COAL BED METHANE POTENTIAL AND BIOGASIFICATION OF SOMA LIGNITE

by

Mustafa Baysal

Submitted to the Graduate School of Engineering and Natural Sciences
in partial fulfillment of
the requirements for the degree of
Master of Science

Sabancı University

2011–2012, Fall

COAL BED METHANE POTENTIAL AND BIOGASIFICATION OF SOMA
LIGNITE

APPROVED BY:

Prof. Dr. Yuda Yürüm (Thesis Advisor) ....

Assoc. Prof. Dr. Serhat Yeşilyurt ....

Assoc. Prof. Dr. Selmiye Alkan Gürsel ....

Assist. Prof. Dr. Gözde İnce ....

Assist. Prof. Dr. Fevzi Çakmak Cebeci ....

DATE OF APPROVAL: ...01.02.2012...................

1

To my father
Mehmet Şevki Baysal

COAL BED METHANE POTENTIAL AND BIOGASIFICATION OF SOMA LIGNITE

Mustafa BAYSAL

MAT, Master of Science Thesis, 2012

Thesis Supervisor: Prof. Dr. Yuda Yürüm

Keywords: Coal bed methane, Biogasification, Coal, Adsorption

Abstract

Coal bed methane (CBM) can arise from both thermogenic and biogenic activity on the coal beds and adsorb on the porous matrix of the coal. Therefore, investigation of pore structure and gas capacity of the coal is essential for accurate estimations of coal bed gas potential. Coal samples of lignite to sub-bituminous rank were obtained from different depths of Soma basin and were characterized by low pressure CO_2 adsorption isotherms at 273 K. Micropore surface areas of the samples were calculated by using D-R model, changed from 224.909 m^2/g to 287.097 m^2/g. Micropore volume and capacity were determined by Dubinin-Radushkevich equation to vary between 0.070 and 0.093 cm^3/g and between 39.06 m^3/ton and 48.44 m^3/ton, respectively. Pore widths of all samples were below 1 nm; suggesting that micropore ratios of the samples are very high. On the other hand, high pressure (up to 17 MPa) adsorption isotherms suggest that methane adsorption capacity of the as receive Soma Lignites vary from 12.99 m^3/ton to 18.13 m^3/ton. Effects of outgas temperature, organic carbon content on gas adsorption capacity of the samples were determined. Results showed that microporosity and methane adsorption capacity of the samples increases with increasing micropore ratio. Carbon isotope analyses of the coal gas desorbed from coal core samples of the Soma lignite basin in Turkey suggests bacterial origin. In order to have a better understanding of secondary biogenic gas potential of the samples, biogasification experiments have been conducted. Results have shown that methane production by

using just methanogens is very limited. When, free hydrogen gas was given the system, methane production has gradually increased. This proved that hydrogen was the limited reagent for microbial methane formation. After 20 days of incubation 1 m^3/ton methane production was measured.

SOMA LİNYİT'NİN KÖMÜR GAZI POTENSİYELİ VE BİYOGAZİFİKASYON ÇALIŞMALARI

Mustafa BAYSAL

MAT, Yüksek Lisans Tezi, 2012

Tez Danışmanı: Prof. Dr. Yuda Yürüm

Anahtar Kelimeler: Kömür, Kömür gazı, Adsorpsiyon, Biogazifikasyon

Özet

Kömür kökenli doğal gaz, termojenik ve biyojenik aktivite sonucu oluşup, kömürün gözenkli yapısı içinde adsorblanır. Bu yüzden, kömürün gözenek yapısının incelenmesi ve ardından gaz kapasitesinin bulunması kömür kökenli doğal gaz potensiyelinin doğru hesaplanması için çok önemlidir. Soma havzasından, olgunlukları linyitten altbitümlü kömüre kadar değişen örnekler karakterize edilmiş ve 273 K'de düşük basınç CO_2 izotermleri ile mikro gözenek yapıları bulunmuştur. D-R adsorpsiyon modeli ile kömürlerin mikro gözenek yüzey alanlarının 224.909 m^2/g dan 287.097 m^2/g 'a kadar değiştiği hesaplanmıştır. Örneklerin mikro gözenek hacimleri ve CO_2 adsorpsiyon kapasiteleri sırası ile 0.070 - 0.093 cm^3/g ve 39.06 - 48.44m^3/ton arasında bulunmuştur. Örneklerin gözenek boyutu dağılımları ise 1 nm'nin altındadır. Ardından, yüksek basınçta (17 MPa'a kadar) metan adsorpsiyon deneyleri ile örneklerin metan kapasiteleri bulunmuştur. Bu deneylerde, degaz yapılmayan örneklerin metan adsorpsiyon kapasiteleri 12.99 m^3/ton'dan 18.13 m^3/ton' kadar değişmektedir. Bunun yanında nem oranınının, degaz sıcaklığının ve organik karbon miktarının adsorpsiyon kapasitesine etkisi gravimetric adsorpsiyon deneyleri kullanılarak incelenmiştir. Sonuçlara gore kömür örneklerinin mikro gözenek miktarları, organic karbon oranı arttıkça artmaktadır. Örnekelerin ^{13}C izotop analizi Soma havzasındaki kömür gazının kökeninin biyojenik olduğunu göstermiştir. Biyojenik metan gazı oluşum sürecini

anlamak için biyogazifikasyon deneyleri metanojen bakterisi kullanılarak yapılmıştır. Sonuçlar göstermiştir ki, sadece metanojenler kullanılarak kömürden metan üremesi çok sınırlı bir işlemdir. Ama sisteme dışarıdan hidrojen eklendiğinde metan üremesinin zamanla arttığı 20 günlük inkübasyon süresince izlenmiştir. Hidrojenin metan üretiminde sınırlayacı ajan olduğu ve artan hidrojen miktarı ile metan üretiminin de artığı gözlenmiştir. Üretimin 20 gün sonunda 1 m^3/ton'a çıktığı görülmüştür.

Table of Contents

List of Figures

List of Tables

CHAPTER 1

1. Introduction

Energy demand of the world is increasing constantly. At present, coal still keeps its value as one of the primary sources of energy to supply this demand. However, utilization of coal as an energy source has lots of negative impacts on the environment. For this reason, scientists have investigated alternative processes to produce clean energy from coal. In order to achieve that, extraction and production of natural gas from coal has become a more significant subject for the energy providers. Coal bed methane (CBM) production is a large and clean energy source with many advantages. In the USA, 10 % percent of natural gas demand has been supplied by CBM [1]. CBM may have thermogenic or biogenic origin and the coal gas is adsorbed in the porous coal surface. In the last two decades, production of the secondary biogenic methane by utilization of additional microorganisms has been studied by scientists aiming to obtain more of clean energy from coal.

Most important factors that affect physical interaction between adsorbent and the adsorbate are dynamic radius of the adsorbate, temperature and solubility parameters of the materials. In the literature, there are many examples where carbon dioxide gas was used for microporous materials instead of nitrogen [2]. Since, dynamic radius of the CO_2 is relatively smaller than that of N_2 (CO_2: 3.3 Å, N_2: 3.6 Å [3, 4]), also solubility parameter of the CO_2 is far greater than nitrogen (for CO_2 δ=6.1 $cal^{0.5}cm^{-1.5}$, for N_2 δ=2.6 $cal^{0.5}cm^{-1.5}$). Owing to these superior properties, interaction between coal and the CO_2 is better than N_2-coal interaction [5, 6]. The last and the most important parameter is the temperature, for physical adsorption of the CO_2, measurement temperature of the isotherm can be 273 K or 298 K which means that we can avoid slow adsorption equilibrium, diffusion limitations at 77 K, also pore shrinkage of the coal at low temperatures can be overcome by using CO_2 for the micropore characterization of the coal. Therefore, CO_2 can reach narrow and wavy micropore structure of the adsorbates due to the high diffusion rate which is called activated diffusion [7, 8]. With all these advantages, coal micropore characterization has been determined by CO_2 since 1964 [9, 10]. In 1984, Smith and Williams reported a relation between high pressure methane adsorption capacity and low

pressure CO_2 adsorption of coal by comparing the results of these experiment and observed close results which means that low pressure CO_2 adsorption also gives idea of the CBM potential [11].

In 1982, Cohen & Gabrielle published the first report on the biological conversion of the coal by microorganisms [12]. Since that time, biological conversion of the coal has been a major area of interest for scientists. Biological treatment of the coal can be divided into two categories; first one is the removal of the sulfur, nitrogen, metals and other unwanted components of the coal and the second one is the conversion of the coal like liquefaction, microbial gasification and microbial pretreatment.

Usually, biological treatment of the coal takes place under mild conditions at low temperature and pressure unlike the classic thermo-chemical processes. For instance, during the thermo-chemical processes, formation of the gas products and liquid hydrocarbons from the coal have been carried out by the thermo catalytic breakdown of deeply buried organic matter at relatively high temperatures ($> 80^{o}C$). On the other hand, in the anoxic biogasification processes, microorganisms cause degradation of the organic content (aromatic hydrocarbons) of the coal to produce gas and other hydrocarbons.

In this study, our primary objective was to understand CBM capacity of the Soma coal basin. For this reason, porosity of the coal samples must have been determined. Usually, surface area and the porosity of the materials can be calculated through the N_2 physical sorption experiment, in this method entire relative pressure range (10^{-8} to 1) can be analyzed without using high pressure equipments [13]. However, for microporous materials like carbon materials and zeolites physical sorption occurs at very low relative pressure ranges (10^{-8} to 10^{-3}) and experiments that are conducted with N_2 are less reliable due to the low diffusion rate and adsorption equilibrium in the pores between 0.5 to 1 nm at 77 K. It is also known that specifically for carbon materials experiments that are conducted at low temperatures such as N_2 sorption causes pore shrinkage that leads to the low sorption equilibrium [14, 15]. On the other hand, gas capacity of the coal can be found by using high pressure methane adsorption isotherms. For this reason, high pressure volumetric gas adsorption experiments were conducted to as received Soma lignite. There are too many variables which effects gas adsorption capacity of the coal such as moisture,

temperature, type of organic content and amount [16-18]. To understand the parameters which effect adsorption capacity of the Soma Lignite, gravimetric adsorption experiments were performed. For low rank coals, usually methane originated from biogenic activity in the coal beds [19]. Hence, laboratory incubation experiments were conducted by using methanogens to simulate underground methane formation.

CHAPTER 2

2. Literature Review on Coal Bed Methane

2.1. Coal

Coal is a complex, heterogeneous, sedimentary organic rock, originated from land plants which have been consolidated between other rock strata and altered by the pressure and heat over millions of years. It consists of mainly carbon, trace amount of hydrogen, oxygen and nitrogen in its structure [20]. Moreover, coal contains significant amount of inorganic material in its structure such as clay, silt. Due to pressure and heat conditions, chemical and physical changes occur. With increasing heat and pressure, water and water vapor are stated to release from the system and peat form, then lignite start to form while CO and CO_2 are releases with water vapor, after that bituminous coal formation occurs with methane and O_2 discharge, finally, anthracite formed due to the H_2 releases. With proper heat and pressure conditions final formation is the grafite. Total of these steps are called coalification. Coal can be classified into five main ranks according to the calorific values [21];

- **Peat**
- **Lignite** Heating value: below 4610 kcal/kg
- **Bituminous coal** Heating value: between 5390 and 7700 kcal/kg
- **Anthracite** Heating value: over 7.000 kcal/kg
- **Graphite**

2.1.1. Coal in World

Coal has still been one of the most important energy sources of the world, even though it has caused negative impacts for the environment due to the greenhouse gas emission. World electricity needs almost rely on coal, in 2003 40% of the world electricity generated from coal. For some countries, this figure is much higher such as for Poland over 94% of its electricity relies on coal, for china 77%, for Australia 76% [22].

Coal has been the fastest growing energy source of the world which is higher than gas, oil, nuclear, hydro and renewables. In the report of the international energy outlook 2011, coal consumption will increase 50% of the world from 2008 to 2035 regarding any environmental regulations in Figure 2.1. According to the reports, 28% of world energy produced from coal in 2008. 60% of this energy was used electricity producers and 36 percent to industrial consumers [23].
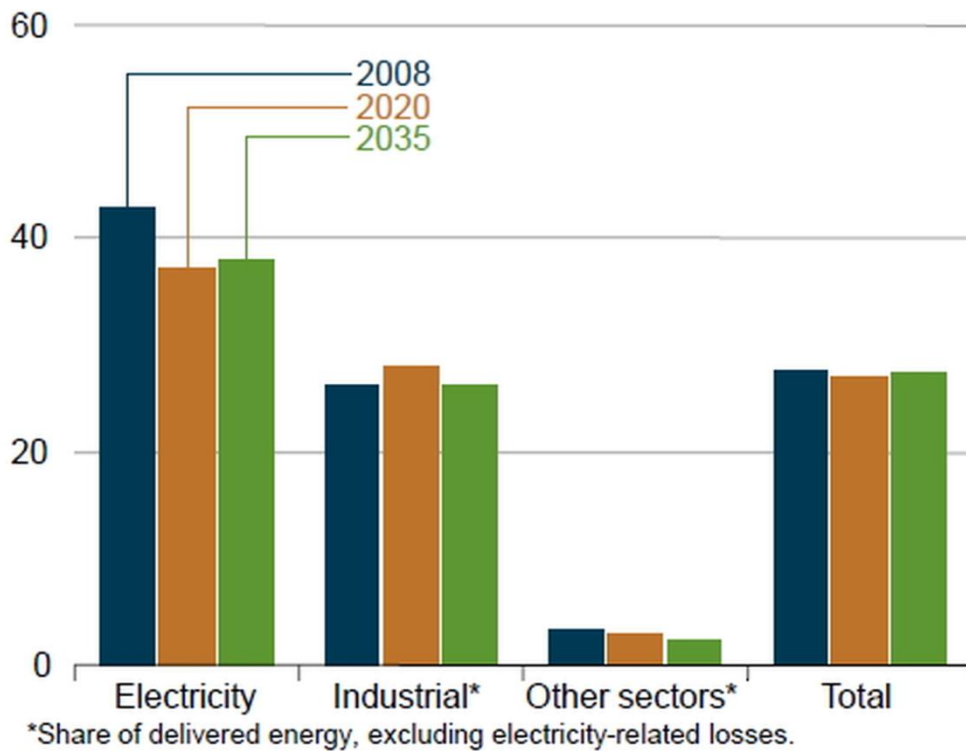
Figure 2. 1: Coal share of world energy consumption by sector, 2008, 2020 and 2035 **[23].**

BP data of 2010 are reflecting a current reserves-to-production ratio of 118 years which is based on proved reserves of the world in table 2.1. Based on the other most used energy sources, coal has the highest reserves to production ratio which indicates that coal will be available to meet demand well into the future since recoverable reserves are less than total coal resources. This mean that further developments such as improving coal mining technology and additional geological assessments of the coal resources, are needed.

Table 2. 1: World coal reserves [24]

Coal: Proved Reserves at end 2010

Million tons	Total	Share of Total	R/P ratio
US	**237295**	27.60%	241
Canada	**6582**	0.80%	97
Mexico	**1211**	0.10%	130
Total North America	**245088**	**28.50%**	**231**
Brazil	**4559**	0.50%	*
Colombia	**6746**	0.80%	91
Venezuela	**479**	0.10%	120
Other S. & Cent. America	**724**	0.10%	*
Total S. & Cent. America	**12508**	**1.50%**	**148**
Bulgaria	**2366**	0.30%	82
Czech Republic	**1100**	0.10%	22
Germany	**40699**	4.70%	223
Greece	**3020**	0.40%	44
Hungary	**1660**	0.20%	183
Kazakhstan	**33600**	3.90%	303
Poland	**5709**	0.70%	43
Romania	**291**	w	9
Russian Federation	**157010**	18.20%	495
Spain	**530**	0.10%	73
Turkey	**2343**	0.30%	27
Ukraine	**33873**	3.90%	462
United Kingdom	**228**	w	13
Other Europe & Eurasia	**22175**	2.60%	317
Total Europe & Eurasia	**304604**	**35.40%**	**257**
South Africa	**30156**	3.50%	119
Zimbabwe	**502**	0.10%	301
Other Africa	**1034**	0.10%	*
Middle East	**1203**	0.10%	*
Total Middle East & Africa	**32895**	**3.80%**	**127**
Australia	**76400**	8.90%	180
China	**114500**	13.30%	35
India	**60600**	7.00%	106
Indonesia	**5529**	0.60%	18
Japan	**350**	w	382
New Zealand	**571**	0.10%	107
North Korea	**600**	0.10%	16
Pakistan	**2070**	0.20%	*
South Korea	**126**	w	60
Thailand	**1239**	0.10%	69
Vietnam	**150**	w	3
Other Asia Pacific	**3707**	0.40%	114
Total Asia Pacific	**265843**	**30.90%**	**57**
Total World	**860938**	**100.00%**	**118**

of which: OECD	**378529**	44.00%	184
Non-OECD	**482409**	56.00%	92
European Union #	**56148**	6.50%	105
Former Soviet Union	**228034**	26.50%	452

Source of reserves data: Survey of Energy Resources, World Energy Council 2010.
* More than 500 years.
 Less than 0.05%.
Notes: Proved reserves of coal - Generally taken to be those quantities that geological and engineering information indicates with reasonable certainty can be recovered in the future from known deposits under existing economic and operating conditions.
Reserves-to-production (R/P) ratio - If the reserves remaining at the end of the year are divided by the production in that year, the result is the length of time that those remaining reserves would last if production were to continue at that rate.

Coal resources are widely distributed all over the world. China, USA, India, Indonesia, Australia and South Africa are the most notable coal producer table 2.2.   Most of the top producers are also top consumer. Only around 18% percent of hard coal is in the international coal market.

Table 2. 2: World coal production [24]
Production*

Million tons oil equivalent	2007	2008	2009	**2010**	Change 2010 over 2009	2010 share of total
US	587.7	596.7	540.9	**552.2**	2.1%	14.8%
Canada	36.0	35.6	32.5	**34.9**	7.2%	0.9%
Mexico	6.0	5.5	5.1	**4.5**	-11.4%	0.1%
Total North America	**629.7**	**637.8**	**578.5**	**591.6**	**2.3%**	**15.9%**
Brazil	2.3	2.5	1.9	**2.1**	8.2%	0.1%
Colombia	45.4	47.8	47.3	**48.3**	2.1%	1.3%
Venezuela	5.6	4.5	2.7	**2.9**	8.1%	0.1%
Other S. & Cent. America	0.3	0.4	0.5	**0.5**	-7.0%	◆
Total S. & Cent. America	**53.6**	**55.2**	**52.4**	**53.8**	**2.6%**	**1.4%**
Bulgaria	4.7	4.8	4.6	**4.8**	5.8%	0.1%
Czech Republic	23.3	21.1	19.5	**19.4**	-0.7%	0.5%
France	0.2	0.1	†	†	–	◆
Germany	51.5	47.7	44.4	**43.7**	-1.5%	1.2%
Greece	8.6	8.3	8.4	**8.8**	5.0%	0.2%
Hungary	2.0	1.9	1.9	**1.9**	1.0%	0.1%
Kazakhstan	50.0	56.8	51.5	**56.2**	9.2%	1.5%
Poland	62.3	60.5	56.4	**55.5**	-1.6%	1.5%
Romania	6.7	6.7	6.4	**5.8**	-9.2%	0.2%
Russian Federation	148.0	153.4	142.1	**148.8**	4.7%	4.0%
Spain	6.0	3.7	3.5	**3.3**	-6.3%	0.1%
Turkey	15.8	17.2	17.4	**17.4**	◆	0.5%
Ukraine	39.9	41.3	38.4	**38.1**	-0.8%	1.0%
United Kingdom	10.3	11.0	10.9	**11.0**	1.6%	0.3%
Other Europe & Eurasia	16.7	17.3	16.9	**16.1**	-4.3%	0.4%
Total Europe & Eurasia	**446.1**	**452.0**	**422.1**	**430.9**	**2.1%**	**11.5%**
Total Middle East	**1.0**	**1.0**	**1.0**	**1.0**	**–**	◆
South Africa	139.6	142.4	141.2	**143.0**	1.3%	3.8%
Zimbabwe	1.3	1.0	1.1	**1.1**	–	◆
Other Africa	0.9	0.9	0.8	**0.8**	–	◆
Total Africa	**141.8**	**144.2**	**143.1**	**144.9**	**1.3%**	**3.9%**
Australia	217.2	220.7	228.8	**235.4**	2.9%	6.3%
China	1501.1	1557.1	1652.1	**1800.4**	9.0%	48.3%
India	181.0	195.6	210.8	**216.1**	2.5%	5.8%
Indonesia	133.4	147.8	157.6	**188.1**	19.4%	5.0%
Japan	0.8	0.7	0.7	**0.5**	-28.4%	◆
New Zealand	3.0	3.0	2.8	**3.3**	16.8%	0.1%
Pakistan	1.6	1.8	1.6	**1.5**	-5.2%	◆
South Korea	1.3	1.2	1.1	**0.9**	-17.3%	◆
Thailand	5.1	5.0	5.0	**5.0**	0.5%	0.1%
Vietnam	22.4	23.0	25.2	**24.7**	-2.0%	0.7%
Other Asia Pacific	23.3	24.3	29.2	**33.4**	14.5%	0.9%
Total Asia Pacific	**2090.2**	**2180.1**	**2314.8**	**2509.4**	**8.4%**	**67.2%**
Total World	**3362.4**	**3470.3**	**3511.8**	**3731.4**	**6.3%**	**100.0%**
of which: OECD	1036.6	1039.3	978.2	**996.0**	1.8%	26.7%
Non-OECD	2325.8	2431.1	2533.7	**2735.5**	8.0%	73.3%
European Union	177.4	167.7	157.7	**156.0**	-1.1%	4.2%
Former Soviet Union	239.0	252.9	233.2	**244.4**	4.8%	6.5%

2.1.2. Coal in Turkey

In the last report of the BP statistical Energy Survey 2011, Turkey has approximately 2243 million tons of coal reserves, 0.3% of the world. Among these reserves, lignite has the highest availability, around 1814 million tons. For 2010, coal production in Turkey is given 17.4 million tons oil equivalent, 0.5% of the world.

Turkey can be considered as medium level in lignite and low level for bituminous coal production of the world. Lignite reserve of Turkey is around 12.4 billion tons and workable reserves around 3.9 billion tons. Most of the lignite reserves were used in thermal power plants due to their low calorific values. In 2008, 82% of the coal was used in thermal power plants, 12% was used in heating and industry. Afşin-Elbistan basin has the highest lignite reserves around 46% of the total [25]. On the other hand, highest bituminous coal reserves are gathered in Zonguldak Basin which are around 1322 billion tones and workable reserve 519 million tons [26]. In 2004, 60 percent of lignite production belongs to the TKI (Turkish Coal Enterprises), EÜAŞ has 32 percent and only 8% percent is produced by private sector [27]. In 2008, TKİ has owned 48% of the lignite production and the other part belongs to the EÜAŞ and private sector. In 2008, coal share is 28% of the total energy consumption in Turkey [28].

Research on coal mining in Turkey has been expanding since 2005. The time between 2005 and 2008, 4.1 billion tons new lignite reserves were found in Turkey [25].

2.2. Coal Bed Methane

Large amounts of methane, light hydrocarbons, carbon dioxide and nitrogen formed during the coalification process of coal. Methane rich gas which is known as coal bed methane (CBM) or coal seam gas has been stored in porous structure of the coal. This trapped methane gas released during the coal mining processes. CBM has been a well known mine hazard subject since the first reported coal mine explosions in USA and France in 1810 and1845, respectively [29].

However, last three decades CBM has attracted attention as a potential energy source. Because coal has a high micropore surface area which is allowed to store six or seven times more methane into these porous structure than conventional natural gas reservoir of the same volume. Beside high methane storage potential of coal, there are many

9

advantages of the coal bed methane such as most of the coal wells which stored methane lies at the shallow depths which is easy to drill and inexpensive to complete. Also most of the methane gas lies in the coal beds therefore there is no need to be exploration cost because most of the national coal resources of the countries are well known [30]. Most of the methane produced on the coal mines has been vented on air. Methane has 21 times more potent a greenhouse gas than is CO_2. Therefore, using these methane gas as an energy source will reduce the greenhouse effect according to the ventilation of methane during the coal mining operations [31]. The other fact is the using CBM as an energy source is more cleaner way than conventional carbon based energy sources because combustion of the natural gas cause 50% less CO_2 emission than combustion of coal and it does not produce SO_2 or particulates [32].

Adsorption in the coal wells is a complicated process. Since coal is a porous material and it has unique adsorption procedures unlike conventional gas reservoirs. Adsorption of coal bed methane occurs in four ways. Firstly, gas molecules adsorbed within the micropores. Secondly, gas is trapped in meso and macropores. Then excess gas is adsorbed in cleat and fractures of coal. In final step, gas is dissolved in ground water within coal fractures. Gas amount decreases from step 1 to 4. Because of the four mode of adsorbed gas in the coal, estimation of the total gas amount in coal beds and forecasting production history have been less predictable than conventional gas resources. It is a problematic issue for exploration and exploitation of coal bed methane [33].

Coal bed methane extraction studies have been conducted since 1980's in USA. In 2007, CBM covers over 10% of the US domestic natural gas supply. In Australia, there were not any CBM production until 1995, however now Australia is the second CBM producer in the world around 4 billion m^3 in 2008. Also, CBM production is a rapidly growing industry in China due to the high CBM potential of the nation [34]. Coal bed methane production is a new developing subject for countries which has high coal reservoir which is shown in Figure 2.2. Researches have been focused on new safe mining operation and utilization of methane as an unconventional energy source [29].
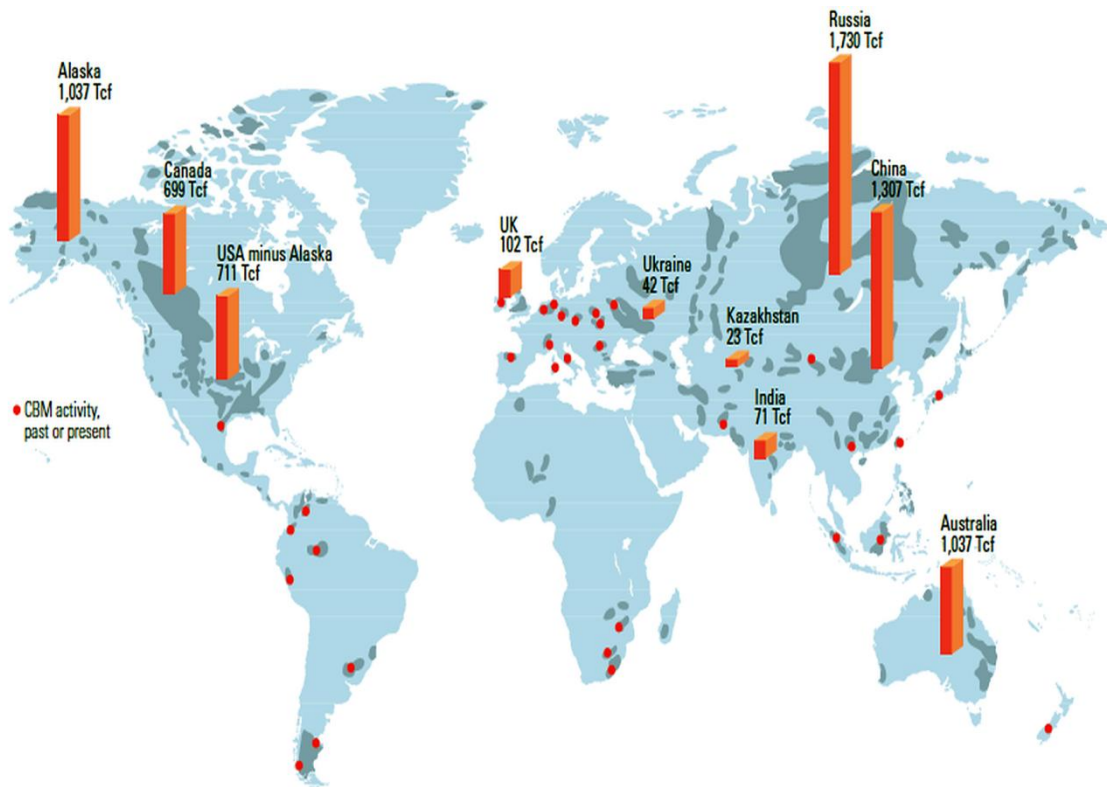
^ CBM reserves and activity. Major CBM reserves (dark blue) are found in Russia, the USA (Alaska alone has an estimated 1,037 Tcf), China, Australia, Canada, the UK, India, Ukraine and Kazakhstan. Of the 69 countries with the majority of coal reserves, 61% have recorded some form of CBM activity—investigation, testing or production. (US DOE, reference 3, and BP Statistical Review, reference 5.)

Figure 2. 2: CBM reserves in present [34].

Coal bed methane extraction has been conducted in USA for three decades. Extraction of coal bed methane is also different from extraction of gas and oil. Since oil and gas production is located above water contact. However for CBM, water is completely permeates coal beds and its pressure causes gas molecules to be adsorbed into coal structure. For CBM production water must be drawn of coal reservoir first, by this way pressure in the coal bed started to reduce and methane will desorbs from the coal structure and then flow to the well bore in Figure 2.3.
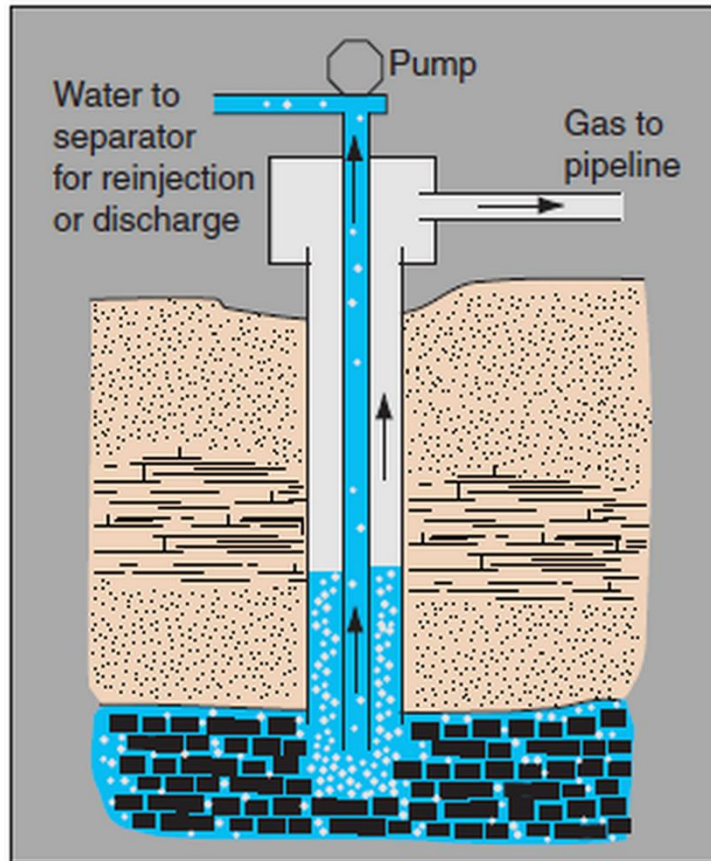
Figure 2. 3: Production scheme of gas and water for a typical coal-bed methane well [30].

On the other hand, CBM production is also environmentally problematic issue because of disposal of the large volumes of water which are produced from CBM wells. Due to the chemical contain and characteristic of the produced water, it can be reinjected into the subsurface or if it is not contain environmentally dangerous materials, it may be dispersed on the surface, pump into evaporation ponds or released directly into local streams.

2.2.1. Thermogenic Coal Bed Methane

Coal bed methane can be originated from thermogenic or biogenic processes [35]. During coalification process, maturity of coal which exposed to high temperature and pressure at deeper ground has increased. With increasing maturity, carbon amount of coal have increased and large amount of volatile matter which contain high amount of hydrogen and oxygen released. Methane, carbon dioxide and water formed during this coalification process [19].

δ^{13}C isotope analysis can be used for determination of origin of the coal bed methane. With increasing coal maturity, deuterium rich methane formed (more positive δD) which leads to more positive heavy isotope δ^{13}C values, it means that methane is originated more from thermal activity than biogenic activity [19].

Methane originated from thermal activity have occur at medium volatile bituminous and higher rank coals which is R_o is greater than 0.6. In USA, Black Warrior Basin (Wyoming) Appalachian Basin (West Virginia, Illinois, Pennsylvania) are the example of the thermogenic gas reservoirs [36] and in Turkey, due to the limited high rank coal resources, methane with thermogenic origin can only be found in Zonguldak Basin [37].

2.2.2. Biogenic Coal Bed Methane

Biogenic gas formed in coal basins is a result of the decomposition of the complex matrix of the coal into the smaller fragments and followed by conversion to the methane by microorganism [1]. Usually, strict anaerobic conditions, high organic content, also low sulfate amount, high pH, low temperature less than 100°C, and proper pore size are required for the generation of the significant amount of coal [19].

Two types of biogenic methane are formed; first one is the methyl type fermentation. In this mechanism, methyl groups converted to methane and carboxyl groups converted to the carbon dioxide. The other type is the carbon dioxide reduction by methanogens; carbon dioxide can be formed by both early bacterial processes and thermal decomposition of the organic matter of the coal [19]. Primary biogenic methane occurs after peat deposition. However, secondary biogenic methane occur all stage of coalification, in this stage surface waters move through the permeable coal beds, by this way microorganisms also move with the waters and start methanogenesis in the coal bed [38], then generated methane adsorb on the internal surface on the coal in Figure 2.4.
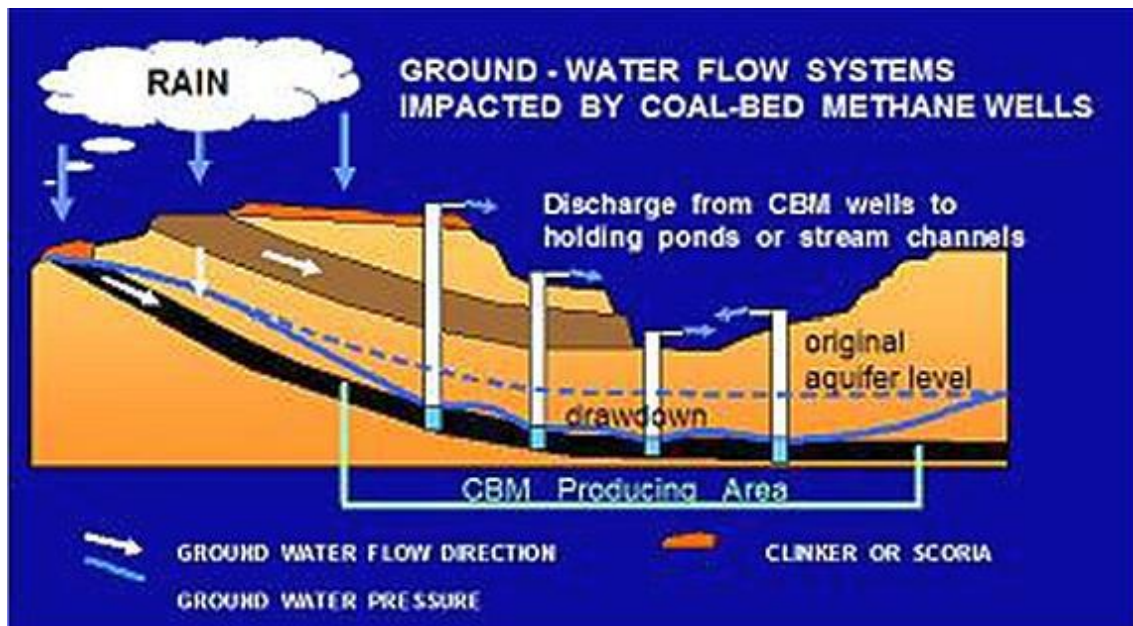
Figure 2. 4: Generation of biogenic methane

Biogenic methane formation favorable in the low rank coals such as lignite, sub bituminous coal. Also significant amount of biogenic methane presence can found in the bituminous coal [39].

2.3. Petrography and Chemical Analysis of Coal

Coal is not a homogeneous substance; it contains various minerals in its structure. Determination of these physical components, systematic and descriptic studies are needed [40]. In order to classify coal and determine its constituents, petrography analyses have been conducted.

2.3.1. Classification and Description of Macerals

Macerals are microscopic constituents of the coal analogous to the minerals of inorganic rocks. Macerals can be classified three groups: vitrinite also called huminite in low rank coals, liptinite or exinite and inertinite.

2.3.1.1. Vitrinite

Vitrinite can be considered as the standard coalification product of woody and cortical tissues. Types of vitrinite macerals are shown in table 2.3. Vitrinite is the most abundant macerals in the coal and more homogeneous than other macerals.

Vitrinite reflectance is used to determination of the coal thermal maturity. It is proportional to the percentage of the directly incident light which is reflected from vitrinite surface [41]. Results can change according to the type of polarization. If plain polarized light is using, reflectance value change during the rotation of the sample between maximum and minimum values [41]. In standard technique, reflectance of the 100 particles are measured and arithmetic mean maximum (R_{max}) is given as a result. If non-polarized light is used to measure vitrinite reflectance, the reflection from all of the direction on the vitrinite surface integrated to give a random reflectance R_r. But usually R_{max} is used to determine rank of the coal [41].

According to the coal maturity from lignite to anthracite, the color of the transmitted light on vitrinite surface change from yellow-orange, red, red brown, dark brown to opaque. On the other hand, color of the incident light varies from dark grey, light gray and white depending on the coal maturity [42].

Table 2. 3: Nomenclature of vitrinite and huminite macerals [43].

Maceral group	Maceral	Maceral subgroup	Source
Vitrinite	Telinite		Woody tissues, leaves, bark, branches, roots, etc.
	Collinite		Humic gels
	vitrodetrinite		Degraded fragments of other vitrinite macerals
Huminite	humotelinite	Textinite ulminite	Woody tissues
	humodetrinite	Attrinite densinite	Finely comminuted humic detritus
	humocollinite	Gelinite corpohuminite	Colloidal humic gels Condensation products of tannis

2.3.1.2. Liptinite

Macerals which have higher hydrogen content than vitrinite are called liptinite groups [41]. Their origin is also related to the plants other than woody tissue such as spore and pollen coats, cuticles and resins etc. Type of liptinite macerals and their sources are shown in table 2.4. Their reflectance values are too low compared to the other macerals with the same rank [42].

Table 2. 4: Nomenclature of liptinite maceral [43].

Maceral group	Maceral	Source
liptinite	sporinite	Spores and pollens
	cutinite	cuticles
	resinite	Resins and waxes
	alginite	algae
	Suberinite	Bark tissues
	liptodetrinite	Degradation products of liptinite maceral

2.3.1.3. Inertite

The last type of macerals which have less hydrogen content than vitrinites called inertites shown in table 2.5. In carbonization, they behave inert or semi-inert. Inertites are formed from intensive degradation of the matrix which induced by microorganisms [41].

Table 2. 5: Nomenclature of liptinite maceral group [43].

Maceral group	Maceral	Source
liptinite	Fusinite	Woody tissue
	semifusinite	Woody tissue
	macrinite	Uncertain-oxidation of gelified plants
	Micrinite	Secondary Maceral
	Sclerotinite	Fungie remains
	inertodetrinite	Degraded fragments of inertinite

2.3.2. Ultimate and Proximate Analysis of Coal

The proximate analysis gives the relative amounts of moisture, volatile matter or fixed carbon. Also, calorific value and tar yield sometimes are given as a result of proximate analysis.

Ultimate analysis is used for the determination of chemical elements in coal like C, H, O,N and S [41].

2.4. Gas Adsorption

There are lots of different methods to characterize porous materials such as neutron scattering, small angle X-ray, SEM, TEM, mercury porosimetry etc. They are all used in the different applications. Gas adsorption is the most favorable porous method characterization method among them. In gas adsorption method wide range of pore sizes can be determined easily (from 0.35 nm to ≥100 nm) [14]. There are lots of options and parameters can adjust according to the experiment such as gas type, temperature, pressure range, adsorption model.

Adsorption can be described as attachment of the particles on the surface. Particles can move through the surface by two ways. In elastic scattering, atoms hit to the surface and bounced back without any energy loss. In inelastic scattering, atoms hit the surface and losses or gains energy.   In gas adsorption, gas solid interface occurs. Solid is called adsorbent or substrate. And gas molecule which adsorbs on the solid surface is called adsorbate.   Amount of adsorbed gas molecule depend on absolute temperature, the pressure and interaction potential between gas and the surface. Due to the interaction strength of the molecules, adsorption can be divided into two categories; chemisorptions and physisorption [14]. Differences are shown in Table 2.6.

2.4.1. Chemisortion

If the interaction energy between adsorbate and adsorbent exceed an absolute potential, irreversible adsorption or chemisorption occurs (Figure 2.5). In chemisorption, actual chemical bonds formed between the gas-solid interfaces which lead to high heat of adsorption. All chemical bonds form when certain activation energy exceed, on the surface there can be different sites which has different activation energies. With the help

of the chemisorption, active sites on catalyst surface can be measured by the determination of the amount of the chemisorbed gas [14].
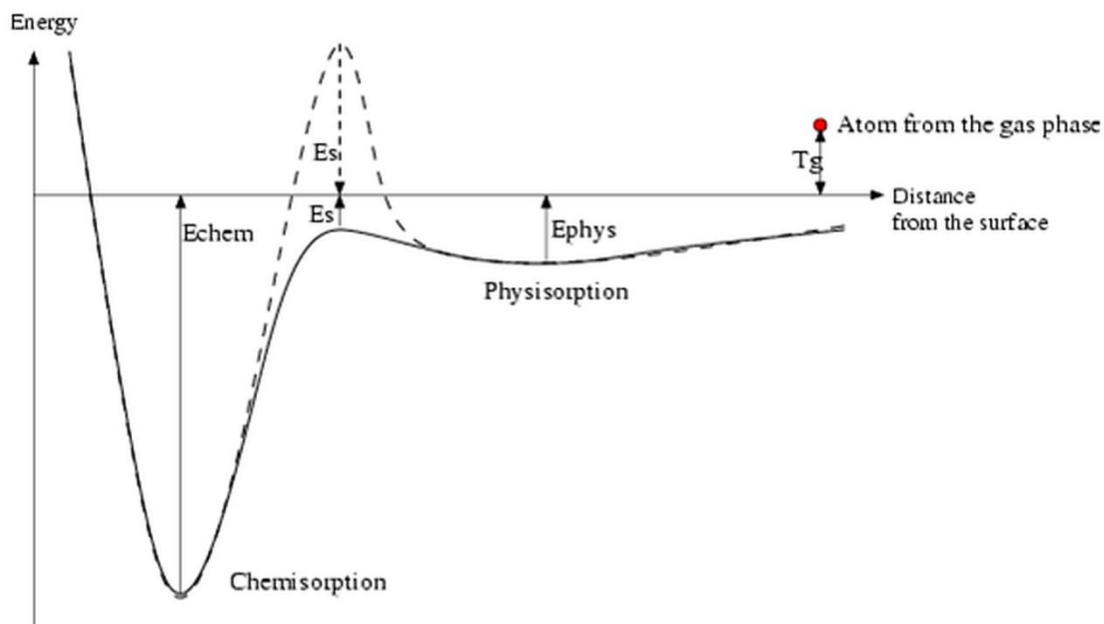
Figure 2. 5: Energy of adsorption [44].

Table 2. 6: Differences between chemisorptions and physisorption [45].

Physical Adsorption	Chemical Adsorption
Low heat of adsorption (≤ 2 or 3 times latent heat of evaporation)	High heat of adsorption (≥ 2 or 3 times latent heat of evaporation)
Non specific regarding adsorbate species	Highly specific regarding adsorbate species
Monolayer or Multilayer. No dissociation of adsorbed species. Only significant at relatively low temperatures	Monolayer only. May involve dissociation. Possible over a wide range of temperature
Rapid, non-activated, reversible. No electron transfer although polarization of sorbate may occur.	Activate, may be slow or irreversible. Electron transfer leading to bond formation between sorbate and surface.

2.4.2. Physisorption

When adsorption on the gas molecules on surface happened via weak van der Waals forces, reversible adsorption also called physisorption occurs since there is no chemical bond formed between adsorbate molecules and the solid surface. It is an exothermic process and energy of adsorption is not much larger than energy of condensation of the adsorbate (between 8.37-41.84 kJ/mol). Usually at low pressure monolayer adsorption, at higher pressure multilayer adsorption is favorable depend on the type of the adsorbent and the adsorbate [46].

2.4.2.1. Porosity

Most of the materials contain free volume in its structure. They can distributed in the material and differ from each other by size and shape. Total of this free volume is called porosity [42]. Pores in the material allow to the fluids to flow in or out of the material. Porosity strongly affects mechanical and chemical properties of the material. Two types of porosity can be observed; first one is the closed pores. They are not connected to the external surface and they are not open for adsorbent molecules, they only affect density and mechanical strength of the material. The second types of pores are called open pores which are connected to the external surface of the material. These pores are accessible to the gas or fluid [42].

2.4.2.2. Pore Size Distribution

In 1982, IUPAC are subdivided pores in the material into three classes according to the their sizes; micropores are the pores internal width less than < 2nm and mesopores with the internal width between 2 and 50 nm, and pores internal width higher than > 50 nm is called macropores [47].

Adsorption behavior in macropores is different from mesopore and micropore due to their size they behave like flat surface. However sorption behavior in micropores is dominated by the interaction between adsorbent molecules and the pore walls; in fact adsorption potentials of the opposite pore walls are overlapping. In adsorption on mesopore, in addition to the adsorbent pore wall interaction, interaction between adsorbent molecules get important additionally which may lead to capillary condensation. It means that gas molecules condenses to a liquid phase in pore at pressure less than saturation pressure of bulk fluid [14].

2.4.3. High Pressure Adsorption

Conventional gas adsorption experiments are usually conducted at atmospheric pressures. On the other hand, most of the coal bed methane measurements are conduct at high pressure. Theories and simulation on gas adsorption based on absolute thermodynamic variables. However experimental results generally give excess thermodynamic variables. At low pressure, differences between absolute and excess values are negligible but at high pressure differences became very important [48].

For CBM potential investigation or ECBM procedures, gas adsorption potential which is found by excess sorption values provides insufficient information, because excess sorption considers the void volume that can be occupied by the gas as a constant disregarding the volume of the gas in its sorbed phase. For this reason, using absolute isotherms values is preferable therefore it considers the total amount of gas that can be sorbed per unit mass of sample included gas amount in its sorbed phase [49].

2.4.3.1. Excess/Absolute Isotherm

- Excess (Gibbs) Adsorption

Excess adsorption values can be found from experimental data. This does not refer to the real adsorption values. Since, it neglects adsorbed gas phase amount. In volumetric gas adsorption systems, known amount of pure gas injected to the system n_{inj} and some of the injected gas adsorb in the pores and some of the gas retained equilibrium without being adsorb in free gas phase called n_{unads}^{Gibbs} . Then adsorb gas amount calculated from equation 2.1;

$$n_{ads}^{Gibbs} = n_{inj} + n_{unads}^{Gibbs} \qquad\qquad 2.1$$

Injected amount of gas calculated from gas conditions, shown in equation 2.2 ;

$$n_{inj} = \left(\frac{P\Delta V}{ZRT}\right) \qquad\qquad 2.2$$

Z is the compressibility factor of the gas at injected temperature and pressure. Different equation of states can be used for determination of Z. It is a very important parameter for gas adsorption experiment especially at high pressures where gas molecules diverge from ideal gas behavior.

Unabsorbed (free) gas amount can be found by using equation 2.3.

$$n_{ads}^{Gibbs} = \left(\frac{P V_{void}}{ZRT}\right)_{cell} \qquad 2.3$$

V_{void} must be found before experiment by using helium according to the formula 2.4.

$$V_{void} = \frac{\left(\frac{P \Delta V}{ZRT}\right)_{injection}}{\left(\frac{P_2}{Z_2 T} - \frac{P_1}{Z_1 T}\right)_{cell}} \qquad 2.4$$

State 1 refers cell condition before gas injection and state 2 is the equilibrium conditions after gas injected in the cells.

- Absolute Adsorption

In absolute adsorption, volume of gas adsorbed phase included. Absolute adsorption data can be calculated from excess adsorption results. In absolute adsorption, we can talk about two gas phase; free gas q_{gas}^{bulk} and adsorbed gas phase q_{gas}^{ads} . As a result of this, total volume of the system contains gas volume V_{gas}, solid volume V_{solid}, and adsorbed phase volume V_{ads}.

$$V_{top} = V_{gas} + V_{solid} + V_{ads} \qquad 2.5$$

According to equation 2.5, void volume can be found equation 2.6;

$$V_{void} = V_{gas} + V_{ads} = V_{total} - V_{solid} \qquad 2.6$$

Quantity of the gases can be written;

$$n_{ads} = n_{total} - n_{unads} \qquad 2.7$$

The only differences between excess and absolute adsorption is the calculation of the n_{unads} value.

In excess adsorption, n_{unads} can be written;

$$n_{ads}^{Gibbs} = n_{total} - V_{void} P_{gas} \qquad 2.8$$

In absolute adsorption, n_{unads} can be written;

$$n_{ads}^{abs} = n_{total} - V_{gas} P_{gas} \qquad 2.9$$

By using equations 2.8 and 2.9, we can find relation between excess and absolute adsorption;

$$n_{ads}^{Gibbs} = n_{ads}^{abs} - V_{ads} P_{gas}$$ 2.10

Adsorbed gas volume can be written;

$$V_{ads} = \frac{n_{ads}^{abs}}{q_{ads}}$$ 2.11

If we can write equation 2.11 inside the equation 2.10, excess adsorption amount can be expressed by two type of gas density;

$$n_{ads}^{Gibbs} = V_{ads} (q_{ads} - q_{gas})$$ 2.12

Lastly, by using equation 2.11 and 2.12,

$$n_{ads}^{abs} = n_{ads}^{Gibbs} \left(\frac{q_{ads}}{q_{ads} - q_{gas}} \right)$$ 2.13

By using equation 2.13, we can calculate absolute adsorption amount by using excess adsorption amount.

- At low pressure $q_{ads} \gg q_{gaz}$; excess and absolute values very closed to the each other $n_{ads}^{abs} = n_{ads}^{Gibbs}$.

- At higher pressure q_{gas} start to increase and after certain pressure value, it can be very closed to q_{ads} value. And differences between excess and absolute adsorption became significant.

2.5. Coal as a Solid Colloidal

At any rank, coal possesses certain porosity because of its solid colloidal structure.

2.5.1. Porosity of Coal

As explained before, porosity is the free volume of the material occupied by the pores. Porosity of the material can be determined by density measurements. Helium and mercury displacement methods are generally used for density measurements of coal. Other gases and vapors also can be used for the density measurement but their

penetration in the coal structure can be completely or partially, depends on the molecular dimension and the molecular interaction with the coal.

At low pressures, helium is capable of penetrate complete pore structure of the sample but mercury doesn't. Even if high pressures were applied, mercury could not penetrate the whole pore structure of the coal. This means that coal contains two pore systems: macropore and micropore system which mercury cannot penetrate [41].

2.5.1.1. Internal Surface of coal

In the first attempts to measure surface area of the coal, heat of wetting values of methanol are measured. In 1944, Griffith and Hirst measured internal surface area of wide range of coal by determining heats of wetting in methanol which changes from 10 to 200 m^2/g [41].

Then, low pressure gas adsorption method was been used to determine the surface area of the coal from BET method. Nitrogen or argon at very low temperature were used as an adsorbent and measured values are vary from 0.1 to 10 m^2/g. Results were very low compared to the heat of adsorption experiment's results. The reason of these results can be explained by the very low diffusion rate of nitrogen in coal at these temperatures and also pore shrinkage of the coal which prevents nitrogen molecules to penetrate micropore structure of the coal. Surface area of the coal measured by gas adsorption experiments always gives different result at different temperature and different gases (Figure 2.7).

Table 2. 7: Surface Areas of the coal measured by different adsorbates at different temperatures [50].

C (%)	Surface area (m^2/g)				
	N_2 (-196°C)	Kr (-78°C)	CO_2 (-78°C)	Xe (-78°C)	CO_2 (25°C)
95.2	34	176	246	226	224
90.0	Nil	96	146	141	146
86.2	Nil	34	107	109	125
83.6	Nil	20	80	62	104
79.2	11	17	92	84	132
72.7	22	84	198	149	139

This causes controversial results of determination of coal surface area. The problem was resolved by the low temperature He adsorption experiments. At low temperatures, helium is not affected by the thermal contraction of coal. It means that pore shrinkage is not the only effect on the low surface area values of coal. Dimension of the adsorbent molecule is very important to penetration of the gases in to the microporous structure of coal. Nitrogen and methane too big to penetrate these micropores however helium is not affected due to its small size.

After that carbon dioxide was used as an adsorbent to eliminate pore shrinkage at low temperatures and its small molecular dimensions. In 1965, Marsh used carbon dioxide isotherms to determined coal surface area of coal by using Dubinin-Polanyi methods [10].

2.6. Coal Bed Methane Capacity

Coal bed methane have been considered to be a potential energy source, on the other hand it is also a potential danger for underground coal mining. Either way, quantity of

the methane in the basins must be determined. When amount of underground gas was determined, it is very important to determine the content of the gas components. Oppose to the free gas in the conventional rock gas reservoirs, gas in the coal beds exist in a condensed phase due to the physical adsorption into the pores [51].

2.6.1. Direct Coal Bed Methane

In direct methane measurements, total gas content in the coal bed is divided into a 3 groups; lost gas, desorbed gas and residual gas.

- Lost gas: During sample collection and retrieval to the desorption canister, some gas from the coal escape which is called lost gas. Amount of lost gas is only related to the sampling time. If sampling time is too much, lost gas amount is also large or vice verse. There is no other control over lost gas for this reason it is the least reliable part of the total gas. Also it cannot directly measured it must be estimated from the measured desorbed gas volume data (Figure 2.6) [52].
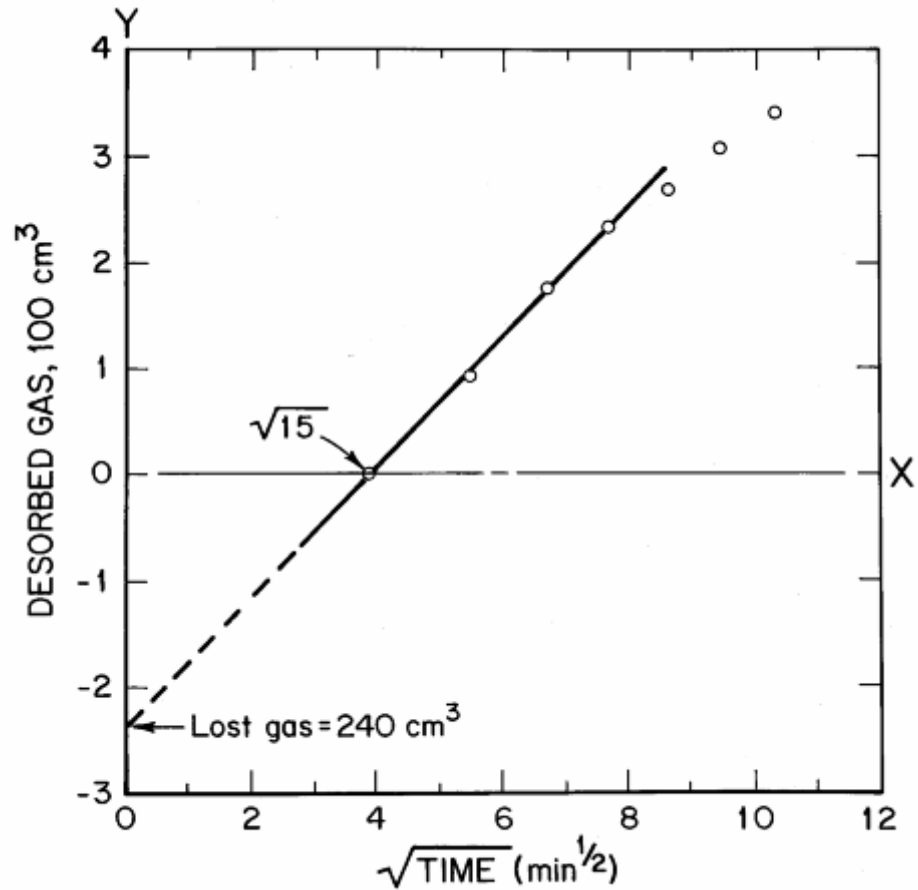
Figure 2. 6: USBM direct method lost gas estimation graph [52].

- Desorbed gas: When sample collect and sealed in canister, significant amount of gas desorp from the coal due to pressure differences which is called desorbed gas. Determination of the desorp gas amount based on periodically measuring pressure differentials in desorption canister as gas is released over time, and calculating the desorbed gas volume utilizing the ideal gas law.

- Residual gas: when desorption rate of the gas in the canister reach very low values, desorp gas measurement is terminated. However, there is still trapped methane gas at 1 atm inside the pores which is called residual gas [53]. Crushing of the sample in an air tight container and measuring the released gas volume as the same as desorp gas measurement method [54].

There are some method to determined total gas amount of the coal such as Bertard's Direct Method [55] , U.S. Bureau of Mines Direct Method and The NIOSH modified direct method which provides a significant level of increased accuracy [52].
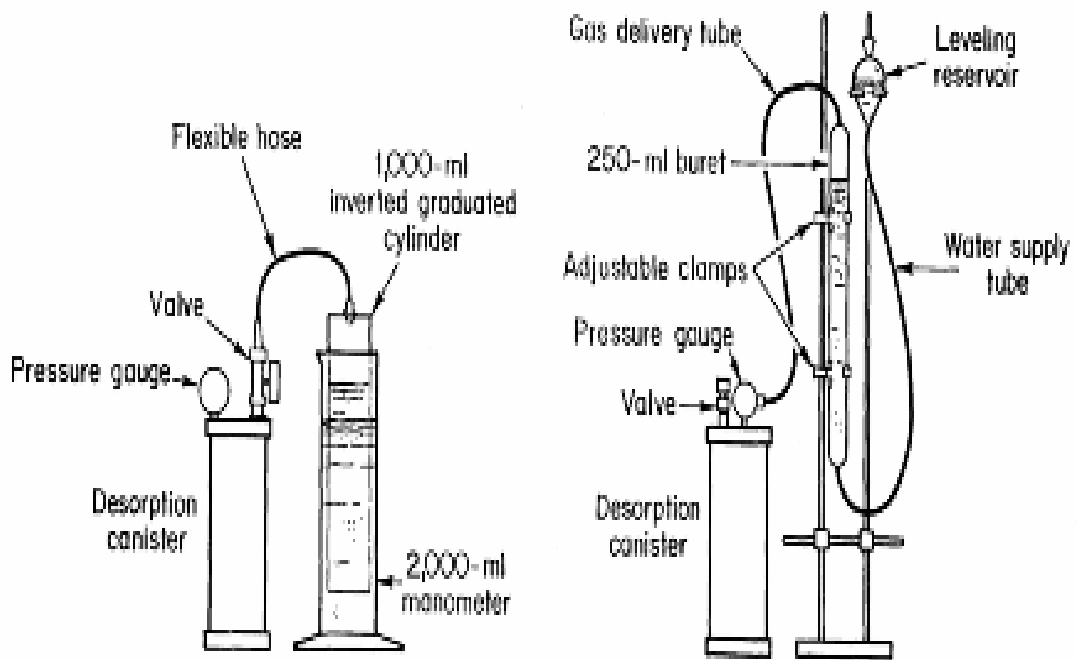
Figure 2. 7: Examples of desorp gas measurements techniques [52].

2.6.2. Indirect Coal Bed Methane

Total gas content of the coal bed can be also found by indirect gas measurements. In this method high pressure gas adsorption isotherms are used. Methane is amount determined by the pressure change and the temperature. Isotherms provide information of maximum amount of methane sorption or maximum storage capacity of the coal beds. However, total methane amount calculated from the isotherm data are not the actual data since all coal beds are not fully saturated with methane especially beds in the shallow depths. Therefore indirect gas measurements are not the crucial factor for mine safety but it can be very useful for preliminary assessment tool for mine planning purposes or targeting potential areas for commercial coal bed methane exploration [52]**.**

2.6.3. Factors Effecting Coal Bed Adsorption Capacity

There are several factors affecting the coal bed adsorption capacity of coals significantly. They must be carefully determined to correct estimation of the coal bed methane potential of the reservoir.

2.6.3.1. Temperature

Coal bed temperature is the one of the most important parameter to change adsorb gas amount in the coal beds. At higher temperatures, gas in the free state in the coal mines is higher than adsorbed state. Adsorption in the gas phase is an exothermic process which means that at lower temperature, equilibrium favors to the adsorption in the coal on the other hand desorption is the dominant process at higher temperatures [56]. At elevated temperatures gas potential of the coal bed start to decrease due to decrease of the adsorbed gas amount [42].

2.6.3.2. Moisture

Gas sorption of the coal is decreasing with the increasing moisture content of the coal. It can be explained that water molecules adsorb the porous structure of the coal as a result of this; accessible micropore volume on the coal is reduced. Usually dry coal adsorbs more gas than moist coal. Studies show that linear decreasing on the methane capacity of coal with increasing moisture content [16]. However above certain moisture content, adsorption amount of the coal does not change which means that water adsorbed all possible sites which they can, the other sites available for the gas molecules. Researchers show that 1% moisture content can reduce 25% adsorption capacity of the coal and in another study 5% moisture cause 65% decrease in the adsorbed gas amount [57].

2.6.3.3. Ash Content

Adsorption capacity of the coal is increasing with decreasing ash content. Mineral matter in the coal adsorbed negligible amount of gas in its structure and also block the micropores in coal. Studies show that isotherms are drew against ash free based gives significantly higher adsorb gas amount then original isotherms [17].

2.6.4. Enhanced Coal Bed Methane

Coal bed methane is a new and can be a considerably large energy source which takes large amount of interest on it. In classic ways, recovery of the coal bed methane has been done by reducing the hydrostatic pressure of the coal beds through dewatering. Main disadvantage of the process is the low yield around 20-60% of gas can be recovered and high amount of waste water produced during the process [46]. The other

proposed method is the CO_2 injection wellbores into the coal bed to recover methane due to the preferential adsorption of the CO_2 to methane which is called enhanced coal bed methane (ECBM) recovery. Another idea is to inject flue gas (CO_2 and N_2) into the seam, in this case N_2 acts as a stripping agent which is called flue gas-enhanced coal bed methane recovery [49]. ECBM is a novel technology which increase methane yield and due to the CO_2 storage it reduce CO_2 emission in to the atmosphere. There have been some field examples of the ECBM in the world to improve its potential and usage [58].

To understand ECBM technology, CO_2, N_2 and methane adsorption in to the coal must be determined at different pressures and temperatures. Also chemical analysis of the coal must be studied. Lots of studies have been conducted on ECBM technologies; all of them show that CO_2 adsorption is always more than methane adsorption at the same pressure and temperature by a factor between 2 and 10 [59]. Therefore, coal beds are significant CO_2 sealing places and allow to store more carbon dioxide that produced by the combustion of the recovered methane.

There are too many benefits of ECBM except from high efficiency methane recovery and reducing carbon dioxide emission. Another important benefit of this technology is that coal beds which cannot be profitably mined used due to the making available substantial amounts of fossil fuel that could otherwise not be used for energy production. And this technology gathers most of the energy sources together closed to the coal basins and reduce energy transportation [16].

2.7. Secondary Biogenic Methane

During coalification, thermogenic and biogenic processes result in methane production. Losses in primary biogenic methane makes it impossible to be used, however, secondary methane is produced by microbes that are transported to mature coal seams by meteoric recharge [60, 61]. Optimum conditions for methane biogenesis can be summarized as: low rank, high permeability and high water content [19]. Essential comprehension of biogenesis reactions are compulsory if coal bed methane is active, in order to maximize the yield.

2.7.1. Methanogenesis of the Coal Beds

Methane gas is produced by anaerobic microorganisms that are called methanogens. Unfortunately, the number of simple carbon compounds that can be converted to methane by these microorganisms is limited. H_2-CO_2 and acetate are the most important ones, as well as methanol. Methylotrophs are the methanogens that use methanol, methylamines, and dimethyl sulfide as their carbon source [62]. There are also some methanogens that utilixe formate, ethanol and isopropanol. Conversion of coal to methane becomes easier as the carbon chains become smaller. Therefore, fermantative and acetenogic bacteria addition to methanogens are necessary to increase the conversion. Complex substrates are hydrolyzed and fermented by bacteria, that results in acetate, longer chain fatty acids, CO_2 H_2, $NH_4 +$, and $HS-$ formation. H_2 and CO_2 are converted to acetate by H_2-utilizing acetogenic bacteria. Those microorganisms can also convert demethoxylate low-molecular-weight ligneous materials and ferment some hydroxylated aromatic compounds to acetate [35]. Aside from H_2 utilizing acetogens, there is also H_2 producing acetogens which produce H_2, carbon dioxide, and acetate. Those can then be converted to methane by methanogens. This collection of different microbial species is referred to as a consortium; for methanogenic consortia, interdependencies such as interspecies H_2 transfer are common [62].

2.7.2. Coal Bioavailability

By inserting bacterial consortia and nutrients into the coal beds, new methane production potential is increased in addition to enhanced reservoir permeability via the microbial consumption of coal, waxes, and paraffins [35]. According to biodegradation studies, endemic bacteria performs as well as, if not better, than any foreign microorganisms site. Therefore, special attention should be payed during the selection of bacteria in the consortia. Limiting nutrients shall be included in the consortia as well, in order to promote endemic organisms. Since it is easier to break low molecular weight carbon chains, which is the common character of low rank coal, low rank coal is open to microbial degradation [35].

CHAPTER 3

3. Experimental

In this chapter, coal characterization steps, characterization devices, gas adsorption equipments, and detailed bioprocess experiments were explained. Chapter focused on volumetric and gravimetric high pressure gas adsorption mechanism and experiments.

3.1. Coal Preparation and Preservation

Characterization of the coal samples which were excavated in different depths from Soma Basin in Turkey was performed.

Coal samples which come from Soma basin were broken and grinded into small particles, and then passed through the sieve to reduce particle size to 150 μm. Resulting samples were preserved at nitrogen atmosphere.

Six Soma Samples were used for the analyses. And two Zonguldak coal samples which have high maturity were used to compare different types of Turkish coals.

Sample	Origin
JK-1122	Soma
JK-1126	Soma
JK-1135	Soma
JK-1137	Soma
JK-1389	Soma
JK-1408	Soma
JK-1414	Zonguldak
JK-1415	Zonguldak

Table 3. 1: Origin of the samples

3.2. Coal Characterization Experiments

3.2.1. Ultimate and Proximate Analysis

In order to understand the basic characteristic of our samples ultimate and proximate analysis were performed in TÜBİTAK Marmara Research Center (MRC) Energy Institute.

3.2.2. Rock-Eval Pyrolysis

Rock-Eval pyrolysis was conducted for determination of level of maturity and type of the organic matter contained in the samples. Rock Eval pyrolysis was done using the Delsi-Nermag Rock Eval II plus TOC module at TÜBİTAK Marmara Research Center (MRC) Earth and Marine Sciences Institute.

3.2.3. Reflectance Analysis

Petrographic analysis was performed in TÜBİTAK Marmara Research Center (MRC) Earth and Marine Sciences Institute by using Leitz MPV microscope that was equipped with photomultiplier. 32X optical lens was oiled with immersion oil (refractive index %1,518). Fort reflection analysis, a sapphire standard (R= %0,592) was used.

3.2.4. FT-IR Analysis

FT-IR analyses of the samples have been conducted by using Thermo Scientific - Nicolet İS10 FTIR with KBR transmittance accessory. KBR pellets were prepared 1/100 sample ratio at 9 ton pressure.

3.3. ^{13}C isotope Analyses

To understand origin of the coal bed gas, ^{13}C isotope analyses were conducted by using Continuous Flow Gas Chromatography—Isotope Ratio Mass Spectrometer (GC-IRMS) at TÜBİTAK Marmara Research Center (MRC) Earth and Marine Sciences Institute (EMSI).

3.4. Solubility Experiments

For the chemical solubilization experiments, sodium oxalate, sodium carbonate and sodium phosphate were used as Lewis bases. 10 ml, 0.1 M aqueous solutions of sodium oxalate, sodium carbonate and sodium phosphate at varying pH values (4-12) were

prepared. Then 50 mg of coal was added to these solutions. Mixtures were shaken at 200 rpm, for 24 hours on a rotary shaker. After that time, aliquots were centrifuged at 5000 rpm for 20 min and absorbance intensities of final solutions were determined by using UV-visible spectrometer.

3.5. Low-Pressure Carbon Dioxide Adsorption Experiments

Low pressure CO_2 micropore surface area and micro porosity experiments were conducted at 273 K by using Quantachrome Autosorb Automated Gas Sorption System. Samples were outgassed at 373 K for 6 h prior to measurements, this temperature was chosen due to the fact that high temperature could cause the collapse of the organic matrix of the coal and also low temperature cannot remove water molecules from pores.

3.6. High Pressure N_2 and Methane Adsorption Experiments

High pressure adsorption experiments were conducted by two different techniques; Gravimetric method and volumetric method. In Gravimetric method, nitrogen and methane adsorption experiments were conducted by Intelligent Gravimetric Analyzer (IGA).

3.6.1. Intelligent Gravimetric Adsorption (IGA) Experiments

High pressure gas adsorption experiments were performed by using Hiden Isochema Intelligent Gravimetric analyzer (IGA-003) with nitrogen and methane. The IGA has a fully automatic microbalance system that allows measuring the weight change as a function of time, gas pressure and the sample temperature. The precision of the measurement can be controlled by a PC. Long term stability of microbalance is $0.1\mu g$ with a weighting resolution of 0.2 μg and temperature stability is 0.1^oC. For nitrogen adsorption experiments samples were outgassed at 105^oC 3 hours under 10^{-6}mbar vacuum, for methane experiments samples were only outgassed under vacuum without any heat treatment. In order to understand the effect of outgas temperature to methane adsorption capacity of the coal, only one sample was outgassed at 105^oC 3 hours. For nitrogen experiments, linear driving force mass transfer model was used to get asymptotic uptake for every pressure point at 298 K up to 9 bar. For methane experiment only 6 hours interaction time was used to get thermodynamic equilibrium at 298 K up to 9 bar without using PC control asymptotic uptake value.

3.6.2. Volumetric Adsorption Experiments

The methane excess sorption isotherms of the coal samples were determined using the manometric method in Aachen University, Institute of Geology and Geochemistry of Petroleum and Coal. Measurements were conducted at 45°C on powdered 'as-received' coal samples.

Experimental set up is shown Figure 3.1. It consists of reference cell and stainless steel sample cell separated with actuator-driven valves and a high precision pressure transducer between them. The reference (void) volume is determined by helium pycnometry with a calibration experiment.

Reference volume: V_{ref}

Sample cell volume: $V_{sample\ cell} = V_{sample} + V_{void}$ 3.1

Temperature control was provided by temperature controlled oven with high accuracy. Before the experiment, sample cell volume which is not occupied by the sample (void) is determined by He as an adsorbate. By this method, volume of the sample can be found. Gas sorption experiment can be explained in 5 steps. In the first step, experimental setup (reference cell and sample cell) was evacuated to establish proper conditions then shot-off valve between reference cell and sample cell is closed. In the second step, certain amount of gas introduced to the reference cell volume and valve 1 closed. Successively, 60 minutes are allowed for pressure and temperature equilibrium (step 3). In the fourth step, valve between cells is opened and gas is admitted to the sample cell. In this step, gas begins to adsorb on the sample and measured pressure start to decrease due to the decrease in the free gas amount. When the system comes to equilibrium in a certain amount of time that can be change with 1 hour to 20 hours depending on the experiment conditions, equilibrium pressure is recorded and valve between two cells is closed. This procedure is repeated for every pressure level until the maximum pressure is reached [16, 59, 63].

The excess amount (excess mass; m_{excess}) is defined as:

$m_{excess} = m_{total} - V^0_{void} \cdot \rho_{methane}\ (T\ ,\ p\ )$ 3.2

Here m_{total} denotes the total mass of methane transferred into the measuring cell up the corresponding pressure step, V^0_{void} is the initial void volume of the cell (as determined

by helium pycnometry). The density $\rho_{methane}$ (T, p) of the gas phase as a function of pressure and temperature is calculated using the equation of state (EOS) for CH_4 of Setzman and Wagner [64]. Helium density is calculated using the reference equation of state GERG-2004 for natural gases and other mixtures [65, 66].
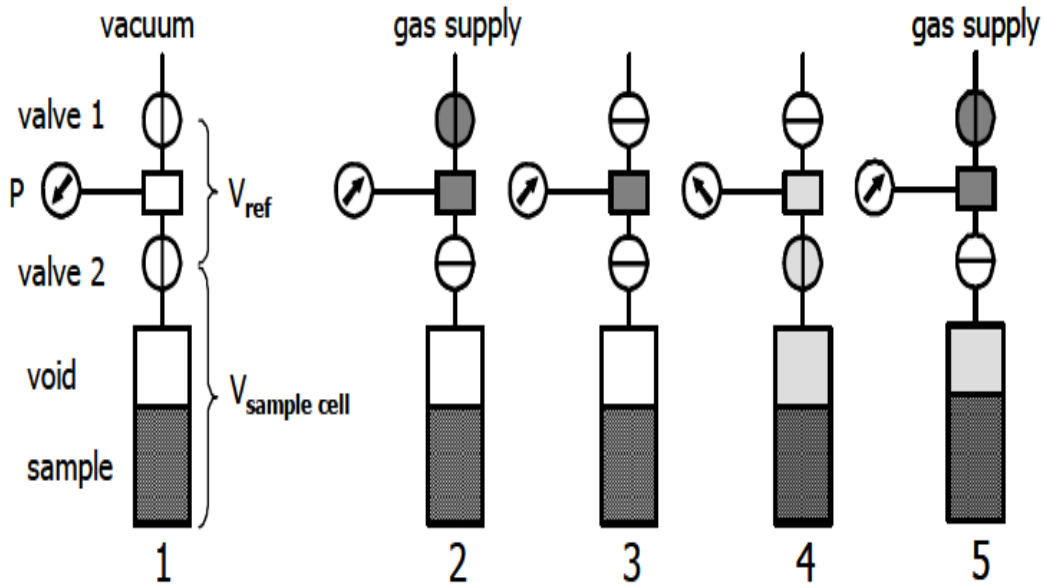
Figure 3. 1: Schematic flow diagram of volumetric system [66]

3.7. Biogasification Experiments

For the biogasification experiments, methanobacterium formicicum was brought DSMZ as an active culture. And "ATCC medium: 1045 methanobacteria medium" was used. This medium was chosen due its Lewis base potential.

3.7.1. Media Preparation

Following solutions were prepared.

Mineral Solution 1:

K_2HPO_4 ....6.0 g

Distilled water..1.0 L

Mineral Solution 2:

KH$_2$PO$_4$ ....6.0 g

(NH$_4$)$_2$SO$_4$...6.0 g

NaCl...12.0 g

MgSO$_4$.7H$_2$O ....2.4 g

CaCl$_2$.2H$_2$O ....1.6 g

Distilled water...1.0 L

Sodium Carbonate Solution:

Na$_2$CO$_3$ ....8.0 g

Distilled water...100.0 ml

And Wolfe's mineral and vitamin solutions were purchased from ATCC as a ready to use solutions. Their composition is given below.

Wolfe's Mineral Solution:

Nitrilotriacetic acid...1.5 g

MgSO$_4$.7H$_2$O ....3.0 g

MnSO$_4$.H$_2$O ....0.5 g

NaCl...1.0 g

FeSO$_4$.7H$_2$O..0.1 g

CoCl$_2$.6H$_2$O ....0.1 g

CaCl$_2$ ....0.1 g

ZnSO$_4$.7H$_2$O ....0.1 g

CuSO$_4$.5H$_2$O ....0.01 g

AlK(SO$_4$)$_2$.12H$_2$O...0.01 g

H$_3$BO$_3$ ....0.01 g

Na$_2$MoO$_4$.2H$_2$O...0.01 g

Distilled water...1.0 L

Wolfe's Vitamin Solution:

Biotin..2.0 mg

Folic acid..2.0 mg

Pyridoxine hydrochloride..10.0 mg

Thiamine . HCl...5.0 mg

Riboflavin...5.0 mg

Nicotinic acid...5.0 mg

Calcium D-(+)-pantothenate...5.0 mg

Vitamin B12..0.1 mg

p-Aminobenzoic acid...5.0 mg

Thioctic acid..5.0 mg

Distilled water...1.0 L

Reducing Agent: Reducing agent is used for the most anaerobic media to reduce redox potential at optimum level. In this study, L-Cycteine.HCl and Na$_2$S.9H$_2$O were used as a reducing agent.

For 20 ml solution, 300 mg L-Cystein.HCl was added to 10 ml water and 300 mg Na$_2$S.9H$_2$O to 10 ml water separately in a serum bottles and flow with nitrogen at least 30 minutes by using sterile 15 cm needles and sealed with butyl rubber stopper and aluminum crimp under nitrogen gas. Then two solutions were autoclaved at 121°C for 15 minutes and allow cooling. After that, equal amount of L-Cystein.HCl and Na$_2$S.9H$_2$O were mixed in glovebox under argon gas. Final solution was clear and used just for two weeks. Once in every two weeks fresh reducing agent was prepared.

Resazurin (Oxygen Indicator, Redox Sensitive Dye): To control anaerobic condition of the media, redox potential of the media must be observed. For this reason redox

sensitive dye resazurine was used since it is non-toxic to bacteria and very effective at low concentrations. Resazurine is originally dark blue color (inactive form) and it must be reduced to be activated. Therefore in first step, resuzurin reduced to resorufin which has a pink color, which is an irreversible step, by boiling mineral media which contains resazurin under oxygen free gas. After the first step, reversible second step occurs and hydroresorufin formed which is colorless, which indicates that oxygen free media is produced. Resorufin/hydroresorufin redox couple turns into colorless below a redox potential of about -110mV and regains a pink color at a redox potential above -51mV.
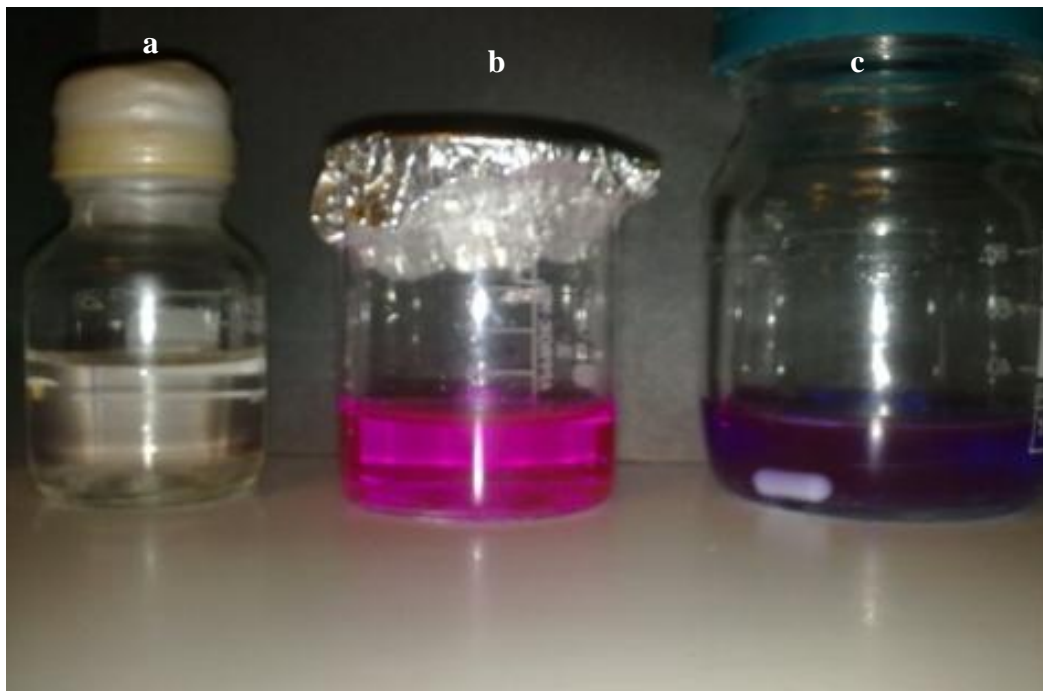
Figure 3. 2: a) Hyrdroresorufin (completely oxygen free media) **b)** resorufin reduced form (activated) **c)** Inactive resazurin

3.7.2. Anaerobic Incubation in Serum Bottle Experiments

For biogasification experiments, firstly mehanobacterium formicicum was grown on the 20 ml medium in 100ml serum bottles. Briefly, 20 ml medium contained;

16.62 ml double distilled water, 1.0 ml Mineral solution 2, 0.5 ml Mineral solution 1, 1.0 ml 8.0% Na_2CO_3 solution, 0.2 ml Wolfe's Mineral solution 0.2 ml Wolfe's Vitamin soltion, 0.4 ml Reducing agent, 0.08 ml Resazurin (from 0.025% resazurin solution).

First of all water and mineral solution 1, mineral solution 2, Na_2CO_3 solution and Wolfe's mineral solution were mixed. Then resazurin was added to the solution and pH

was adjusted to 7.2 by using 1 M NaOH and HCl. Then, serum bottles were boiled under high purity nitrogen which is passed through the cotton packed syringe barrel with sterile needles, during boiling, loss water was compensated with additional water whose pH was adjusted to 7.2 before. When the solution is reduced, pink color forms. However, when high purity nitrogen is passed, colorless solution is not formed due to the high amount of oxygen.

Figure 3. 3: Medium prepared by using nitrogen.

For this reason, high purity carbon dioxide which has oxygen content below 5 ppm was used as an oxygen free gas due to the higher density than air and good solubility in water. When CO_2 was used, medium became colorless after prolonged times. Therefore, while gassing of the medium, adding 0.2 ml reducing agent shortens the time, and medium turns into colorless in around 2 hours. When the media was completely reduced (free of oxygen), needles were removed and septum sealed with aluminum crimp by using crimper.
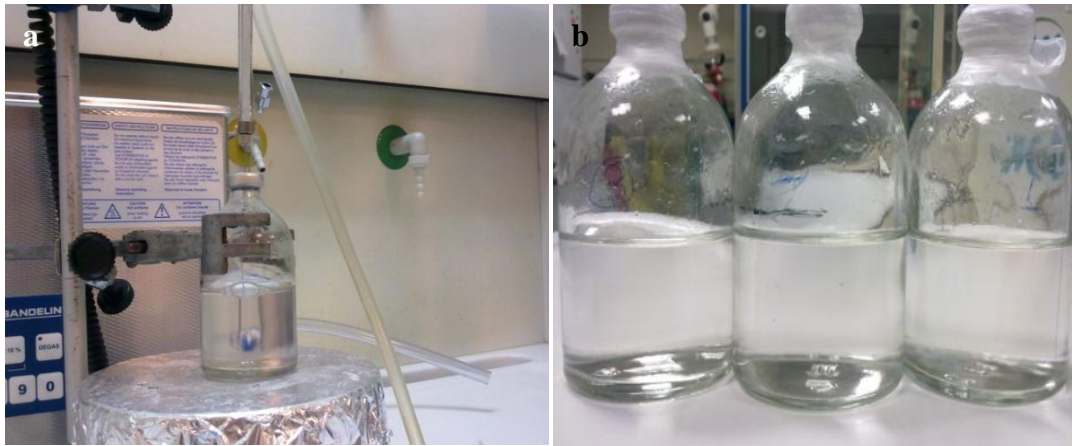
Figure 3. 4: : a) Gassing of the media **b)** Reduced media inside the serum bottles.

Then, reduced medium was autoclaved at $121^{o}C$ for 15 minutes and cooled under argon atmosphere in glovebox. Glovebox was sterilized by using UV lamb for 1 hour before every usage. Then, 0.2 ml Wolfe's vitamin solution and 0.2 ml reducing agent was added to the medium by using sterile syringes. Finally, 20 ml medium were inoculated with 0.5 ml active methanobacterium formicicicum culture inside the glovebox. After that, media was removed from the glovebox and 80% H_2 and 20% CO_2 gas mixed was passed through the media for 5 minutes with sterile needles and cotton filled syringe barrels. Bottles placed in a shaker at $37^{o}C$ and agitated at 150 rpm for 3 days. After 3 days of incubation 5 ml culture medium was transferred to the 60 ml pre-reduced media and 80% H_2 and 20% CO_2 gas mix was passed through the media again. Some of the samples turn to pink color during incubation and they were terminated. Only successful incubations were used. The microorganism incubation procedure is summarized in Figure 3.6.

Figure 3. 5: Successful incubation (colorless), failed incubation (purple)

```
┌─────────────────────────────────────────┐
│ 16.62 ml DDI water                       │
│ 1.0 ml Mineral solution 2                │
│ 0.5 ml Mineral solution 1                │
│ 1.0 ml  8.0% Na₂CO₃ solution             │
│  0,2 ml Wolfe's Mineral solution         │
│ 0,08 ml resazurin                        │
│ was mixed in a serum bottles             │
└─────────────────────────────────────────┘
```

$$1.0 \text{ ml } 8.0\% \ Na_2CO_3 \text{ solution}$$

⇩

pH was adjusted to 7.2 by using 1 M HCl and 1 M NaOH

⇩

Oxygen free gas was passed through the cotton filled syringe barrel to the media while boiling by using sterile needles

⇩

0.2 ml Reducing agent was added

⇩

When the solution became colorless, bottles were sealed with alimunium crimp

⇩

Autoclaved at 121°C for 15 minutes

⇩

Cooled under oxygen free gas inside the glovebox

⇩

0.2 ml Wolfe's vitamin solution and 0.2 ml reducing agent were added with sterile syringes

⇩

0.5 ml active culture added with sterile syringe inside the glove box

⇩

Media was removed from the glovebox and 80% H₂ and 20% CO₂ gas mixed was passes through the media for 5 minutes with sterile needles and cotton filled syringe barrels

⇩

Bottles placed in a shaker at 37°C and agitated at 150 rpm for 3 days

⇩

After 3 days of incubation, 5ml culture medium were transferred to the 60 ml pre-reduced media
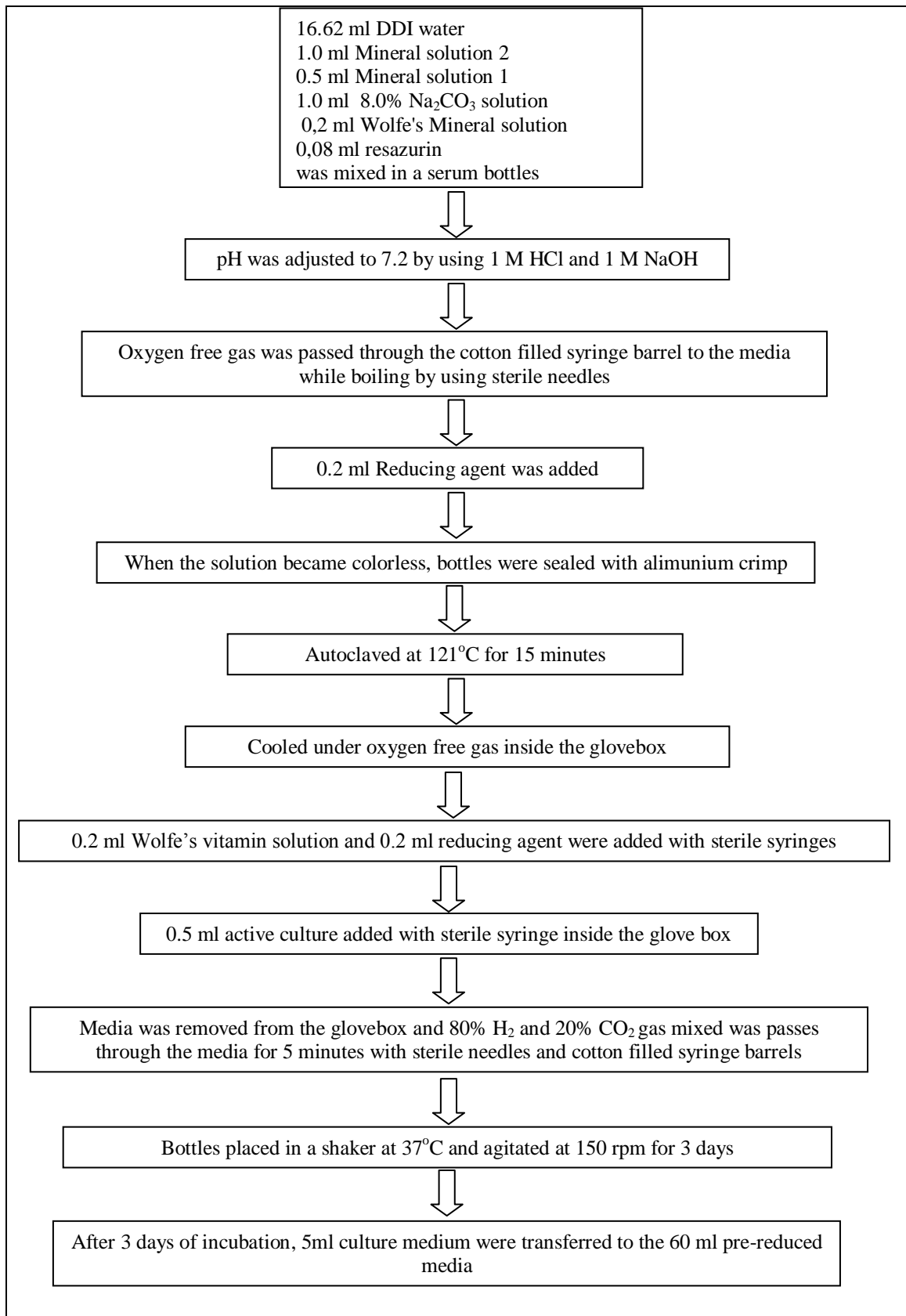
Figure 3. 6: Microorganism incubation procedure.

3.7.2.1. Anaerobic Incubation with coal in Serum Bottles

2 g Soma lignite (particle size less than 150 µm) was added to 20 ml medium reduced with high purity argon (oxygen level below 3 ppm) while gas was passing through the medium. Prior to inoculation, the sealed, pressurized bottles were sterilized in an autoclave at 121°C for 15 minutes and cooled inside the glovebox. Then, 0.2 ml Wolfe's vitamin solution and 0.2 ml reducing agent was added to the medium by using sterile syringes. Afterwards, 5 ml of 60 ml methanobacterium formicicicum active culture which has been grown for three days was added on top of them with sterile syringe inside the glovebox. Final bottles were pressurized different gases and placed the incubator at 37°C and 150 rpm.

Four types of incubation were prepared:

1st Set: 2 g Coal in 20 ml medium + 5ml microorganism + 80% H_2 and 20% CO_2 were passed through the media for 5 minutes

2nd Set: 2 g Coal in 20 ml medium + 5 ml microorganism + 100% H_2 was passed through the media for 5 minutes

3rd Set: 2 g Coal in 20 ml medium + 5ml microorganism + 100% Argone was passed through the media for 5 minutes

4th Set: 2 g Coal in 20 ml medium without Na_2CO_3 solution + 5 ml microorganism + 100% Argon was passed through the media for 5 minutes

3.7.3. Anaerobic Incubation in Bioreactor

For the bioreactor experiment, Sartorious-Stedim Biostat A-plus autoclaveable bioreactor with 1 liter working volume was used. Before the experiment, pH and oxygen probes were calibrated. Oxygen probe was calibrated by using high purity nitrogen for zero oxygen and dry air for 100% of oxygen value. Reactor was designed to working with air, oxygen, nitrogen and carbon dioxide but not hydrogen. Therefore all sealing screws were reversed and 2 o-rings were used for every screw to seal the reactor against any hydrogen leakage.

1 liter anaerobic medium was prepared, for the first irreversible reduction step of resazurin, media must be boiled. However, reactor is not designed for the high

temperature processes due to the heating jacket. Therefore, 1Liter medium was boiled on the heater. When resazurin was reduced to resorufin, media was placed the bioreactor and gassed with high purity carbon dioxide shown in Figure 3.7.a. Although, oxygen probe indicated the 0% oxygen value, medium did not turn into colorless. This result indicates that, the zero set of oxygen probe is not sufficient for the process. Therefore, it has been decided to take the electric current value reading from the probe as a reference instead of the zero set of the probe. When the solution became colorless, electric current reading from the probe was 1.8 nA shown in Figure 3.7.b. After that, 75g Soma lignite whose particle size is below 150 µm was added into the solution and the bioreactor was sealed. Carbon dioxide flow was stopped. During this procedure pH was kept at 7.2 by the pH controller. Before autoclaving, pH controller was removed from the system in order to avoid any oxygen from the 1 M HCl and NaOH solutions. Following that, bioreactor was autoclaved at 121°C for 15 minutes and cooled under CO_2 flow. After addition of coal inside the medium, there was no color control for oxygen, therefore, electric current value was followed for the oxygen level in the medium. When the current value reading was 1.8 nA, 30 ml of 60 ml methanobacterium formicicicum active culture which has been grown for three days was added by using sterile syringe and gas flow were changed to 80% H_2 and 20% CO_2. Gas flow was continued about 15 minutes then gas flow was stopped and sealed. Then bioreactor was adjusted at 37°C and 150 rpm shown in Figure 3.7.c.
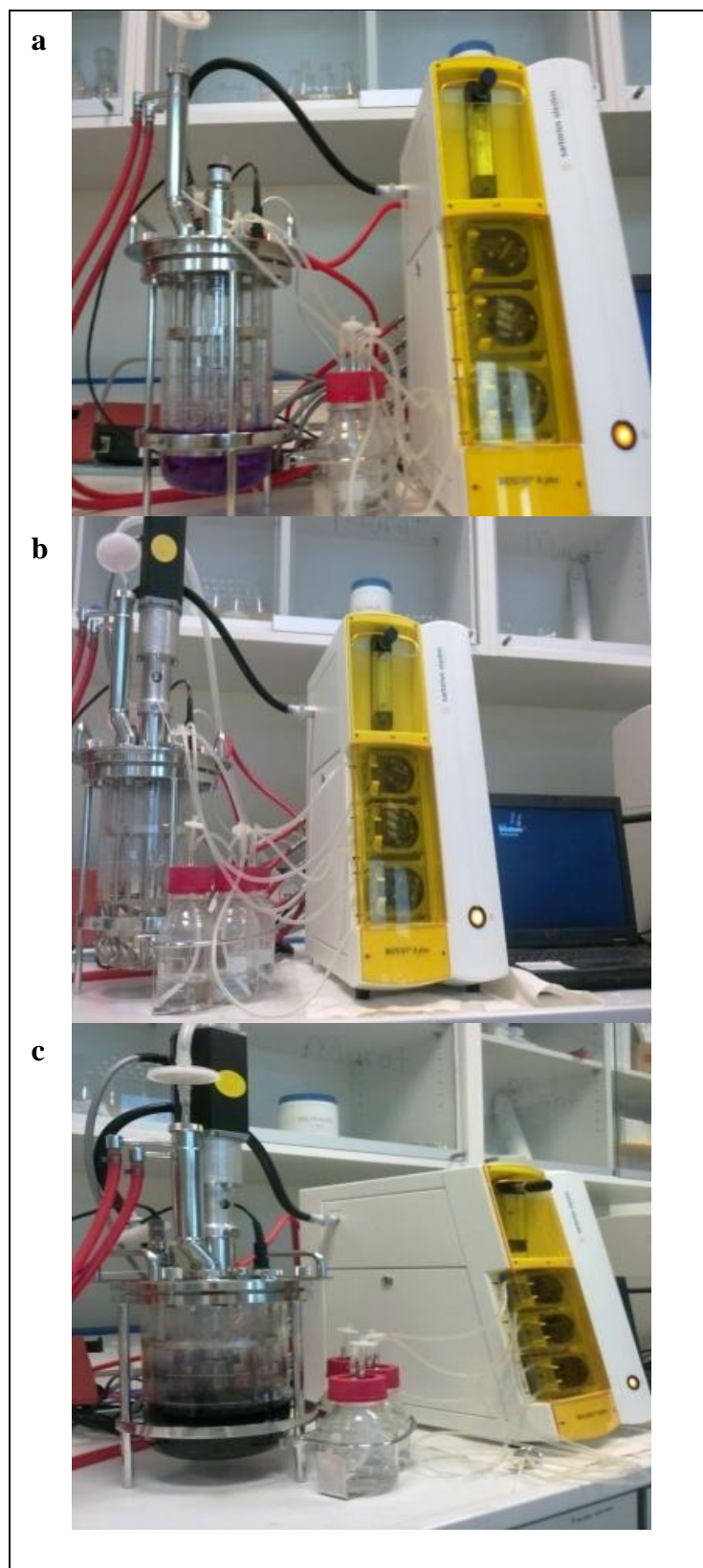
Figure 3. 7: Media in bioreactor. **a**) Reduced media, **b**) Completely colorless oxygen free media **c**) Coal-medium slurry.

In this experiment, methane generation was not determined. Only small amount of sample was removed after 10 days of incubation and investigated under optical microscope.

3.7.4. Methane Determination

Culture tube headspace samples were drawn using aseptic, anaerobic technique with a 50 μL gas syringe (SGE, 100 μL Gas sealing gland (GSG) syringe) equipped with removable 25 gauge needle. Methane analysis was performed using a Shimadzu GCMS-QP2010 Plus gas chromatograph-mass spectrometer, equipped with a Restek RT-Q-Band 30×0.32 mm fused silica capillary column. The injection port was maintained at 180 °C, the oven temperature was kept at 35 °C for 2 minutes and started to increase up to $250^{o}C$ with the rate $20^{o}C/min$, ion source was at $230^{o}C$ and the detector was operated at 250°C. The retention time for methane was 1.5 min. Calibration standards consisting of 4% or 10% methane compensated with helium (from Linde Gas) were injected at atmospheric pressure to generate the calibration plot. For calibration and real measurements same method file was used and methane was determined on a daily basis.

For calibration sampling, 50 ml bulb Erlenmeyer flask with stopcock control outlet which is closed by butyl rubber stopper, connected with the Sigma-Aldrich freeze and thaw glass equipment was used. Freeze and thaw glass equipment has two outlets, one of the outlets was sealed with butyl rubber stopper and the other one was connected the vacuum pump system and operated at least 15 minutes. Then shut off valve was closed and vacuum was closed. After that, sealed outlet was opened and calibration gas was connected to the system and opened at 1 atm pressure adjusted by a regulator. Gas started to flow from one outlet to the other about 5 minutes to clear the air from the free space. While gas was flowing, shut off valve was opened and gas filled the vacuumed Erlenmeyer flask and valve was closed again and 50 μL of sample was removed from the system. Diagram of the gas sampling system was described at Figure 3.8.
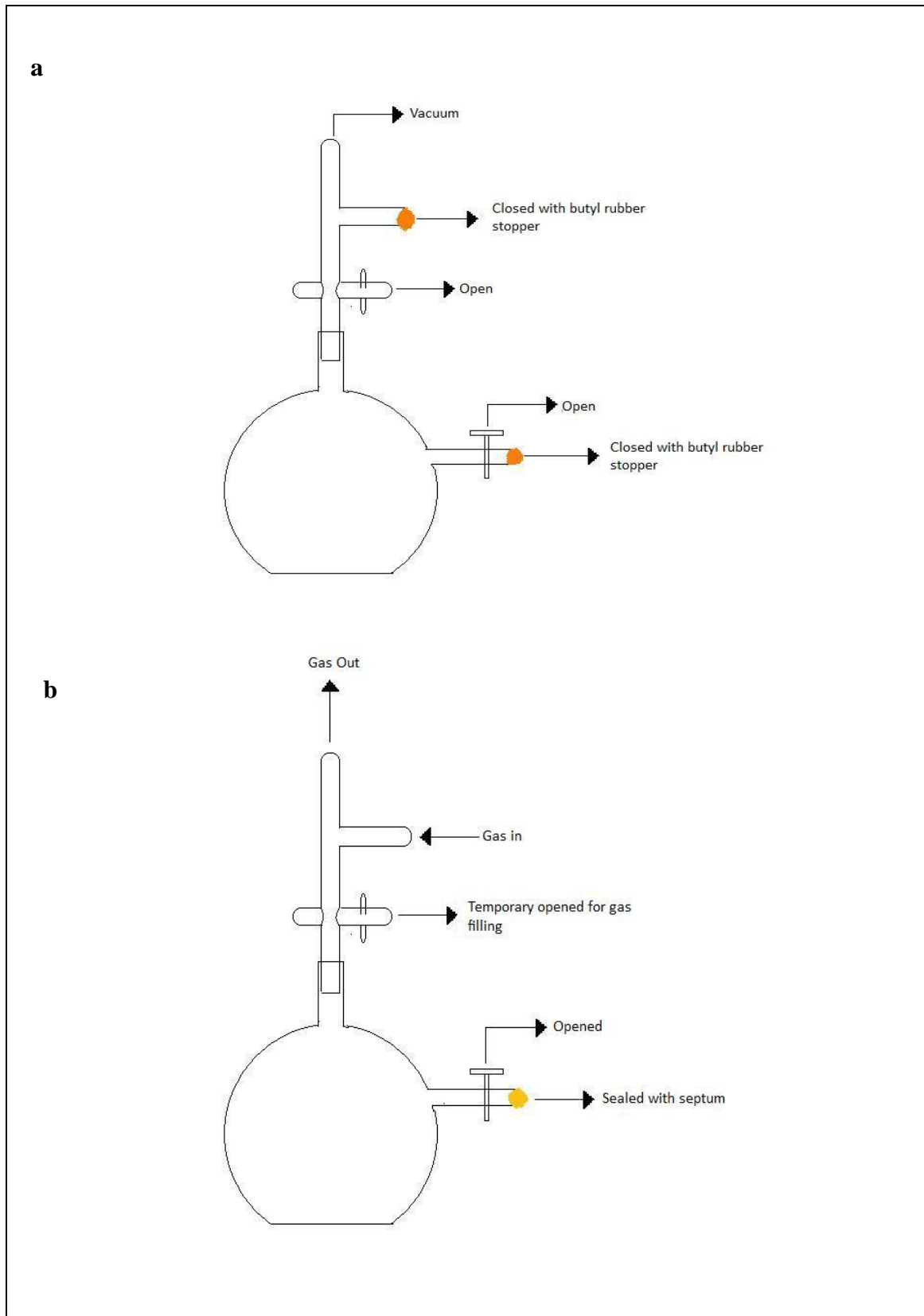
Figure 3. 8: Sampling of the calibration gas **a)** Vacuum process **b)** Gas filling process

CHAPTER 4

4. Results and Discussion

4.1. Coal Characterization

In this Chapter, ultimate and proximate analyses, rock eval pyrolysis, maceral reflectance results and FTIR analysis of the Soma lignite were discussed

4.1.1. Ultimate and Proximate Analyses of Soma Lignite

Ultimate and proximate analyses of the samples were done at TÜBİTAK Marmara Research Center (MRS) Energy Institute. Elemental analyses of the samples were conducted according to the ASTM D 5373 standard and proximate analysis is ASTM D 4239 and D 5142.

Elemental analysis results of the samples were shown in Table 4.1. For six Soma lignite samples, standard %C, %S, %N, %H and %O values change from 59.45-68.5%, 0.8-2.18%, 0.58-2.68%, 4.8-6.23% and 9.99-14.71% respectively. For two Zonguldak samples, values vary from 65.16-85.61%, 0.38-0.52%, 1.69-1.84%, 4.41-5.13% and 1.15-21.57% respectively. Oxygen ratios of the samples were found by using this formula %O = 100 - (ash + moisture + C + H + N + S).

Table 4. 1: Ultimate analysis of the samples

Sample	Original sample							Dry sample				
	C%	H %	N %	S %	O%	H/C	O/C	C%	H %	N %	S %	O%
JK - 1122	67.91	5.85	0.58	2.18	10.59	1.03	0.12	74.94	5.29	0.64	2.41	12.82
JK - 1126	66.75	4.8	1.48	1.01	12.82	0.86	0.14	72.07	4.29	1.6	1.09	14.71
JK - 1135	59.45	5.79	1.89	1.23	11.15	1.17	0.14	63.62	5.41	2.02	1.32	12.69
JK – 1137	65.56	6.23	0.93	1.88	9.26	1.14	0.11	70.53	5.86	1	2.03	10.79
JK - 1389	68.5	5.36	1.15	0.8	10.18	0.94	0.11	76.58	4.67	1.29	0.9	12.69
JK - 1408	68.15	5.74	2.68	0.86	7.33	1.01	0.08	77.98	4.96	3.07	0.98	9.99
JK- 1414	85.61	4.41	1.69	0.38	1.02	0.62	0.01	86.62	4.33	1.71	0.39	1.15
JK- 1415	65.16	5.13	1.84	0.52	21.57	0.94	0.25	86.30	5.05	1.86	0.53	1.75

By using standard elemental analysis values, H/C and O/C ratios of the samples were found and placed into the van Krevelen Diagram which is the statistical diagram that shows origin and maturity of the kerogen in fossil fuel according to the H/C vs O/C values. Figure 4.1 shows that all samples were around type-3 kerogen region, which belongs to the humic and woody kerogens with low H/C and high O/C ratio. This type of kerogen contains high ratio vitrinite or huminite in its structure.
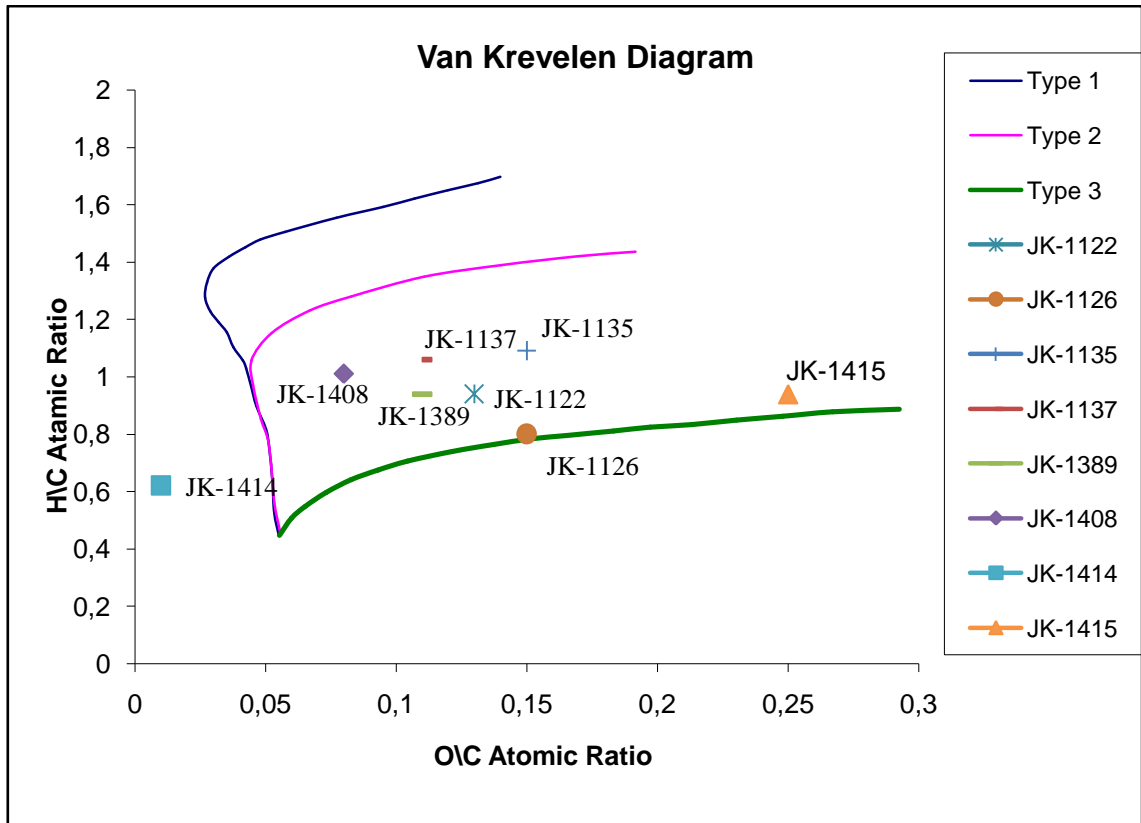
Figure 4. 1: van Krevelen diagram of the samples

Proximate analyses of the standard and dry ash free samples are shown in Table 4.2. Fixed carbon, moisture, ash and volatile matter percentage of the 6 Soma samples vary from 41.56-53.23%, 6.56-12.60%, 33.88-42.30% and 2.64-13.93% respectively. For Zonguldak samples original fixed carbon, moisture, ash and volatile matter percentages change from 61.29-70.21%, 1.16-1.32%, 22.90-32.93% and 4.46-5.73%, respectively. According to the results, Zonguldak samples have higher fixed carbon ratio and lower moisture percentage compared to the Soma Samples which are classified as lignite [67] due to their higher rank.

Table 4. 2: Proximate analysis of the samples.

Sample	Original sample				Dry sample		
	Moisture %	Volatile Matter %	Ash %	Fixed Carbon %	Volatile Matter %	Ash %	Fixed Carbon %
JK-1122	9.37	3.52	33.88	53.23	3.88	37.38	58.74
JK-1126	7.38	5.76	36.01	50.85	6.21	38.87	54.92
JK-1135	6.56	13.93	37.63	41.88	14.91	40.27	44.82
JK-1137	7.04	9.1	42.3	41.56	9.78	45.5	44.72
JK-1389	10.55	3.46	36.83	49.16	3.86	41.17	49.16
JK-1408	12.60	2.64	37.33	47.43	3.01	42.71	54.28
JK-1414	1.16	5.73	22.90	70.21	5.80	23.17	71.03
JK-1415	1.32	4.46	32.93	61.29	4.51	33.37	62.12

4.1.2. Rock-Eval Pyrolysis and Maceral Analysis

Rock Eval pyrolysis is used to identify the type and maturity of organic matter fuel. Program based on heat treatment of the sample in an inert atmosphere and detection of quantative mass loss. A unique property of the program is the selective determination of the free hydrocarbons contained in the sample and the hydrocarbons and oxygen containing compounds (CO_2) which are volatilized during the cracking of the unextractable organic matter in the sample (kerogen).

For specific determination of hydrocarbon, gradual increase in temperature is necessary. In the first step, temperature of the oven was kept for three minutes at $300^{o}C$ to volatilize free hydrocarbons which is called S_1 in the program and detected by flame ionization detector. In the second step, temperature is increased from $300^{o}C$ to $550^{o}C$ with heating rate $25^{o}C/min$. In this step, volatilization of heavy hydrocarbons ($>C_{40}$) and

cracking of the nonvolatile organic carbons occur which is called S_2 peak in the program. The hydrocarbons released from this thermal cracking are detected by FID. S_2 peak is the most important step to determine the maturity of the fuel because in this step maximum temperature, which is called T_{max}, depends on the nature and maturity of the products. In the last step, CO_2 from hydrocarbon cracking process is trapped and then heated. Released CO_2, which is called S_3, is detected by TCD. Total organic carbon (TOC) amount of the samples can also be found by this process. Organic matter remaining in the sample after pyrolysis is oxidized and detected. Finally, sum of the pyrolysis products and the oxidized organic matter gives TOC of the sample.

Hydrogen index (HI = (100 x S_2)/TOC) and oxygen index (OI = (100 x S_3)/TOC) are used for the determination of type and maturity of the sample. Rock Eval pyrolysis data of the samples are given Table 4.3. Soma samples have lower hydrogen content and higher oxygen content compared to the Zonguldak samples. TOC values of the Soma Lignite are much closed to the each other, changes from 61.3 to 68.31%, much higher than Zonguldak samples.

Table 4. 3: Rock-Eval pyrolysis of the samples

Sample	Depth (m)	S1	S2	S3	HI	OI	Tmax (^{o}C)	Organic Carbon %
JK-1122	793.50-793.70	0.24	79.77	4.6	118	7	396	67.55
JK-1126	826.65	0.49	61.19	18.77	90	27	412	68.31
JK-1135	725.90-726.20	1.29	103.38	15.14	169	25	408	61.3
JK-1137	736.70-736.90	3.97	161.24	9.42	241	14	393	66.37
JK-1389	1207.2-1208.7	0.48	103.3	15.1	158	23	406	65.43
JK-1408	772.0-773.0	0.68	130.37	10.7	200	16	407	65.29
JK-1414	Kozlu	0.86	105.84	2.43	212	5	456	49.82
JK-1415	Armutçuk	5.93	252.74	2.35	476	4	442	53.07

Modified van Krevelen Diagram gives the relation between hydrogen index and the T_{max} values of the samples. HI data gives the origin of the kerogen and T_{max} data gives maturity of the products. $T_{max} = 400°\text{-}430°C$ represents immature organic matter; $T_{max} = 435°\text{-}450°C$ represents mature or oil zone; $T_{max} > 450°C$ represents the over-mature zone. In Figure 4.2., HI vs T_{max} data are plotted. As it can be seen in Figure 4.2, Soma samples lie in the immature region and type III kerogen. These results are in good agreement with the elemental analysis results. However, Zonguldak Coals lie in the over-mature zone as expected.
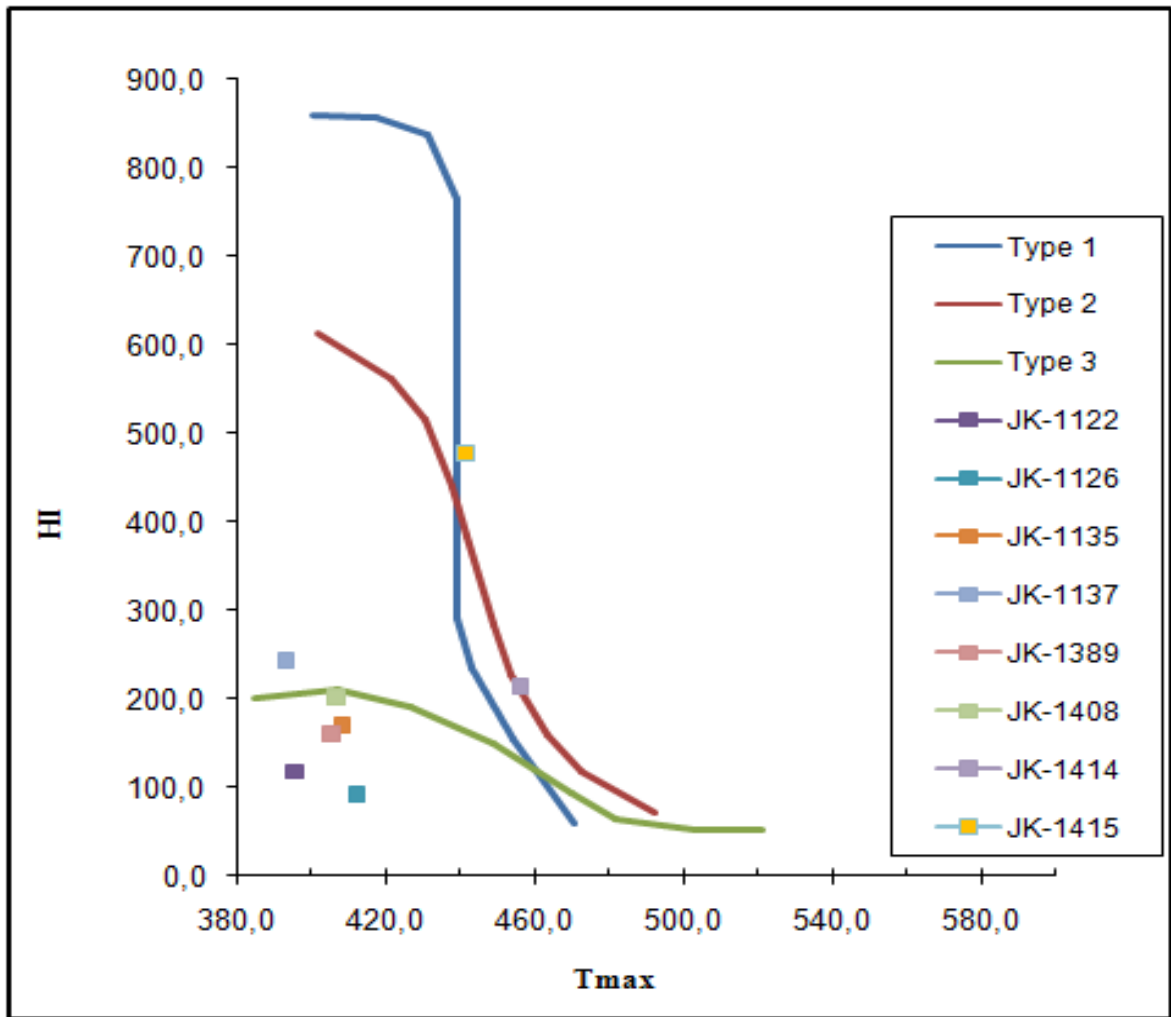
Figure 4. 2: Modified van Krevelen diagram. HI vs Tmax relation of the samples [68].

According to the maceral analysis results of four samples which are given in the table 4.4., huminite is the dominant maceral group in the Soma lignite. Studies show that vitrinite rich coals have higher microporosity [18, 69]. For this reason, high adsorption capacity of the Soma lignite is expected due to the maceral composition which allows the micropore formation.

Table 4. 4: Maceral analyses of the Soma Lignite

Sample No	Depth (m)	Huminite (%)	Liptinite (%)	Inertite (%)	Ro (%)
JK -1122	793.50-793.70	96	2	2	0.46
JK-1126	826.65	87	1	12	0.48
JK-1135	725.90-726.20	78	19	3	0.42
JK-1137	736.70-736.90	82	16	2	0.44

4.1.3. FT-IR Analysis

Figure 4.3 shows that FT-IR spectrum of the lignite samples which were evacuated from different depths of Soma basin. Most of the peaks are common for all samples. The broad band at 3400 cm^{-1} is due to the O-H and N-H groups. The peaks at 2900-2800 cm^{-1} represent C-H stretching vibration of aliphatic and alicyclic methyl, methylene and alkyl groups. The intensity of the peak at 2900 cm^{-1} is greater than intensity of the peak at 2800 cm^{-1}. This shows the presence of long aliphatic chains in the samples. Also, the peak at 1600 cm^{-1} and the shoulder at 1700 cm^{-1} indicate the high concentration of conjugated carbonyl structures and conjugated aromatic structures. Relatively strong band at 1400 cm^{-1} is due to the C-H bend in methyl, methylene or aromatic C-H bending. Usually, peaks between 1100 cm^{-1} - 400 cm^{-1} belong to inorganic mineral matter in the coal.
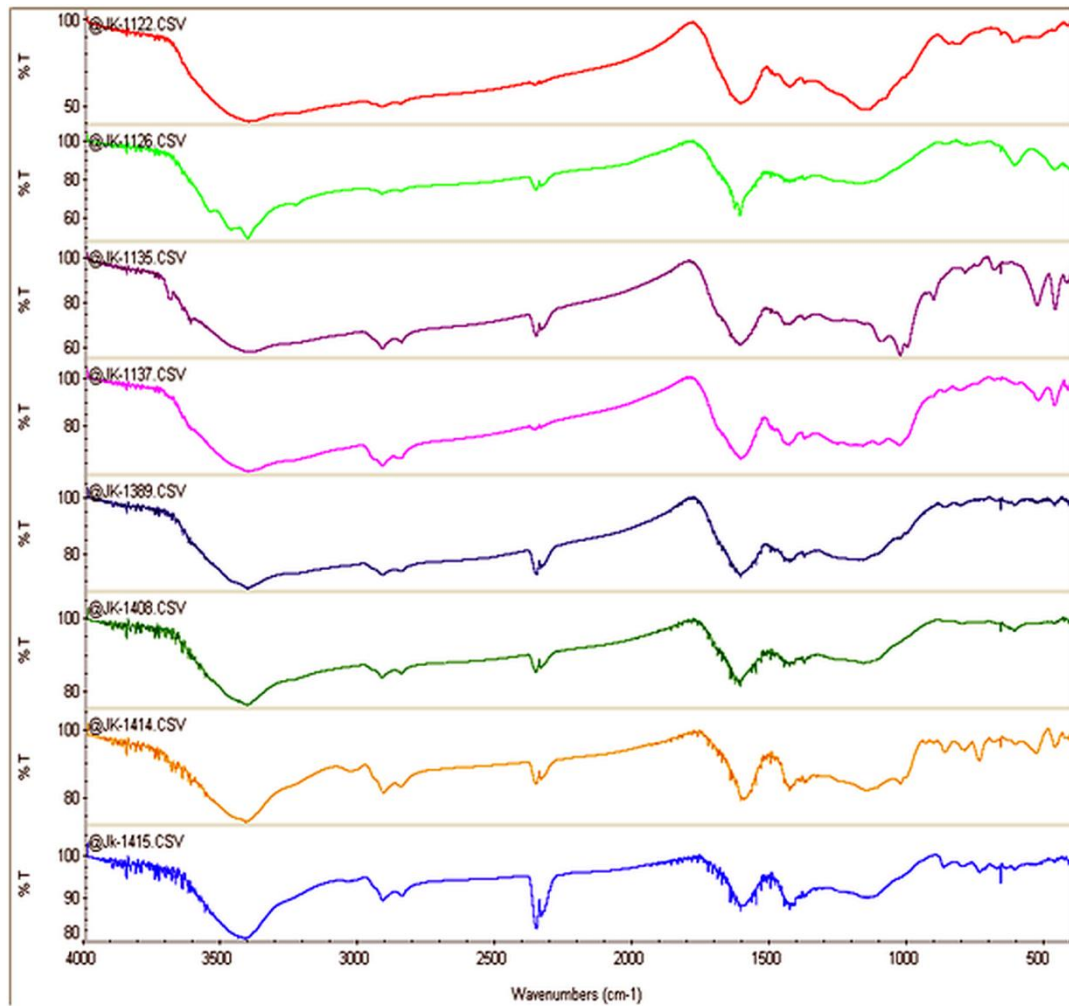
Figure 4. 3: FT-IR results of the samples

4.2. Gas Analysis

4.2.1. ^{13}C isotope Analyses

Origin of the desorp gas from Soma samples was found before making any assumption due to gas generation. For this reason, desorbed gas from the coal samples were collected and used for the determination of the carbon isotopic ratio of the gasses in TÜBİTAK Marmara Research Center (MRC) Earth and Marine Sciences Institute (EMSI). Results are shown in Figure 4.4. According to the results, majority of the collected samples are in biogenic region, represented as a green dot on the Figure 4.4., also one of the samples is in the mixed gas region but very close to the biogenic part, which is shown by red dot on the figure. These results confirm that origin of the CBM is the result of the bacterial activity [67].
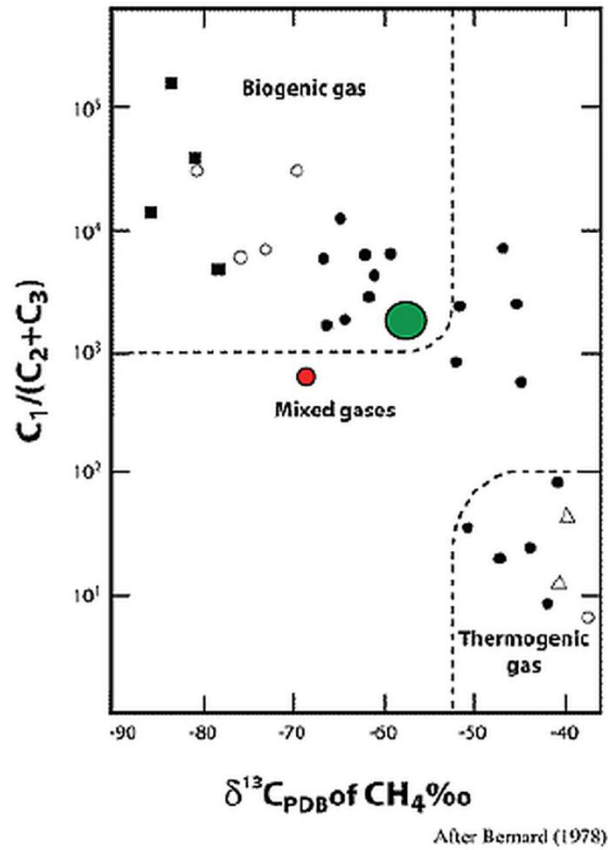
$$\delta^{13}C\text{\textperthousand} = \left[\frac{(^{13}C/^{12}C_{sample}) - (^{13}C/^{12}C_{std})}{(^{13}C/^{12}C_{std})} \right] \times 1000$$

With respect to PDB standard

Figure 4. 4: Differentiation of biogenic and thermogenic gas of Soma Lignite

4.2.2. Direct Method CBM Results

After determination of the origin of the gas in Soma Basin, desorbed gas amount was calculated by the direct method. Four borehole samples were immediately placed in the gas tight canister and gas desorption was measured in certain time periods [52]. Relation with the time and desorption amount was given in Figure 4.5. For all samples, lost gas amount, which is the desorbed gas during the extraction of the sample, is calculated by the extrapolation of the linear increase part of the graph to time zero.

According to the results, gas capacities of the Soma Lignites measured from direct method vary from 1.43 m^3/ton to 3.86 m^3/ton.
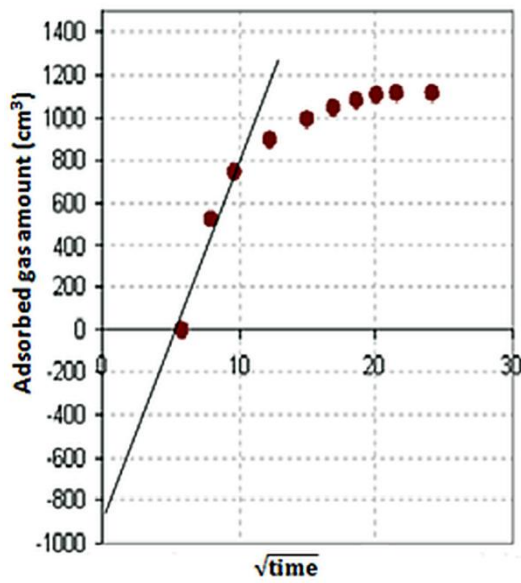
Depth (m)	1207.20 - 1208.70
Coal weight (g)	670
Measured gas amount (cm³)	1110
Lost gas amount (cm³)	900
Gas capacity (m³/tone)	3
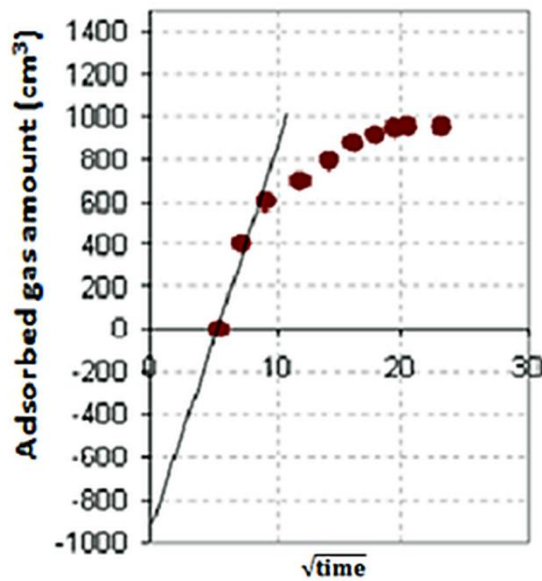
Depth (m)	1207.20 - 1208.70
Coal weight (g)	480
Measured gas amount (cm³)	955
Lost gas amount (cm³)	900
Gas capacity (m³/tone)	3.86

58

Depth (m)	1206.7 – 1207.10
Coal weight (g)	140
Measured gas amount (cm^3)	130
Lost gas amount	70
Gas Capacity (m^3/tone)	1.43

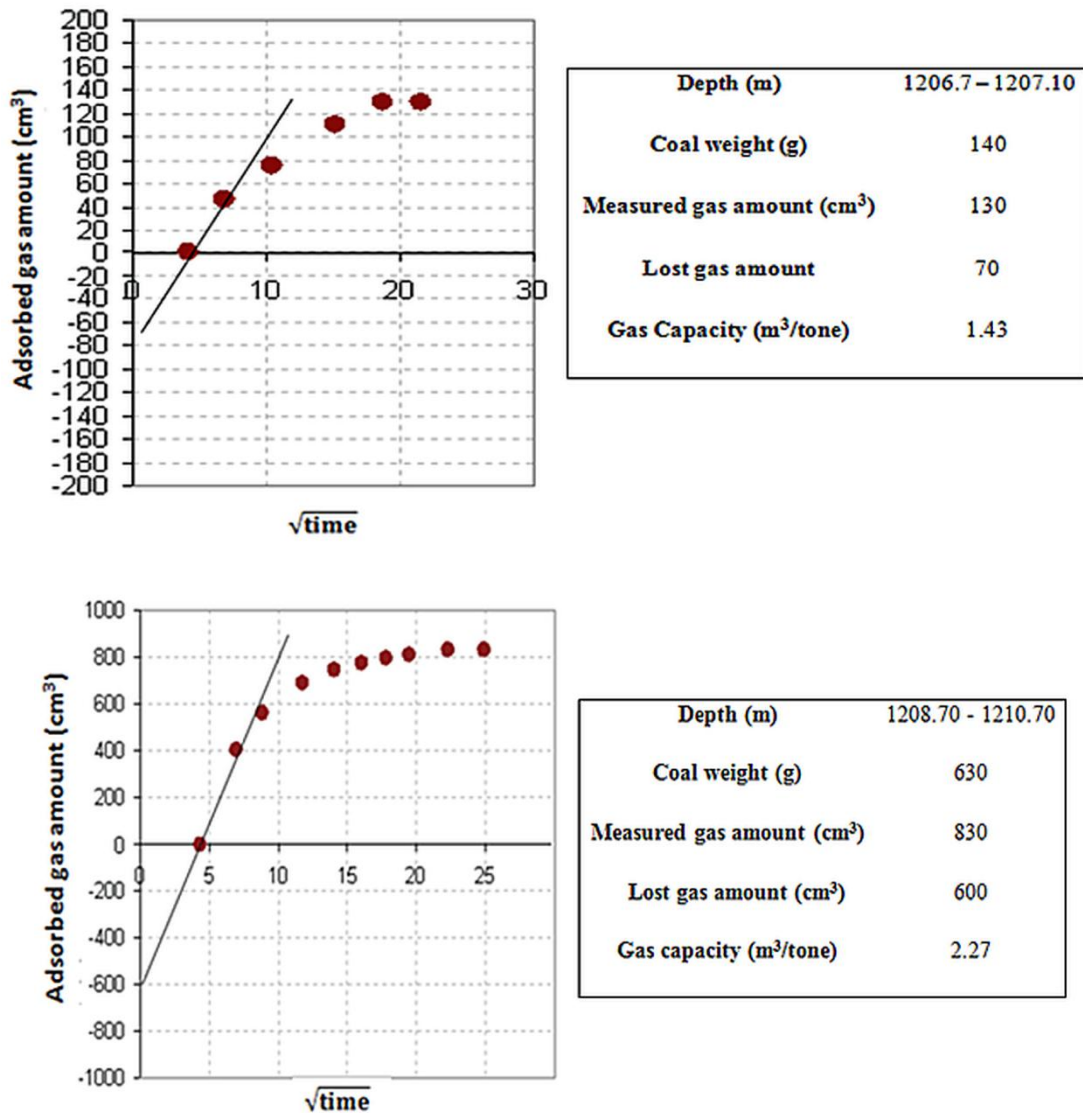| Depth (m)	1208.70 - 1210.70
Coal weight (g)	630
Measured gas amount (cm^3)	830
Lost gas amount (cm^3)	600
Gas capacity (m^3/tone)	2.27

Figure 4. 5: Direct method gas capacities of the samples

4.3. Low-Pressure Carbon Dioxide Adsorption Experiments

Coal is one of the materials with high micropore ratio. Since gas adsorption occurs in this microporous structure, gas capacity of the coal increases with increasing micropore ratio. Even though, there are also other factors that affect the gas adsorption capacity, such as moisture ratio, ash amount, etc., microporosity is the most significant effect on gas adsorption capacity. In that sense, for 6 Soma samples and 2 Zonguldak coals which were characterized before, porosity determination experiments were conducted by using low pressure CO_2 experiments.

59

Usually, surface area and the porosity of the materials can be calculated through the N_2 physical sorption experiments. In this method, entire relative pressure range (10^{-8} to 1) can be analyzed without using high pressure equipments [13]. However, for microporous materials like carbon materials and zeolites physical sorption occurs at very low relative pressure ranges (10^{-8} to 10^{-3}) and experiments that are conducted with N_2 are less reliable due to the low diffusion rate and adsorption equilibrium in the pores between 0.5 to 1 nm at 77 K. It is also known that specifically for carbon materials experiments that are conducted at low temperatures such as N_2 sorption causes pore shrinkage that leads to the low sorption equilibrium [14, 15].

Most important factors that affect physical interaction between adsorbent and the adsorbate are dynamic radius of the adsorbate, temperature and solubility parameters of the materials. In the literature, there are many examples where carbon dioxide gas was used for microporous materials instead of nitrogen [2]. Since, dynamic radius of the CO_2 is relatively smaller than that of N_2 (CO_2: 3.3 Å, N_2: 3.6 Å [4]), also solubility parameter of the CO_2 is far greater than nitrogen (for CO_2 δ=6.1 $cal^{0.5}cm^{-1.5}$, for N_2 δ=2.6 $cal^{0.5}cm^{-1.5}$). Owing to these superior properties, interaction between coal and the CO_2 is better than N_2-coal interaction [5, 6]. The last and the most important parameter is the temperature, for physical adsorption of the CO_2, measurement temperature of the isotherm can be 273 K or 298 K which means that we can avoid slow adsorption equilibrium, diffusion limitations at 77 K. Moreover, pore shrinkage of the coal at low temperatures can be overcome by using CO_2 for the micropore characterization of the coal. Therefore, CO_2 can reach narrow and wavy micropore structure of the adsorbates due to the high diffusion rate which is called activated diffusion [7, 8]. With all these advantages, coal micropore characterization has been determined by CO_2 since 1964 [9, 10].
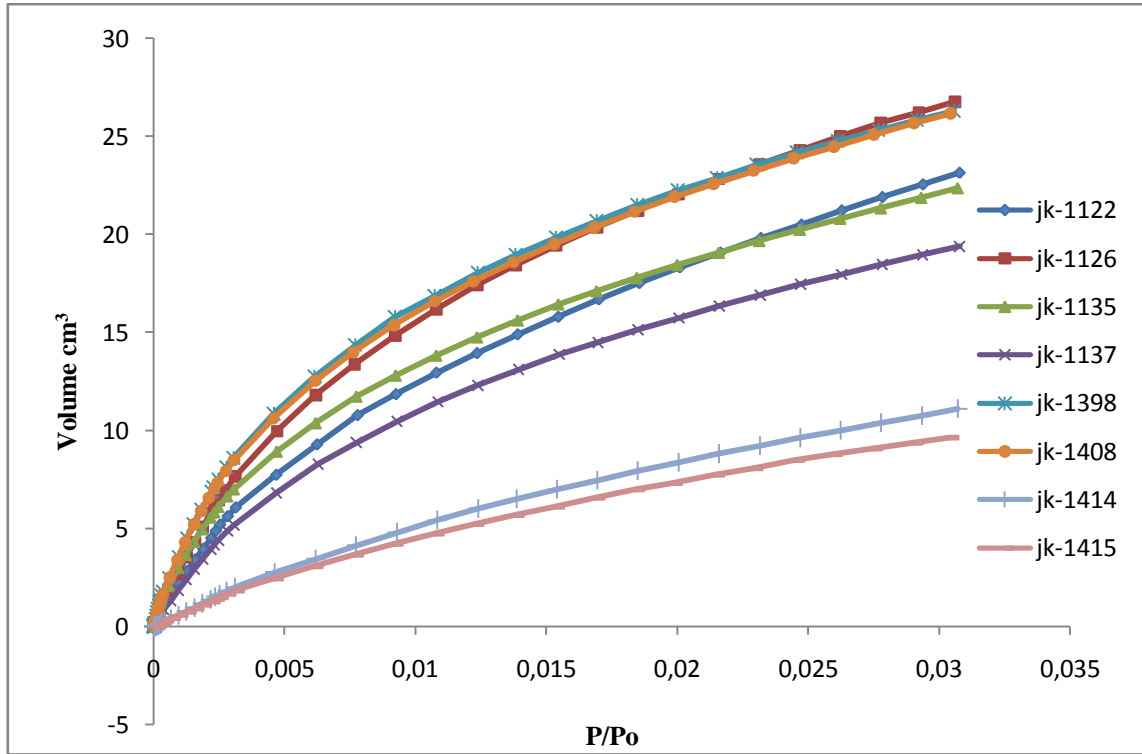
Figure 4. 6: CO_2 adsorption isotherms

Table 4. 5: CO_2 surface characterization results at 273 K

Sample	Organic carbon %	DR surface area (m^2/g)	DR micropore volume (cm^3/g)	DR micropore capacity (cm^3/g)	R^2 values
JK-1122	67.55	248.891	0.083	43.23	0.99861
JK-1126	68.31	274.73	0.092	47.92	0.99758
JK-1135	61.3	224.909	0.075	39.06	0.99955
JK-1137	66.87	232.653	0.078	40.63	0.99941
JK-1389	65.43	280.097	0.093	48.44	0.99977
JK-1408	65.29	278.041	0.092	47.92	0.99977
JK-1414 Kozlu	49.82	157.148	0.052	27.08	0.99803
JK-1415 Armutc uk	53.07	127.646	0.043	22.39	0.99700

For 6 Soma Lignites and Zonguldak samples, CO_2 isotherms can be seen in Figure 4.6. Low pressure isotherms by CO_2 as an adsorbent cannot characterize all relative pressure regions due the high condensation pressure of CO_2 at 0°C which is equal to the 26141 torr. However, microporous materials like coal, porosity characterization of the micropore region can be considered enough for entire porosity since contributions from

meso and macropores are very low. Moreover, 0.03 relative pressure is enough for the micropore filling processes.

Micropore surface areas and pore volumes of the samples were calculated by Dubinin-Radushkevich method. All Soma samples have high micropore surface areas and volume. According to the results in Table 4.5, Micropore surface areas and micropore volumes of the Soma samples change from 224.909 m^2/g to 287.097 m^2/g and 0.070 to 0.093 cm^3/g, respectively. CO_2 micropore capacities of the samples were calculated by a density conversion factor which is equal to the 0.00192 [70]. Calculated capacities of Soma Lignites are vary from 39.06 m^3/ton to 48.44m^3/ton. Zonguldak samples are much lower micropore surface areas than Soma samples. This result proves that gas adsorption capacity is not strongly related to the coal rank at a certain level. Gürdal et al. [70] show that micropore surface area of the coal decreasing with increasing maturity until R_o reach 1.0-1.1 values. After that value, micropore surface area start increased with increasing maturity due to bitumen generation in the structure during coalification which blocks accessible pores. However after certain maturity bitumen is degraded to the gas and pore became accessible again.

JK-1389, JK-1408 and JK-1126 have the biggest capacity of the all samples. They have also highest organic ratio compare to the other samples. Organic carbon structure in the coal is the certain region which allows adsorbent molecule to find high interaction surface due to the physical van der Waals forces between CO_2 molecules and Carbon structure. Organic carbon ratio of the Soma samples very closed to the each other (table 4.5), it is hard to get good correlation. For this reason Zonguldak samples which have low organic carbon ratios were also used. In Figure 4.7, D-R micropore surface areas of the samples are correlated with organic ratios. As it can be seen in the Figure 4.7, microporosity of the samples is increasing with increasing organic carbon ratios.
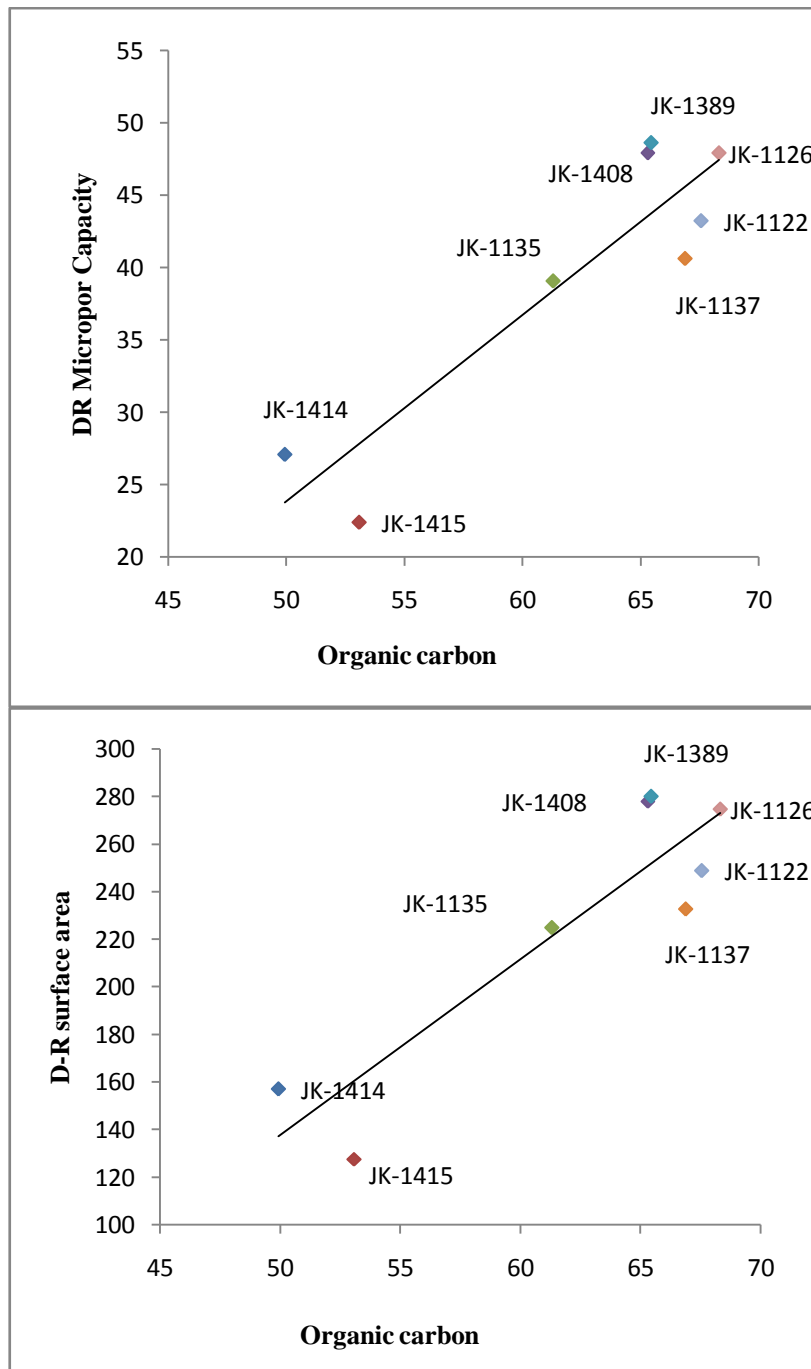
Figure 4. 7: Relation with the organic carbon ratio and surface area

In Figure 4.8, pore size distribution of the six Soma samples can be seen. The graph has been plotted the pores under 15 Å according to the Non Local Density Functional Theory with device software. Pore distribution became intensified 5.5 Å and 8.5 Å for all samples. Results were concluded that Soma lignite did not contain pores bigger than 10 Å and different pore formation have not been observed.
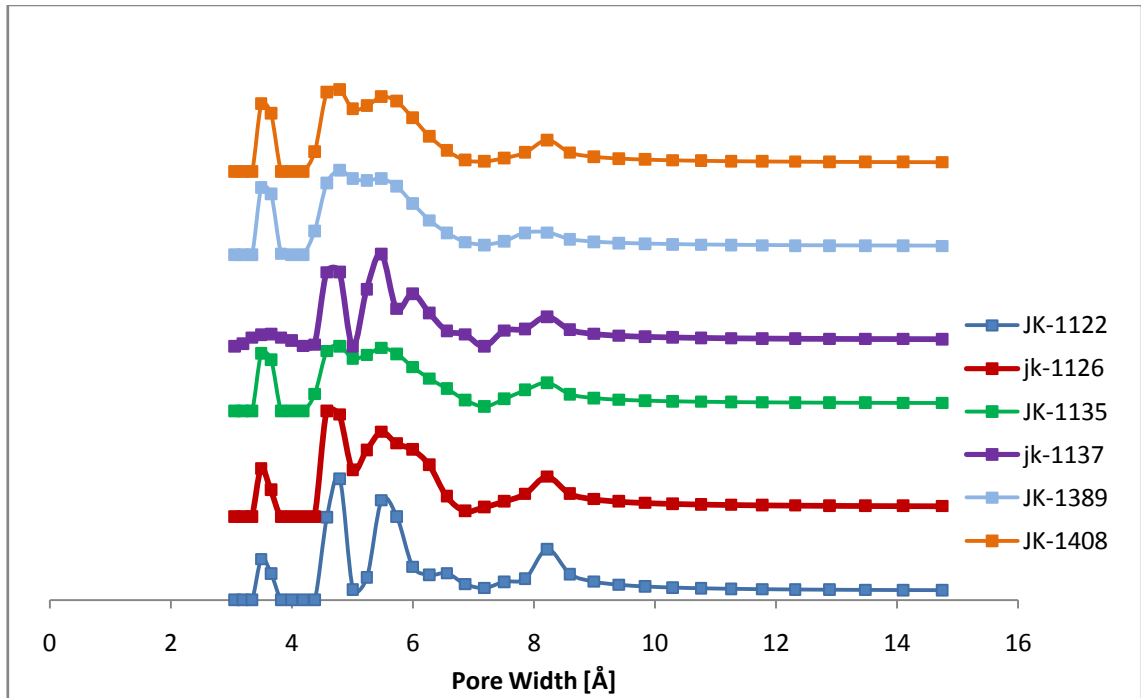
Figure 4. 8: Pore size distribution of the samples

4.4. High Pressure N₂ and Methane Adsorption Experiments

4.4.1. Intelligent Gravimetric Adsorption (IGA) Experiments

To understand gas adsorption behavior of Soma lignite and observe the effects of the gas adsorption capacity, gravimetric gas adsorption experiments were conducted by Intelligent Gravimetric Analyzer (IGA-003) up to 1 MPa.

As explained in Section 3.3., IGA has completely automatic microbalance system which allowed to measure mass uptake in time according to the pressure and temperature change. High precision measurements could be attained by gravimetric method with long term stability 0.1μg and very low temperature deviation around 0.1°C. The software of the device used two mass transfer methods (Linear Driving Force and Avrami Model) for the get asymptotic uptake for one isotherm point. In Figures 4.9 and 4.10, IGA system and process schematics can be seen. IGA working principles were explained in previous sections.
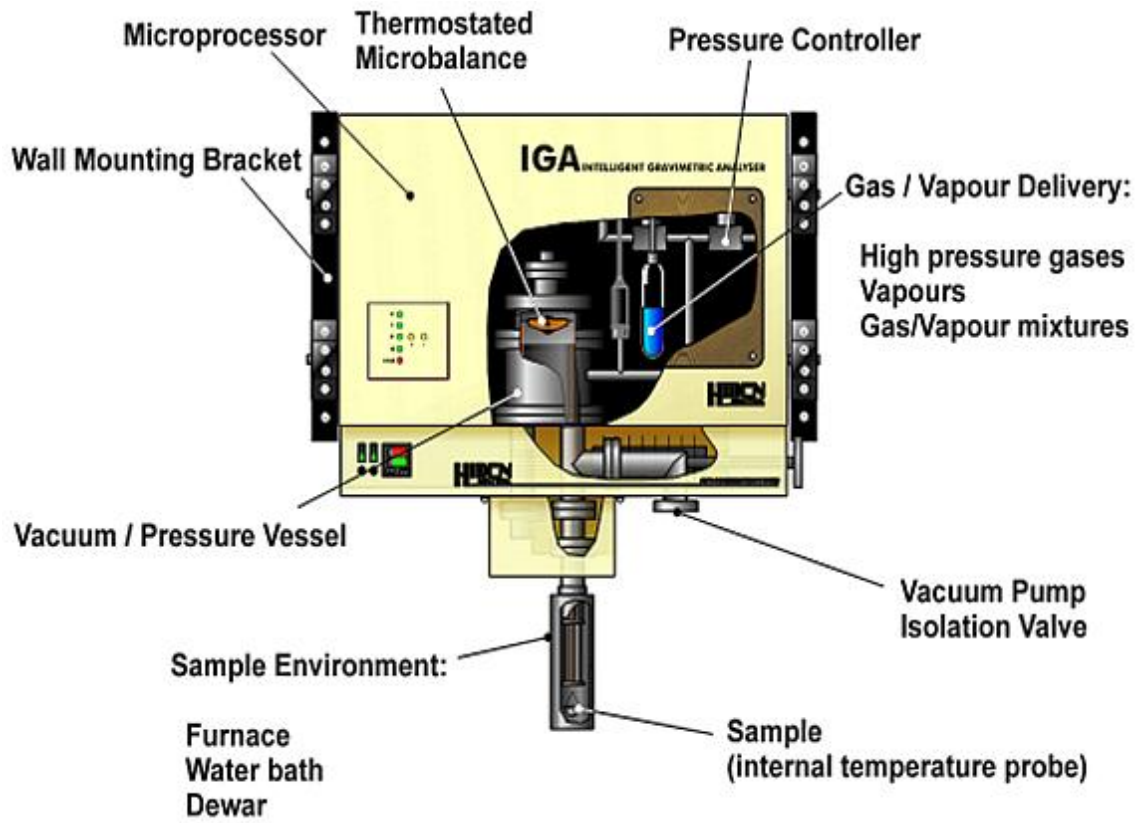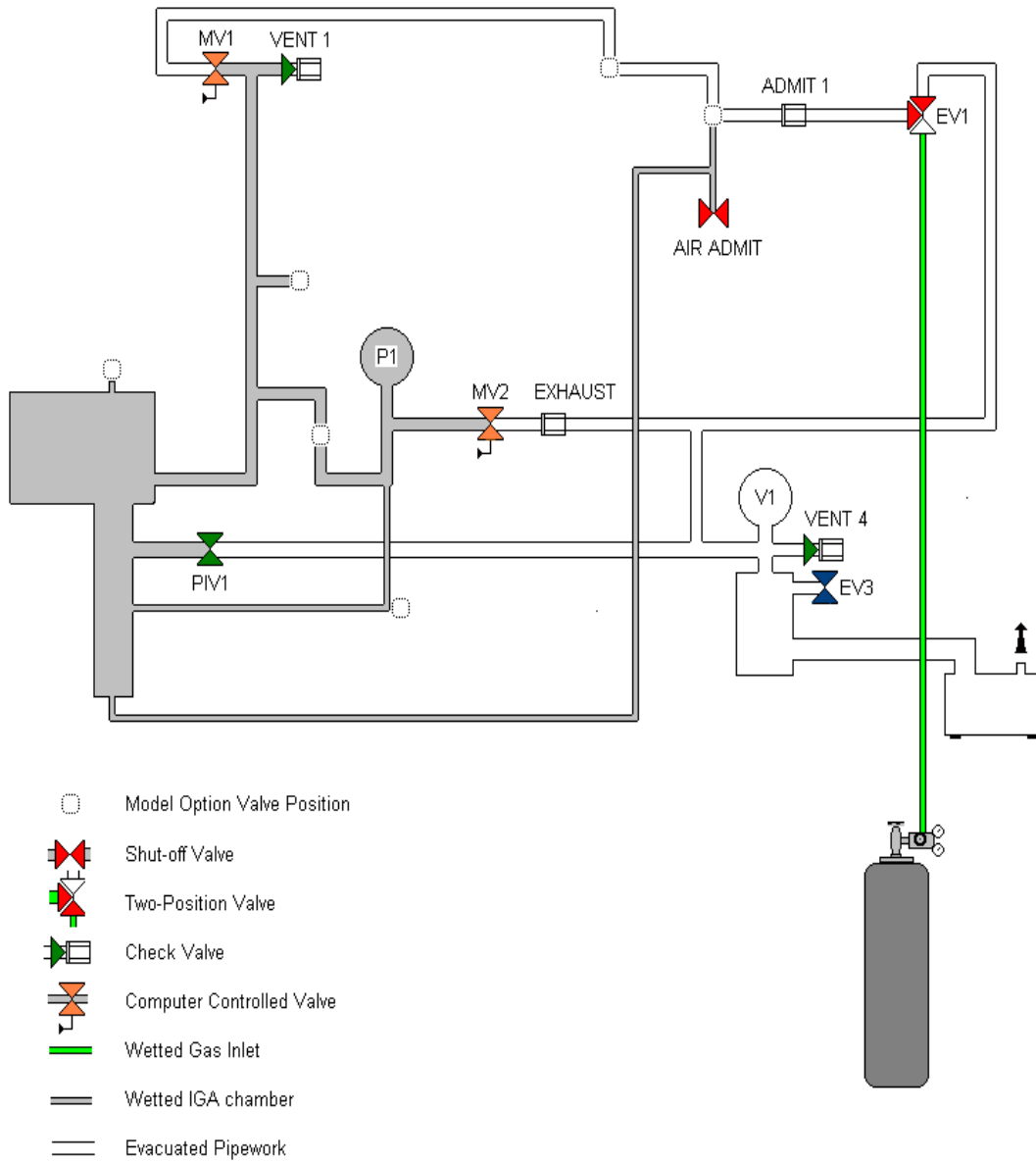
Figure 4. 9: IGA system

Figure 4. 10: Process schematic of IGA

4.4.1.1. IGA Buoyancy Correction:

Gas adsorption experiments can be conducted by volumetric and gravimetric methods. Gravimetric method can be more accurate and sensitive. It allows high vacuum operations and more parameters like pressure and temperature adjustment. In volumetric method, dead volume measurement calibration at certain pressure is the source of the errors in the measurement. In gravimetric method, buoyancy correction is corresponding to dead volume correction applied in volumetric systems. Error is absolute and is proportional to pressure, unlike volumetric systems where the error is

also cumulative from point-to-point thus making detailed isothermal studies counter-productive. Effect can be used to determine unknown sample density. Buoyancy calculator incorporated in software which allows for provision of non-ideality via use of van der Waal's constants or Peng-Robinson EOS or compressibility tables.

$$Dm_b = Dp\ M\ [(dV_c/Z_c\ T_c)-(dV_s/\ Z_sT_s)] / R \qquad (4.1)$$

Dp-pressure change

M-Molar mass

dV-Volume displaced

T-Temperature

R-Gas constant

Z -Compressibility

c - Counterweight

s - Sample

4.4.1.2. Nitrogen Adsorption Experiments up to 10 bar

For nitrogen experiments, coal samples were outgassed at 105^oC for three hours under vacuum level 10^{-9} bar around Ultra High Vacuum (UHV). Temperature inside the chamber and the outside the chamber was very different than each other due to the high vacuum level. Therefore, sample temperature was adjusted by the thermocouple inside the sample chamber to make sure that outgas temperature was reached to desired value. Then outgas step have been continued until the constant weight was reached at 10^{-9}bar. The unique property of IGA is the real time processer which realizes to take asymptotic values. In nitrogen experiments, mass uptake was very slow, therefore, easy to understand.

To understand real time processer (RTP) parameters must be known. RTP consist of 8 parameters.

- Mode: This is the most important part of the RTP measurements which requires a mathematical model for the variation of uptake with time. The software of the device has two models, which have in practice both been applied to diverse experimental conditions [71].

  The LDF model of the relaxation $u(t)$ is, F1: $u(t) = u0 + \Delta u(1- exp(-[t – t0') / k))$ where $u0$ is the uptake at the arbitrary time origin $t0'$, k is the exponential time constant and Δu is the change in uptake. The asymptotic uptake is then equal to $u0 + \Delta u$. It is applicable for wide range of unknown sorption processes and diffusive processes, which become single exponential-like in the long time limit.

  Avrami's model of the relaxation $u(t)$ is, F2: $u(t) = u0 + \Delta u(1- exp(-[t – t0']^x / k))$ where $u0$ is the uptake at the arbitrary time origin $t0'$, k is the time constant, x is a variable power and Δu is the change in uptake. The asymptotic uptake is then equal to $u0+ \Delta u$. Designed for metal recrystallization and it is suitable for phase transition.

- Phase: The initial value of the time origin for real-time analysis. Data prior to this time origin is never used for real-time analysis and data collected afterwards may be used although the actual time origin.

- Min Time: It is the minimum time required for data collection.

- Timeout: It is the maximum time to be adjusted during the mass relaxation. For unknown samples, it must be high as possible as to get equilibrium.

- Wait until: Which is the required equilibrium criteria for RTP. It can be defined for the sufficient data is acquired when the uptake has changed by a defined fraction of the difference between the initial reading $u00$ and predicted asymptote ($u0 + \Delta u$).

- RTP min: This is the minimum uptake change for the real time analysis attempt to get asymptote value. Typically 0.1-10 µg.

- RTP tolerance: Which is refer to the deviation of the last reading from the average deviation of the fit trajectory between the time origin $t0'$ and the current time t.

- Acquisition Min.: which is the target interval for weight acquisition

Temperature is another parameter to get asymptotic value for the one isotherm point. IGA did not have computer control water bath therefore temperature equilibrium was provided by the water in a Dewar which ~~is~~ was temperature equal to the room temperature and Temperature Deviation Limit was attained $0.2^{o}C$ by this way.

To understand adsorption of the different gases into coal, nitrogen adsorption experiments were done up to 1MPa. Also, Investigation of the nitrogen adsorption must be very useful for Flue-gas Enhanced Coal Bed Methane mechanism (N_2-CO_2 mixture injected to the underground).
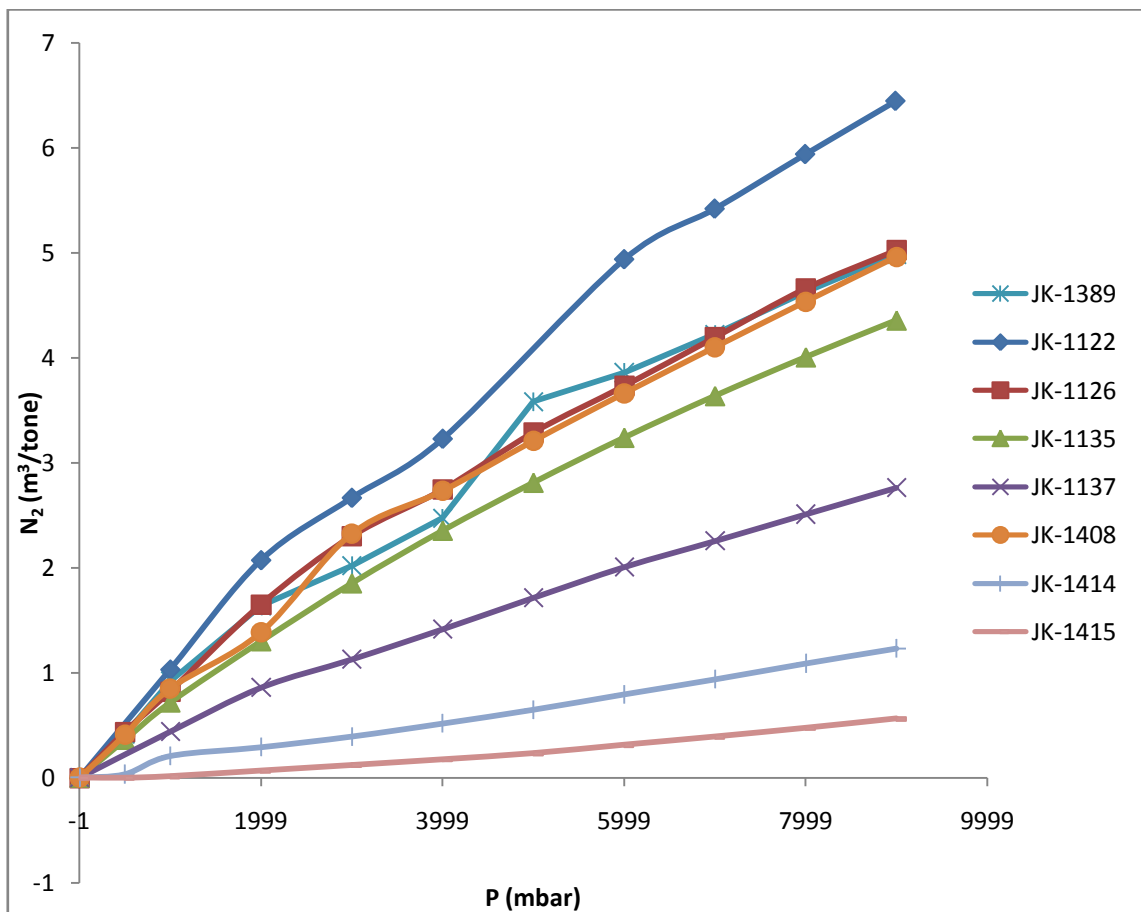

Figure 4. 11: Nitrogen adsorption isotherms at 298 K

In Figure 4.11, nitrogen adsorption isotherms of the samples are shown. Zonguldak coal samples JK-1414 and 1415 have a lower nitrogen adsorption capacity than Soma lignite samples due to their low porosity. Nitrogen sorption in coal was a diffusion limited process, uptake was very low compared to methane and CO_2. Nitrogen could not be adsorbed in micropores of the coal due to its low diffusion rate and high dynamic

radius. Therefore, sorption in the mesopores and macropores was a more effective parameter for N_2 adsorption compared to the methane and CO_2 adsorption. For Soma Lignites nitrogen adsorption capacities changed from 2.76 m^3/ton to 6.44 m^3/ton Nitrogen isotherms up to 9 bar by using asymptotic values show that JK-1122 has higher adsorption capacity than the others.

Interface of the software can be seen in Figure 4.12 for one isotherm point. Adsorption equilibrium can be followed in real time by the software. As it can be seen in the figure, uptake reaches equilibrium while asymptotic value is being recorded.
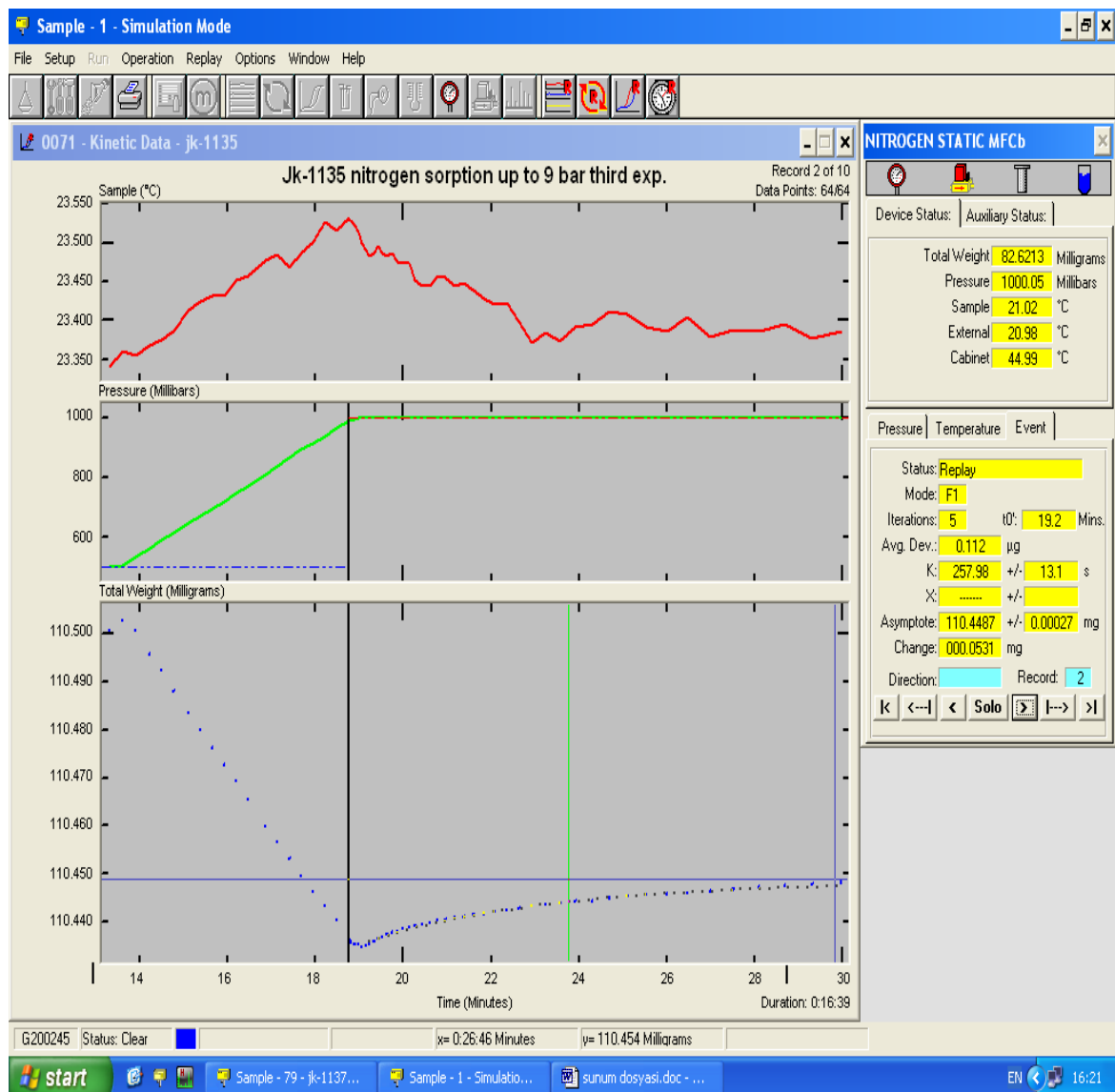

Figure 4. 12: The interface of the software used for one isotherm point

4.4.1.3. Methane Adsorption Experiments up to 9 bar

In methane sorption, real time processer was not used due to the high deviation of the uptake reading. Therefore, 6 hours interaction time was enough to get equilibrium and understand methane adsorption capacity. 6 hours was chosen by trying 3 hours and 10 hours interaction time. 3 hours was too short for the complete equilibrium and 10 hours consumed too much machine time for one isotherm point. Temperature stability was provided by the same method as the nitrogen sorption experiments. In the literature, equilibrium times for methane adsorption vary as a function of particle size. Researchers used different equilibrium times for different particle sizes (Figure 4.13). According to the results, 6 hours interaction time for our 150 µm particles was consistent with literature.

Table 4. 6: Equilibrium times in the literature [49]

Author	Grain Size (µm)	Temperature(K)	WaitingTime (hours)
Chaback et al. 1996	93-300	300-320	6-18
Clarkson and Bustin 1999	1840	273	7
Busch et al. 2006	63-2000	318	1
Goodman et al. 2004	250	295-328	0..5-12
Siemons and Busch 2007	200	318	20
Day et al. 2008	500-1000	326	4
Gruszkiewicz et al.	1000-2000	308-313	50
Majewska et al. 2009	20000x20000x10000	298	440
Goodman et al. 2006	250	328	96
Battistutta et al. 2010	1000-2000	318-328	336

Methane adsorption is far greater than nitrogen adsorption to the coal due to the strong interaction of the C-C van der Waals forces and easy access (i.e.: smaller dynamic radius) to the micropore structure of the coal (see Figure 4.14), JK-1389 which has the one of the highest organic carbon ratio, also has the highest adsorption capacity. Therefore micropore structure of the coal strongly related to the organic carbon pattern so adsorbent finds available sites in these organic patterns.
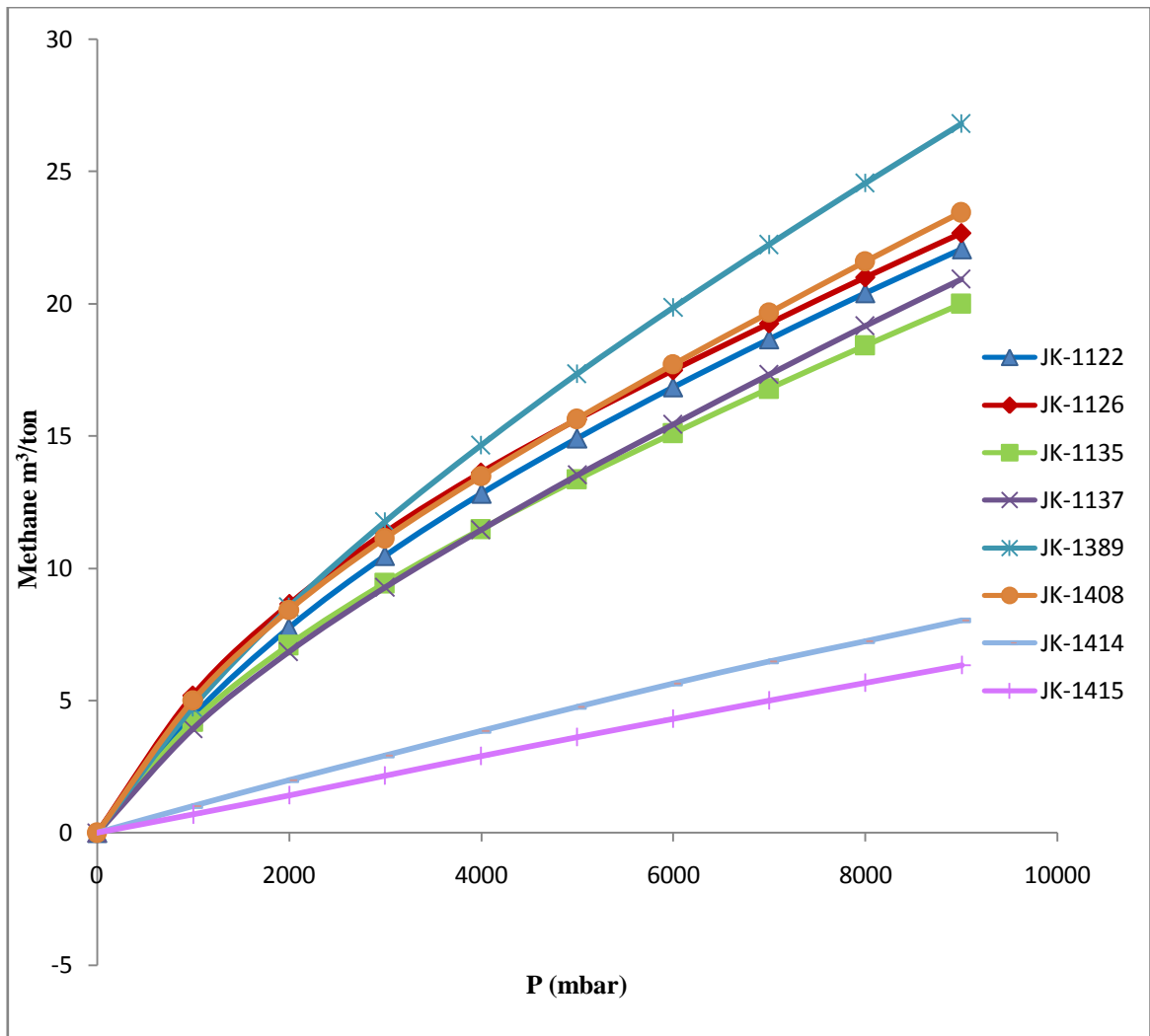

Figure 4. 13: High pressure gravimetric methane adsorption

As it can be seen Figure 4.13, JK-1389 and Jk-1408 had higher methane adsorption capacity than the others like CO_2 adsorption. They also had higher micropore ratio which meant that methane adsorption occurred in micropores. Methane adsorption capacities of outgassed Soma Lignites changed from 19.76 m^3/ton to 26.47 m^3/ton at 1 MPa. JK-1414 and 1415 gives the lowest adsorption capacity due to their low

micropore surface areas. Gravimetric methane adsorption results were in good agreement with the low pressure CO_2 results.

In the literature, there are many arguments about outgas temperature of coal, therefore temperature assisted outgas effect on the methane adsorption capacity of coal was investigated. In Figure 4.15, sample was outgassed in vacuum at 105°C prior to adsorption. Other sample was outgassed only in vacuum. Results show that vacuum outgassed sample has a higher methane adsorption capacity than the other; it means that temperature could cause a collapsed micropore structure of coal, and disturbed structure cannot adsorb methane efficiently.
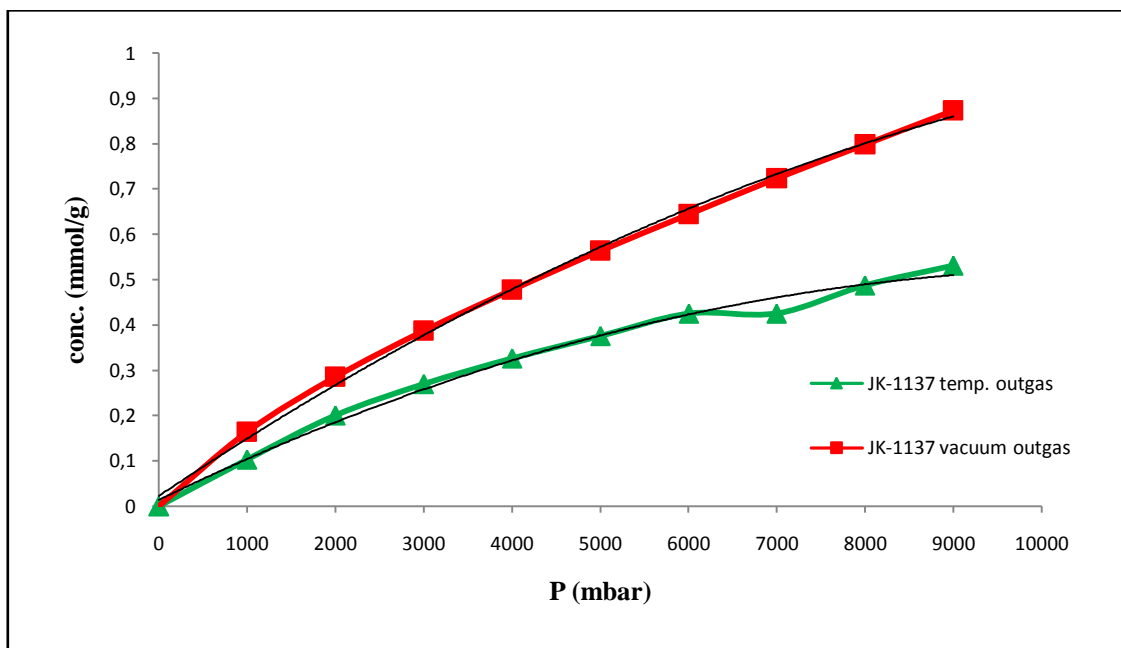

Figure 4. 14: JK-1137 adsorption isotherms at 298 K with and without temperature outgas prior to experiment.

4.4.2. Volumetric Methane Adsorption Experiments

Volumetric adsorption experiments up to 17 MPa were conducted in Aachen University. As received (moisture equilibrated) samples were used and high pressure excess adsorption values are recorded according to the normalized dry, ash-free coal mass since this is the standard procedure that has been encountered in the literature. Maximum excess adsorption values of the samples change from 9.73 m^3/ton to 13.13 m^3/ton as shown in Figure 4.16. In Figure 4.17, absolute adsorption isotherms of the samples are given. Calculated absolute methane adsorption capacities of the samples

varied from 12.99 m³/ton to 18.13 m³/ton. Absolute sorption values were similar to the excess sorption in the low pressure region up to ~3 MPa. At higher pressures, absolute sorption became significantly higher.
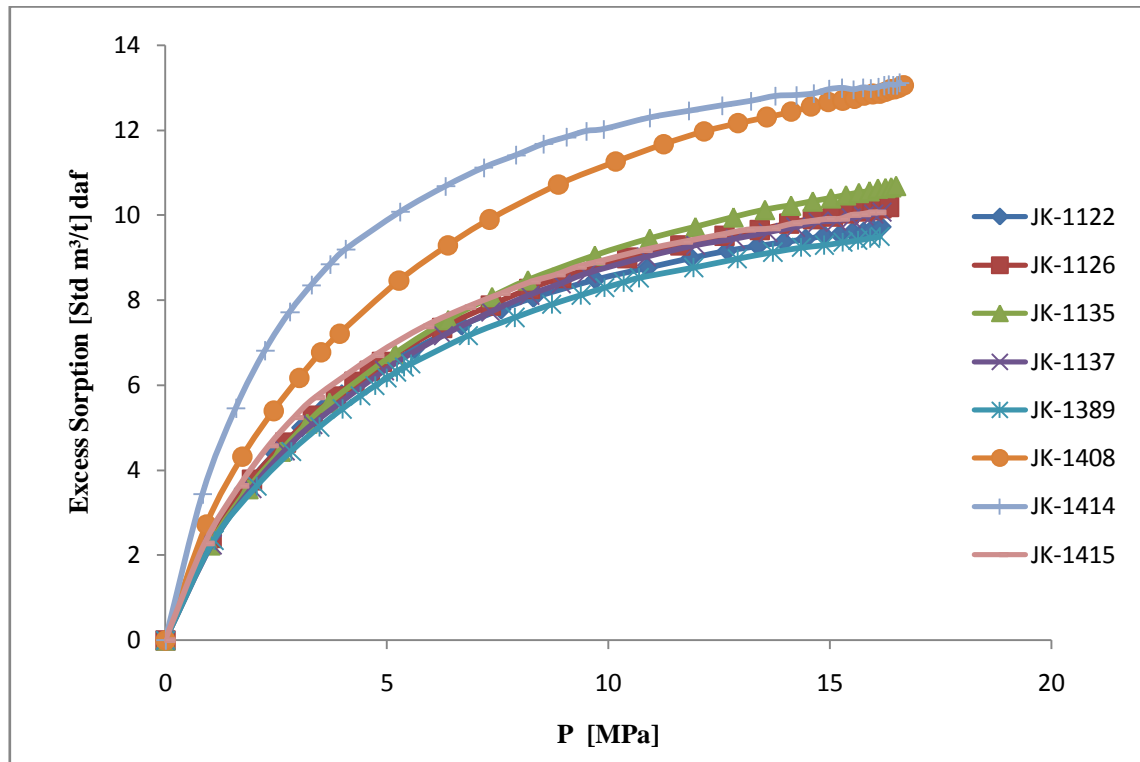

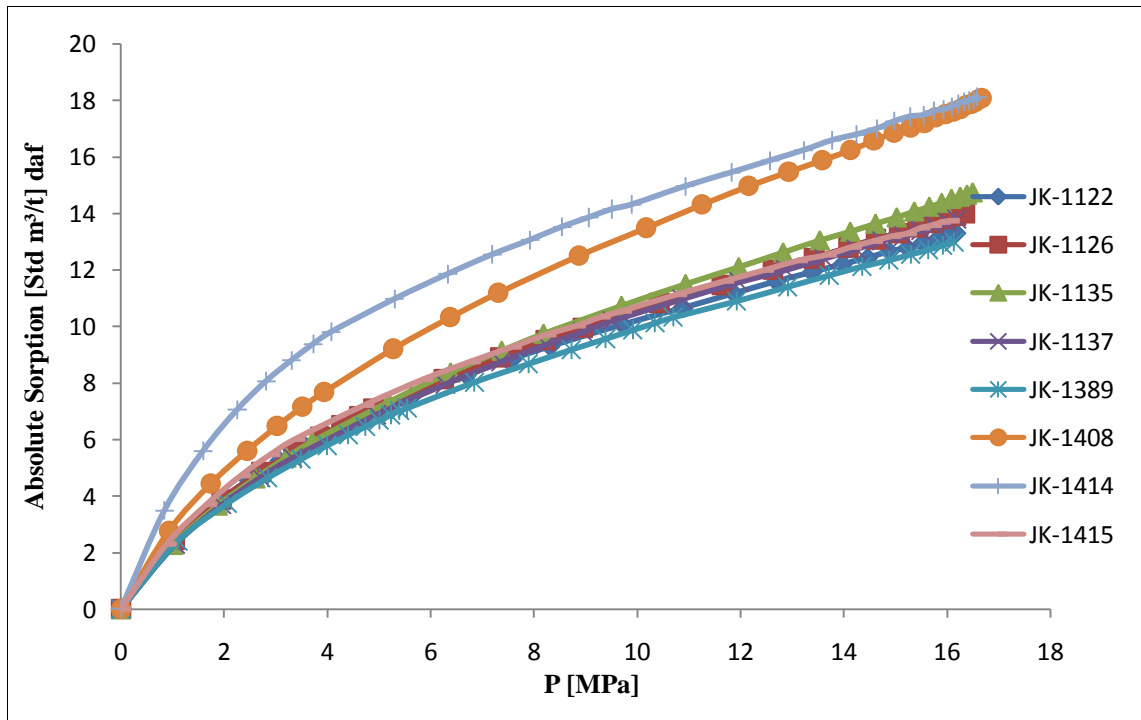**Figure 4. 15:** Excess sorption isotherms of the samples

Figure 4. 16: Absolute sorption isotherms of the samples

Absolute adsorption results of the samples can be considered to be true methane capacities. Since adsorption experiments are conducted on as-received samples without outgassing. For enhanced coal bed methane processes, ratio of CO_2 adsorption to methane adsorption is very important. Therefore, calculated CO_2 micropore capacities of the samples were compared to the absolute methane adsorption capacities. Results are shown in Table 4.6. According to the data, Soma samples adsorbed at least 2.65 times more CO_2 which was a very encouraging result for ECBM processes.

Table 4. 7: CO_2/CH_4 ratio for ECBM processes

	Theoretical CO_2 adsorption capacity (m^3/ton)	Experimental Methane Capacity (17MPa) (m^3/ton)	CO_2/CH_4 Ratio
JK-1122	43.23	13.31	3.247934
JK - 1126	47.92	14.02	3.417974
JK - 1135	39.06	14.75	2.648136
JK - 1137	40.63	13.8	2.944203
JK - 1389	48.44	12.99	3.729022
JK - 1408	47.92	18.08	2.650442
JK-1414 Kozlu	27.08	18.13	1.493657
JK-1415 Armutcuk	22.39	13.74	1.629549

According to the high pressure volumetric adsorption results, Zonguldak samples JK-1414 and JK-1415 had higher adsorption capacities as expected, since they had lower microporosity, lower nitrogen and methane adsorption amount upto 1MPa. However, in all other sorption experiments, outgas was conducted prior to adsorption. Outgas can remove moisture and impurities from the internal surface of the material and make them accessible for gas molecules. However, in volumetric adsorption experiments, moisture equilibrated samples were used. Therefore moisture amount inside the structure affected adsorption capacities, since moisture blocks the pores. Soma Lignites are low rank coals and contain more moisture in their structures compared to the high rank Zonguldak coals which reduce adsorption capacity of Soma lignite more than Zonguldak coal samples. Moisture effect is shown in Table 4.7, at the same pressure, 10% of moisture could reduce approximately 90% of the methane adsorption amount.

Table 4. 8: Effect of outgas on methane adsorption

	Moisture %	Outgassed Methane Capacity at 1 MPa (m³/ton)	Moisture equilibrated Methane Capacity at 1 MPa (m³/ton)	% Methane Capacity Loss
JK-1122	9.37	22.06875	2.30947	89.53511
JK - 1126	7.38	20.00773	2.443769	87.78587
JK - 1135	6.56	22.68581	2.271099	89.9889
JK - 1137	7.04	20.93032	2.285488	89.08049
JK - 1389	10.55	26.79849	2.393407	91.06887
JK - 1408	12.60	23.45107	2.767527	88.19872
JK-1414 Kozlu	1.16	8.034462	3.482192	56.65931
JK-1415 Armutcuk	1.32	6.337493	2.311868	63.52078

4.5. Solubility and Biogasification Results

To understand underground methane production due to bacterial activity, small lab scale anaerobic incubations were investigated.

4.5.1. Solubilization Results

In this study, solubilization of the coal samples was investigated as a beginning. Studies showed that, coal can be solubilized biologically or chemically. In biological methods, wood-rotting fungi species are able to solubilize/depolymerize low rank coals by secreting oxalate ions. Bumpus et al. [72] show that chemically, coal macromolecules are solubilized in an alkaline medium, like aqueous solution of oxalate, carbonate and phosphate ions instead of using any fungi species.
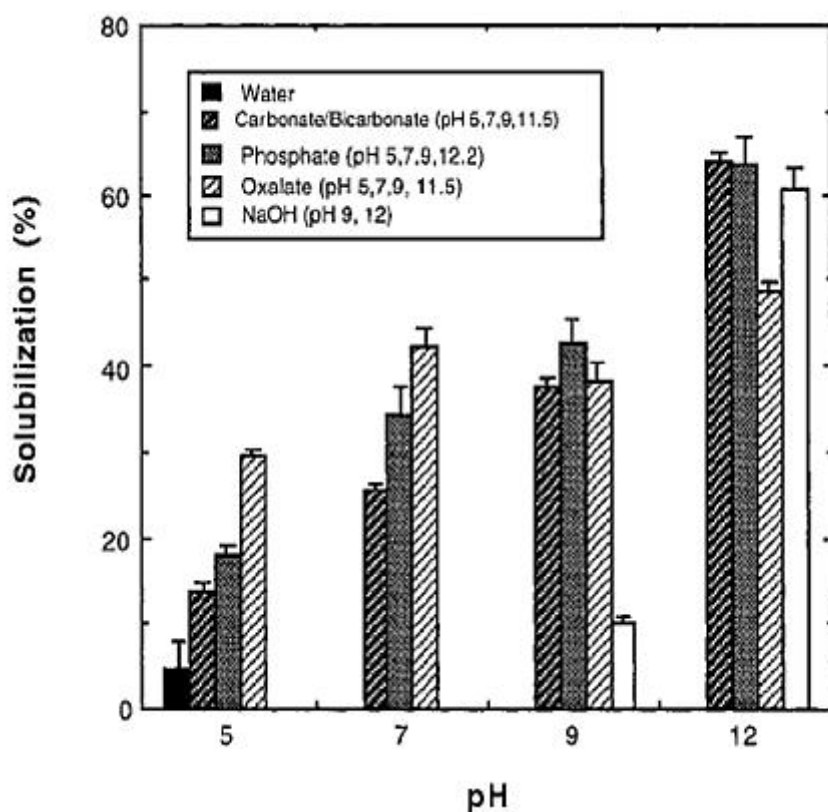

Figure 4. 17: Leonardite solubilization in different Lewis bases in different pH [72].

Carbonate, phosphate and oxalate systems could solubilize around 40% low rank coal, Figure 4.18. That means that coal can be degraded to small fragments by using Lewis bases. In the light of this point, we used different Lewis bases to reach maximum solubilization capacity for our coal samples. Effect of pH on the ability of Lewis bases to solubilize coal was investigated.
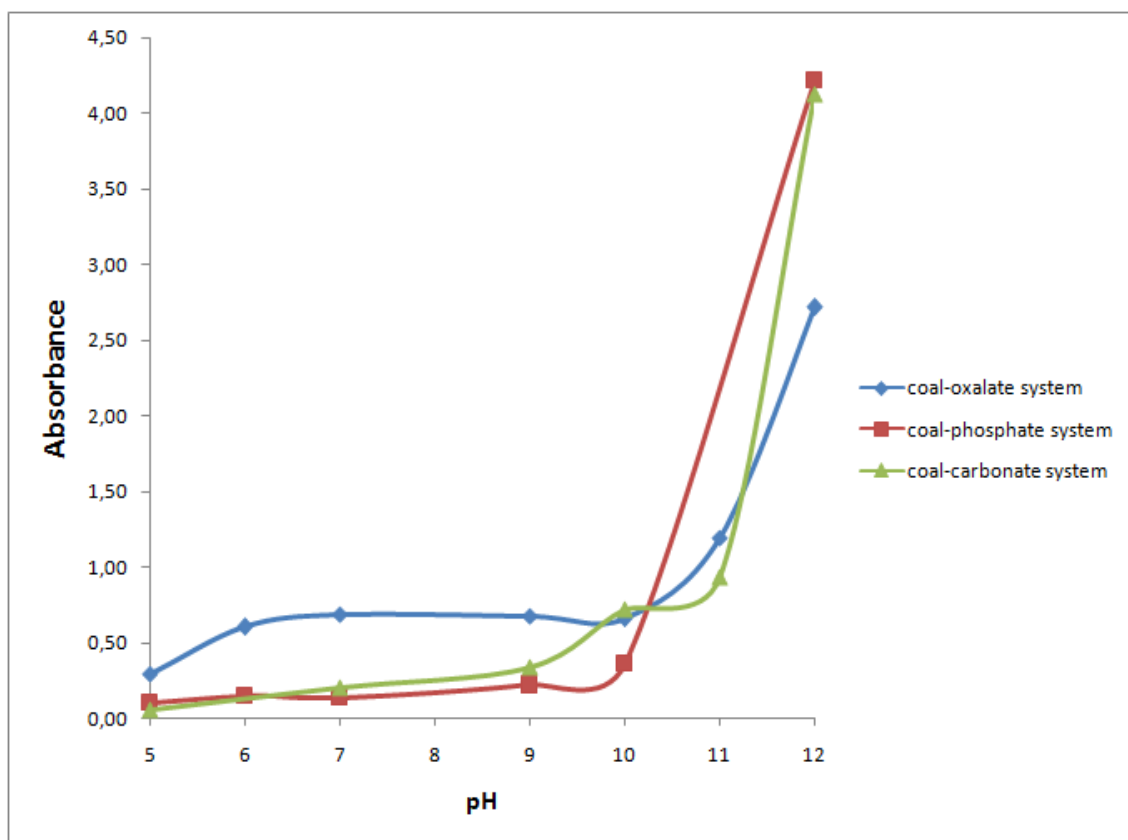
Figure 4. 18: pH dependence of Lignite solubilization

Figure 4.19 shows the comparison of the absorbance intensity at 275 nm of the solubilized coal in the aqueous solution of the different Lewis bases at varying pH. The UV-visible spectrum of this material was uncharacteristic, gradually increasing in intensity through the visible spectrum into the UV. There were no distinct peaks. 275 nm was chosen to compare all results due to the higher absorbance value of the whole spectrum. At high pH values (pH $\geq$10), solubility of the coal was more in carbonate and phosphate anions systems than oxalate anions. On the other hand, at lower pH levels between 9$\geq$ pH $\geq$5, oxalate anion system solubilized coal more effectively. This result was important, since in the microbial gasification processes of the coal, harsh conditions reduce microorganism's activity. Therefore, higher solubilization of the coal at moderate pH levels is a very important parameter to increase the efficiency of the biogasification processes due to the decomposition of the complex structure of the coal into the smaller organic substances which are more easily converted to methane by microorganism.

For the future prospect of this study, Lewis bases will be used for the biogasification of the lignite samples to increase efficiency of these processes.

4.5.2. Biogasification Results

4.5.2.1. Optical Microscope Results

For biogasification experiments, first anaerobic growth of the microorganisms was observed; therefore after ten days of incubation of methanobacterium formicicicum in bioreactor, 1 ml sample was taken and sealed in the test tube. To visualize microorganisms' cell, 10 µl samples dropped on the microscope slide and colored with resazurine dye. In Figure 4.20-a, optical microscope image of bacterial colony was seen in 1000x magnification. In Figure 4.20-b, colored microorganisms can be seen more clearly, opaque samples were coal particles and green round images represented microorganisms after ten days of incubation.
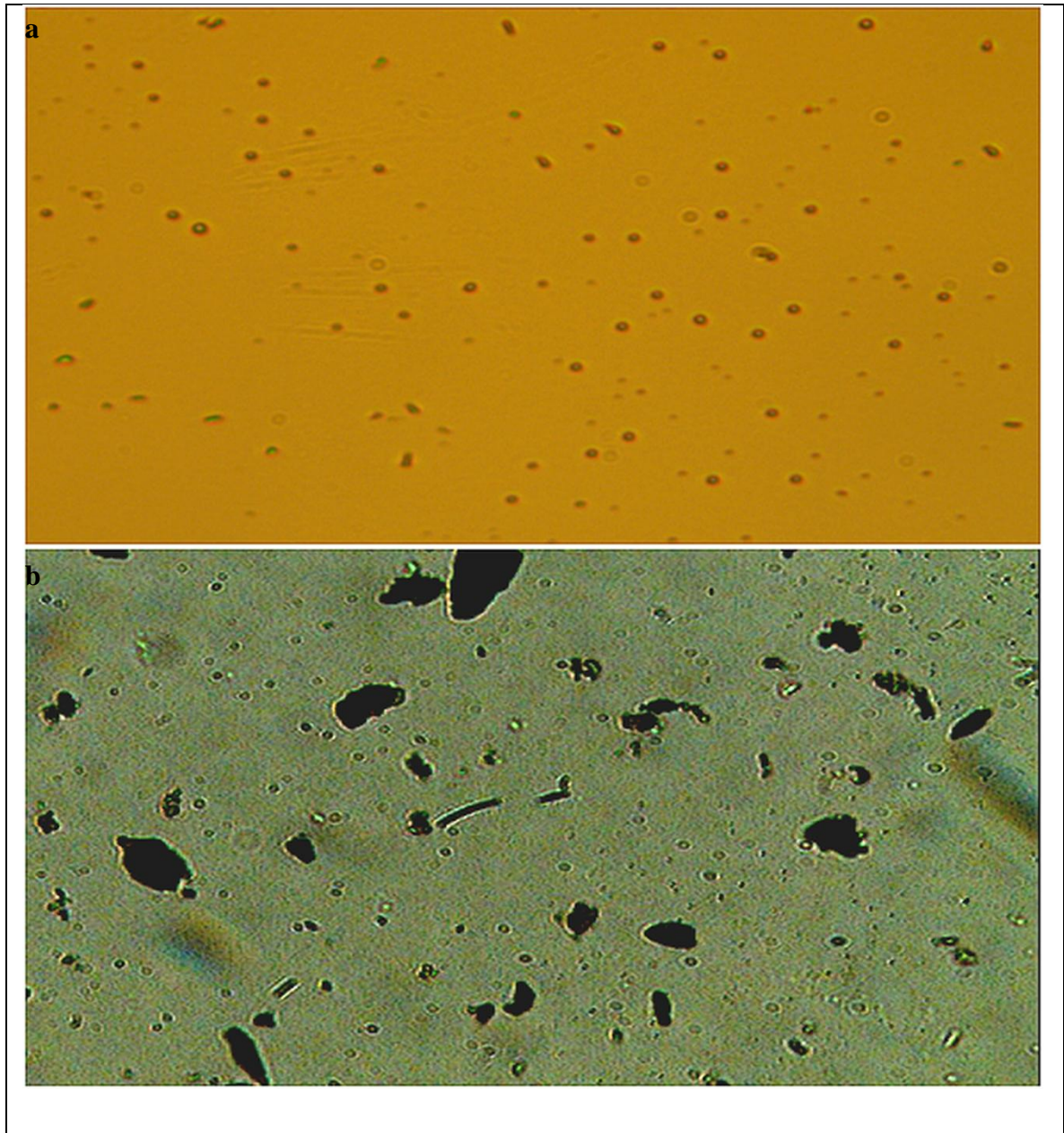
Figure 4. 19: Optical microscope images after 10 days of incubations **a)** Bacterial colony at 1000x magnification **b)** Bacteria and coal particles at 500x magnification

Figure 4.20 showed that after ten days of incubation, microorganisms inside the slurries still active and detectable.

4.5.2.2. Bacterial Methane Production Results

For bacterial gasification process, methanobacterium formicicicum grew in ATCC 1045 methanobacteria medium under H_2/CO_2 as the sole carbon-energy source. Serum bottles of these strains were overpressurized to 0.5 to 1 bar with a gas mixture of 80% H_2 and 20% CO_2. After 3 days of incubation produced methane in the headspace of the bottles

were measured. In figure 4.21 and table 4.8, methane production result of the H_2-CO_2 culture is shown as an example of the GC-MS spectrum of the products.
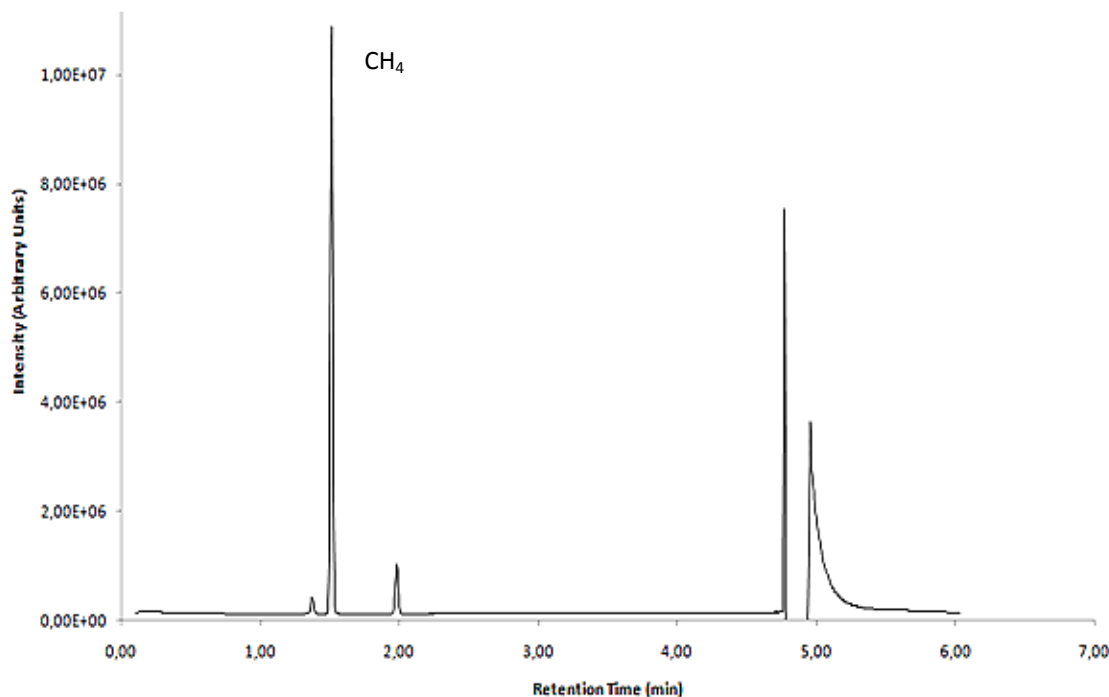

Figure 4. 20: GC-MS spectrum of the produced methane after 3 days of GC-MS spectrum of the produced methane after 3 days of incubation H_2/CO_2 as the sole carbon-energy source

Table 4. 9: GC-MS data of the produced methane after 3 days of incubation H_2/CO_2 as the sole carbon-energy source

Pea k#	Ret. Time	Proc. From	Proc .To	Mas s	Area	Height	A/H	Con c.	Name
1	1,511	1,475	1,55	TIC	12945944	10740490	1,21	40,36	Methane (CAS) Marsh gas

After 3 days of incubation with H_2-CO_2, culture growth was frequently flocculent and formation of large cell aggregates which settled down at the bottom of the bottles have been observed. Optical density of the microorganisms at that time was measured 0.4 at 600 nm. After that soma lignite was incubated with growth microorganisms. Cell concentrations were not quantified, as the presence of coal solids would have interfered with such measurements.

As explained in section 3.7.2.1 four types of incubation were prepared. In the first set, H_2-CO_2 was added to the coal slurry to enhanced microbial growth to convert coal into the methane. Methane production was monitored around 20 days. As it can be seen in Figure 4.22, methane production reached to 11 m^3/ton in three days, after that, significant methane production has not been measured. This result indicated that produced methane was the result of the CO_2 reduction to the CH_4 but not coal conversion.
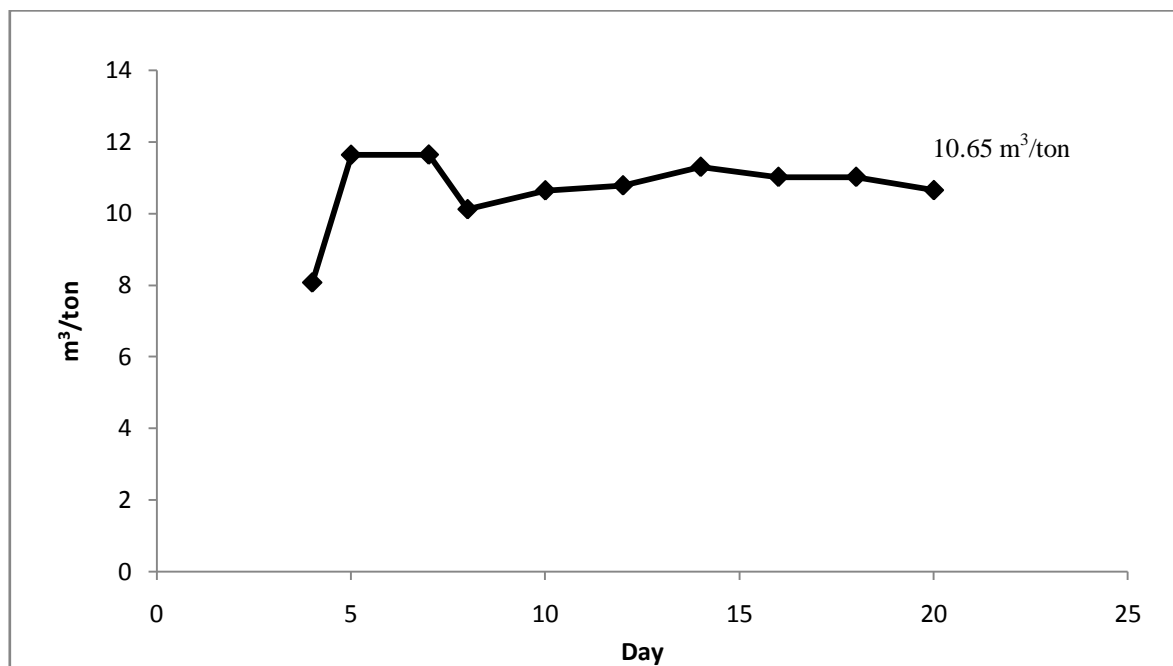
Figure 4. 21: Set 1 - Coal-medium with H_2-CO_2 as the sole carbon-energy source results after 20 days of incubation.

On the other hand, if methane production of the coal degradation occurred, it was too low to be observed compared to the CO_2 reduction to CH_4 by microorganisms.

In the second set, CO_2 was not used; coal was the only source of the carbon conversion. H_2 was added to the substrate and methane production was monitored. As it can be seen on the Figure 4.23, significant increase was observed during incubation.

Figure 4. 22: Set 2 - Coal-medium with H_2 results after 20 days of incubation.
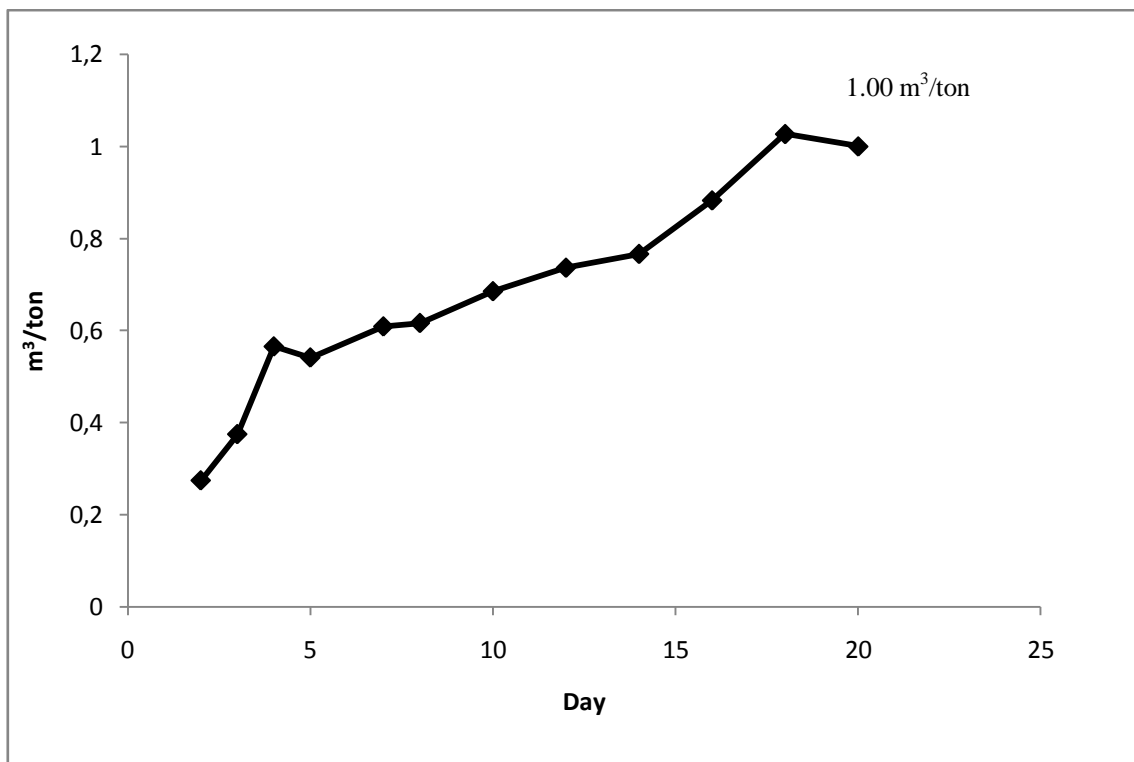
Coal can be solubilized with Lewis Base systems. Methanobacterium medium contain carbonate and phosphate system. Coal can be degraded into small fragments and converted to the methane by methanogenic bacteria. As a result, the coal in this reaction act as sole carbon and energy source in excess but conversion to the methane not only dependent on carbon amount also H_2 is needed to conversion. As it can be observed in the results H_2 is the limiting agent for the methane production from the coal by methanogens. 1 m^3/ton was a good result for methane production compared to the results in the literature. These results also proved that H_2-producing microorganisms must be included in the consortium (collection of different microbial species) in addition to the methanogens.

In the set 3, coal was the only carbon and hydrogen source for the methanogens. Methane production was very limited (Figure 4.24). Because even if, Lewis base system convert complex coal structure to small organic molecules, there was no H_2 in the system for the conversion of the methane for methanobacterium formicicicum. Maximum 0.06 m^3/ton methane production was measured at the end of the 20 day.
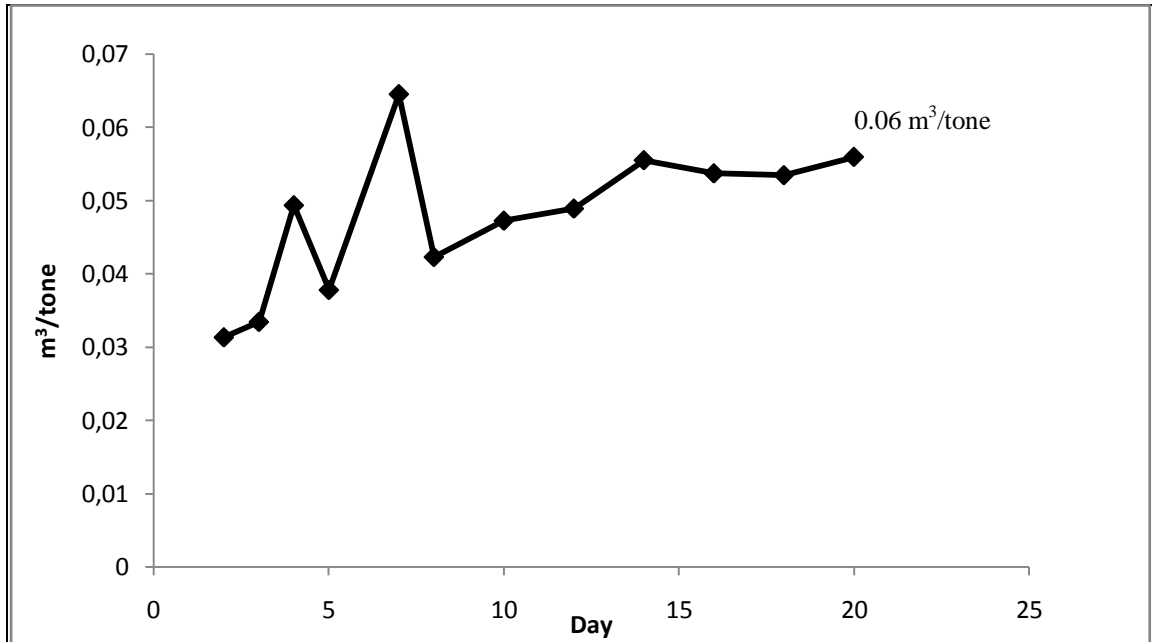
Figure 4. 23: Set 3 - Coal-medium in argon results after 20 days of incubation.

Methanogens can convert small carbon molecules to methane. Carbonate in the medium may have cause additional methane production. To understand methane production due the carbonate conversion, the set-4 was prepared without carbonate in the medium and methane production was monitored. Results are shown in Figure 4.25. There was no additional methane production due to the carbonate in the medium was observed. Methane production was almost the same as of the set-3.

Figure 4. 24: Set 4 - Coal-medium without carbonate in argon results after 17days of incubation.

CHAPTER 5

5. Conclusion

In this study, coal bed methane adsorption capacity of Soma lignite and factors that affect gas adsorption capacity were examined. For this pu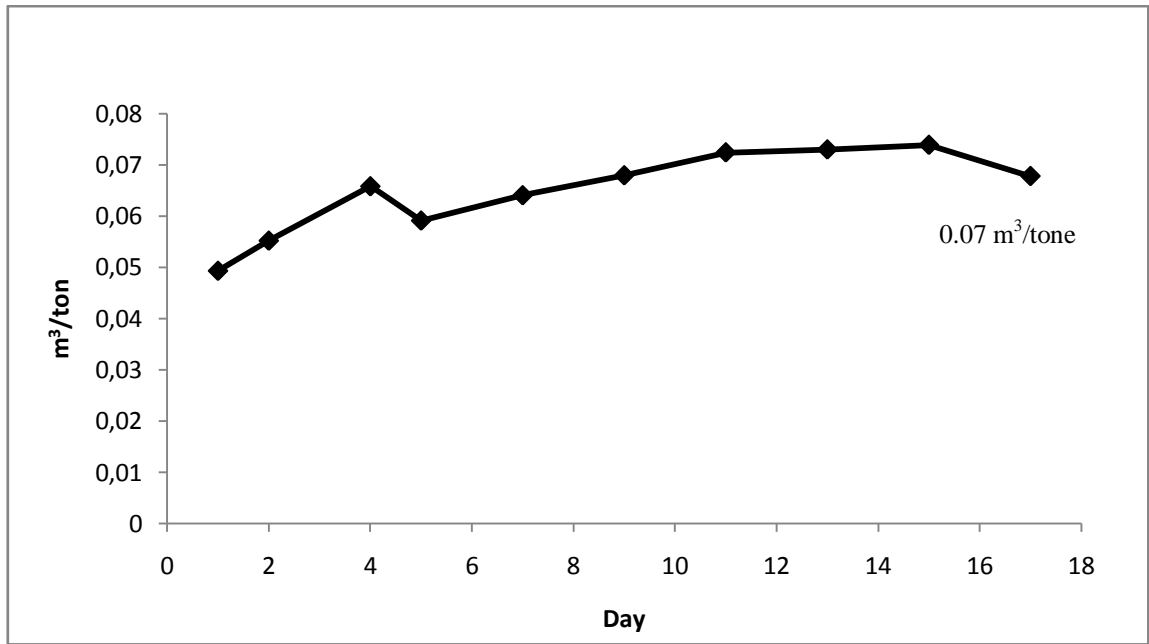rpose, chemical and petrographical analyses of coal were studied. Then, gravimetric and volumetric high pressure gas adsorption experiments were conducted. After determination of biogenic origin of the gas produced in the coal bed, gasification experiments were conducted by using methanogens to simulate methane generation from coal. As a result of this study, following observations were concluded;

- By using standard elemental analysis values, H/C and O/C ratios of the samples were found and placed into the van Krevelen Diagram. Origin of the organic matter in Soma Lignites was found to type-3 kerogen that belongs to the humic (woody) kerogens with low H/C and high O/C ratio. This type of kerogen contains high ratio vitrinite or huminite in its structure. Proximate analyses of the samples showed that Soma lignite samples had high moisture content with low fixed carbon ratio compared to the Zonguldak coals (JK-1414, JK-1415) due to their low rank.

- Thermal analysis (Rock-Eval pyrolysis) results showed that Soma samples were laid in the immature region of the modified van Krevelen diagram due to their low T_{max} values. But they had high organic carbon ratio compared to the mature Zonguldak coal (JK-1414, JK-1415).

- High pressure volumetric adsorption isotherms up to 17 MPa showed that absolute methane adsorption capacities of the as received (without outgas) Soma lignite were vary between 12.99 m^3/ton to 18.08 m^3/ton at 45°C.

- To understand enhanced coal bed methane capacity of the Soma Lignite, calculated carbon dioxide micropore capacity and experimental high pressure methane adsorption capacity of the samples were compared. For Soma Lignite, CO_2 was adsorbed at least 2.5 times more than methane. This was a good result for ECBM processes.

- Low pressure CO_2 adsorption experiments showed that micropore surface areas and micropore volumes of the Soma Lignite changed from 224.909 m^2/g to 287.097 m^2/g and 0.070 to 0.093 cm^3/g, respectively. Results were much higher than mature Zonguldak coal samples. Pore size distribution results were concluded that Soma lignite did not contain pores bigger than 10 Å and different pore formation had not been observed.

- Micropore surface areas of the samples were correlated with organic carbon ratios. Results have shown that microporosity was increasing with increasing organic carbon ratio. Mature Zonguldak samples had lower microporosity and organic carbon ratio according to the results. It has been observed that organic carbon ratio affected microporosity (adsorption capacity) more than maturity of the samples.

- Soma Lignites are low rank coals and contain more moisture in their structures compared to the high rank Zonguldak coals. To understand the effect of moisture on the adsorption capacity, gravimetric adsorption results with high vacuum outgassed samples and volumetric adsorption results on as received samples were compared at the same pressure. Moisture could approximately reduce the methane adsorption amount by 90% due to blockage of the microporosity of the coal structure by water molecules. Also outgas conditions were investigated by using gravimetric adsorption experiments. High temperature used 105°C during outgas with high pressure vacuum conditions reduced adsorption capacity significantly compared to the only vacuum outgassed results. Removal of moisture at this high temperature regime caused some thermal expansion of the coal and the micropore structure to collapse. Therefore this disturbed structure could not adsorb methane efficiently.

- Four types of microbial gasification experiments were conducted by using methanobacterium formicicum. Results have shown that methane production by using just methanogens was very limited process due to the low degradation of the complex carbon structure of coal for the methane production. When, free hydrogen gas was given to the system, methane production gradually increased. This proved that hydrogen was the limited reagent for microbial methane formation. After 20 days of incubation 1 m^3/ton methane production was measured which was a promising result compared to the literature.

- According to the results of the set-3 and the set-4 in the biogasification experiments, carbonate in the medium did not affect total methane yield.

5. 1. Future Work

As a future step of our study, thermal expansion of the coal samples up to $150^{\circ}C$ under inert atmosphere can be investigated to understand temperature outgas effect on the coal structure. To investigate enhanced coal bed methane processes, methane-carbon dioxide replacing ratio in the micropores can be found through the CO_2 injection in the methane adsorbed samples by using two gas mass flow systems with pressure and temperature control.

For biogenic methane formation processes, methane production due to the endemic bacterial population of Soma Basin can be determined. For this reason, underground water samples must be collected anaerobically. Moreover, microbial consortium which contains species that produce H_2 shall be prepared. Then, produced H_2 can be used by methanogens. This consortium should contain fermentative and acetenogic bacteria in addition to methanogens are necessary to increase the conversion. By this way, complex substrates are hydrolyzed and fermented by bacteria that result in acetate longer chain fatty acids, CO_2, H_2 formation.

References

1. Harris, S.H., R.L. Smith, and C.E. Barker, Microbial and chemical factors influencing methane production in laboratory incubations of low-rank subsurface coals. International Journal of Coal Geology 2008. **76**: p. 46-51.

2. Mastalerz, M., A. Drobniak, and J. Rupp, Meso- and Micropore Characteristics of Coal Lithotypes: Implications for CO_2 Adsorption. Energy & Fuels, 2008. **22**(6): p. 4049-4061.

3. Breck, D.W., Zeolite Molecular Sieves 1974, New York Wiley.

4. Sing, K.S.W. and R.T. Williams, The Use of Molecular Probes for the Characterization of Nanoporous Adsorbents. Particle & Particle Systems Characterization, 2004. **21**(2): p. 71-79.

5. Barton, A.F.M., Handbook of Solubility Parameters and Other Cohesion Parameters. 1983, Boca Raton, FL: CRC Press.

6. Reucroft, P.J. and A.R. Sethuraman, Effect of pressure on carbon dioxide induced coal swelling. Energy & Fuels, 1987. **1**(1): p. 72-75.

7. Cazorla-Amorós, D., et al., CO_2 As an Adsorptive To Characterize Carbon Molecular Sieves and Activated Carbons. Langmuir, 1998. **14**(16): p. 4589-4596.

8. Nandi, S.P. and P.L.J. Walker, The diffusion of nitrogen and carbon dioxide from coals of various rank. Fuel, 1964. **43**: p. 385-393.

9. Marsh, H., Determination of Surface Areas of Coals - Some Physicochemical Considerations. Fuel, 1965. **44**(4): p. 253-268.

10. Marsh, H. and T. Siemieniewska, The surface area of coals as evaluated from the adsorption isotherms of carbon dioxide using Dubinin–Polanyi equation. Fuel, 1965. **44**: p. 355-367.

11. Smith, D.M. and F.L. Williams, Coal Sience and Chemistry (A. Volborth, Ed.). 1987, Amsterdam: Elsevier.

12. Cohen, M.S. and P.D. Gabriele, Degradation of Coal by the Fungi Polyporus versicolor and Poria monticola. Applied and environmental microbiology, 1982. **44**(1): p. 23-7.

13. Lozano-Castelló, D., D. Cazorla-Amorós, and A. Linares-Solano, Usefulness of CO2 adsorption at 273 K for the characterization of porous carbons. Carbon, 2004. **42**(7): p. 1233-1242.

14. Lowell, S., Characterization of porous solids and powders: surface area, pore size, and density. 2004: Kluwer Academic Publishers.

15. Walker, P.L. and I. Geller, Change in Surface Area of Anthracite on Heat Treatment. Nature, 1956. **178**(4540): p. 1001-1001.

16. Krooss, B.M., et al., High-pressure methane and carbon dioxide adsorption on dry and moisture-equilibrated Pennsylvanian coals. International Journal of Coal Geology, 2002. **51**(2): p. 69-92.

17. Clarkson, C.R. and R.M. Bustin, Binary gas adsorption/desorption isotherms: effect of moisture and coal composition upon carbon dioxide selectivity over methane. International Journal of Coal Geology, 2000. **42**(4): p. 241-271.

18. Crosdale, P.J., B.B. Beamish, and M. Valix, Coalbed methane sorption related to coal composition. International Journal of Coal Geology, 1998. **35**(1–4): p. 147-158.

19. Rice, D., Composition and Origins of Coalbed Gas. AAPG Studies in Geology, 1993. **38**: p. 159-184.

20. COAL. [cited 2012 January]; Available from: http://www.worldcoal.org/coal/.

21. Kömür Nedir. Available from: http://www.tki.gov.tr/dosyalar/komur_nedir.pdf.

22. The Coal Resource: A Comprehensive Overview of Coal 2009; Available from: http://www.worldcoal.org/coal/uses-of-coal/.

23. INTERNATIONAL ENERGY OUTLOOK. 2011; Available from: http://www.eia.gov/forecasts/ieo/pdf/0484(2011).pdf.

24. BP Statistical Review of World Energy. 2010; Available from: http://www.bp.com/liveassets/bp_internet/globalbp/globalbp_uk_english/reports_and_publications/statistical_energy_review_2008/STAGING/local_assets/2010_downloads/statistical_review_of_world_energy_full_report_2010.pdf.

25. Kömür. Available from: http://www.enerji.gov.tr.

26. Bituminous Coal Sector Report. 2009; Available from: http://www.enerji.gov.tr

27. Coal Mining in Turkey - Overview. Available from: http://www.mbendi.com/indy/ming/coal/as/tr/p0005.htm.

28. Coal Sector Report - Lignite 2009; Available from: http://www.enerji.gov.tr

29. Romeo M, F., Coalbed methane: From hazard to resource. International Journal of Coal Geology, 1998. **35**(1–4): p. 3-26.

30. Nuccio, V., Coal-Bed Methane: Potential and Concerns. U.S. Geological Survey, 2000. **Fact Sheet 123-00**.

31. Rice, D.D., Coalbed methane—An untapped energy resource and an environmental concern. U.S. Geological Survey, 1997. **Fact Sheet FS–019–97**.

32. Yip, D. and J. Jacobelli, CBM - Another green solution (Industry Overview), 2007.

33. Bustin, R.M. and C.R. Clarkson, Geological controls on coalbed methane reservoir capacity and gas content. International Journal of Coal Geology, 1998. **38**(1–2): p. 3-26.

34. Al-Jubori, A., et al. Coalbed Methane: Clean Energy for the World. 2009. **21**, 4-12.

35. Green, M.S., K.C. Flanegan, and P.C. Gilcrease, Characterization of a methanogenic consortium enriched from a coalbed methane well in the Powder River Basin, U.S.A. International Journal of Coal Geology, 2008. **76**(1–2): p. 34-45.

36. DeBruin, R.H., et al. Coalbed methane in Wyoming. 2001; Available from: http://www.blackdiamondenergy.com/coalbed3.html.

37. Yalçin, M.N., et al., Carboniferous Coals of the Zonguldak Basin (Northwest Turkey): Implications for Coalbed Methane Potential. AAPG Bulletin, 2002. **86**(7): p. 1305-1328.

38. Andrew R, S., Hydrogeologic factors affecting gas content distribution in coal beds. International Journal of Coal Geology, 2002. **50**(1–4): p. 363-387.

39. Maciej J, K., Composition and origin of coalbed gases in the Upper Silesian and Lublin basins, Poland. Organic Geochemistry, 2001. **32**(1): p. 163-180.

40. Harrison, J.A., H.W. Jackman, and J.A. Simon, Predicting Coke Stability form Petrographic Analysis of Illinois Coals. Illinois State Geological Survey, 1964. **366**: p. 1-20.

41. Krevelen, D.W.v., Coal: Typology - Physics - Chemistry - Constitution 1993, Amsterdam: Elsevier Science. 977.

42. Gertenbach, R.M., Methane and Carbon Dioxide Sorption Studies on South African Coals in Chemical Engineering2009, University of Stellenbosch Stellenbosch. p. 175.

43. Bustin, R.M. and G.A.o. Canada, Coal petrology: its principles, methods, and applications. 1985: Geological Association of Canada.

44. Cazaux, S. and M. Spaans, HD and H(2) formation in low-metallicity dusty gas clouds at high redshift. Astronomy & Astrophysics, 2009. **496**(2): p. 365-374.

45. Ruthven, D.M., Principles of adsorption and adsorption processes. 1984: Wiley.

46. White, C.M., et al., Sequestration of Carbon Dioxide in Coal with Enhanced Coalbed Methane RecoveryA Review†. Energy & Fuels, 2005. **19**(3): p. 659-724.

47. Sing, K.S.W., Reporting physisorption data for gas/solid systems with special reference to the determination of surface area and porosity (Provisional). Pure and Applied Chemistry, 1982. **54**(11): p. 2201-2218.

48. Myers, A.L. and P.A. Monson, Adsorption in Porous Materials at High Pressure: Theory and Experiment. Langmuir, 2002. **18**(26): p. 10261-10273.

49.   Battistutta, E., et al., Swelling and sorption experiments on methane, nitrogen and carbon dioxide on dry Selar Cornish coal. International Journal of Coal Geology, 2010. **84**(1): p. 39-48.

50.   Walker, P.L. and K.A. Kini, Measurement of the Ultrafine Surface Area of Coals. Fuel (London), 1965. **44**: p. 453-459.

51.   Yee, D., J.P. Seidle, and W.B. Hanson. Gas Sorption on Coal and Measurement of Gas Content. 1993 [cited 2012; Available from: http://uwlib5.uwyo.edu/omeka/items/show/1320.

52.   Diamond, W.P., et al. The modified direct method: a solution for obtaining accurate coal desorption measurements. in International Coalbed Methane Symposium. 2001. Tuscaloosa, Alabama.

53.   Levine, J.R., Oversimplifications can lead to faulty coalbed gas reservoir analysis. Journal Name: Oil and Gas Journal; (United States); Journal Volume: 90:47, 1992: p. 63-69.

54.   Diamond, W.P., et al., Results of direct-method determination of the gas content of U.S. coalbeds. 1986: U.S. Dept. of the Interior, Bureau of Mines.

55.   Bertard, C., B. Bruyet, and J. Gunther, Determination of desorbable gas concentration of coal (direct method). International Journal of Rock Mechanics and Mining Sciences & Geomechanics Abstracts, 1970. **7**(1): p. 43-65.

56.   Levy, J.H., S.J. Day, and J.S. Killingley, Methane capacities of Bowen Basin coals related to coal properties. Fuel, 1997. **76**(9): p. 813-819.

57.   Lama, R.D. and J. Bodziony, Outbursts of gas, coal and rock in underground coal mines. 1996: R.D. Lama.

58.   Reeves, S.R., The Coal-Seq Project: Key Results From Field, Laboratory, and Modeling Studies (2000-2004), in 7th International Conference on Greenhouse Gas Control Technologies (GHGT-7)2004: Vancouver, BC, Canada.

59.   Busch, A., et al., Methane and carbon dioxide adsorption–diffusion experiments on coal: upscaling and modeling. International Journal of Coal Geology, 2004. **60**(2–4): p. 151-168.

60.   Scott, A.R., W.R. Kaiser, and W.B. Ayers, Thermogenic and secondary biogenic gases, San Juan Basin, Colorado and New Mexico; implications for coalbed gas producibility. AAPG Bulletin, 1994. **78**(8): p. 1186-1209.

61.   Faiz, M. and P. Hendry, Significance of microbial activity in Australian coal bed methane reservoirs — a review. Bulletin of Canadian Petroleum Geology, 2006. **54**(3): p. 261-272.

62.   Zinder, S.H., Physiological ecology of methanogens, in Methanogenesis: Ecology, Physiology, Biochemistry and Genetics, J.G. Ferry, Editor. 1993, Chapman & Hall: New York & London. p. 128-206.

63.   Busch, A., Y. Gensterblum, and B.M. Krooss, High-Pressure Sorption of Nitrogen, Carbon Dioxide, and their Mixtures on Argonne Premium Coals. Energy & Fuels, 2007. **21**(3): p. 1640-1645.

64.   Setzmann, U. and W. Wagner, A New Equation of State and Tables of Thermodynamic Properties for Methane Covering the Range from the Melting Line to 625 K at Pressures up to 100 MPa. Journal of Physical and Chemical Reference Data, 1991. **20**(6): p. 1061-1155.

65.   Kunz., O., et al., The GERG-2004 wide range equation of state for natural gases and other mixtures: GERG TM15 2007. 2007, Düsseldorf: VDI-Verl. 555.

66.   Siemons, N. and A. Busch, Measurement and interpretation of supercritical CO2 sorption on various coals. International Journal of Coal Geology, 2007. **69**(4): p. 229-242.

67.   İnan, S., et al. Coalbed Gas Potential in the Miocene Soma Basin (Western Turkey). in 27. Pittsburgh Coal Conference. 2010. İstanbul-Turkey.

68.   Mukhopadhyay, P.K., J.A. Wade, and M.A. Kruge, Organic facies and maturation of Jurassic/Cretaceous rocks, and possible oil-source rock correlation based on pyrolysis of asphaltenes, Scotian Basin, Canada. Organic Geochemistry, 1995. **22**(1): p. 85-104.

69. Lamberson, M.N. and R.M. Bustin, Coalbed methane characteristics of Gates Formation coals, northeastern British Columbia; effect of maceral composition. AAPG Bulletin, 1993. **77**(12): p. 2062-2076.

70. Gürdal, G. and M.N. Yalçın, Pore volume and surface area of the Carboniferous coals from the Zonguldak basin (NW Turkey) and their variations with rank and maceral composition. International Journal of Coal Geology, 2001. **48**(1–2): p. 133-144.

71. Isochema, H., IGA Systems User Manual, 2005.

72. Bumpus, J.A., et al., Biomimetic Solubilization of a Low Rank Coal: Implications for Its Use in Methane Production. Energy & Fuels, 1998. **12**(4): p. 664-671.

Curriculum Vitae

Personal information	
First name(s) / Surname(s)	**Mustafa Baysal**
Address(es)	Sedir Mahallesi 728. Sokak Çetintaş Apt. No:34/4 Merkez/Antalya Türkiye
Telephone(s)	+902423344297 Mobile: +905324164599
E-mail	mustafabaysal@sabanciuniv.edu
Nationality	Turkish
Date of birth	29/07/1986
Gender	Male
Work experience	
Dates	October 2009- June 2011
Occupation or position held	Teaching Assistant
Main activities and responsibilities	Recitation Hours, Lab Sessions
Name and address of employer	Sabancı University, Sabancı Üniversitesi Orta Mahalle, Üniversite Caddesi No: 27 34956 Tuzla-İstanbul
Type of business or sector	University
Dates	July 2008- Sept. 2008
Occupation or position held	Undergraduate Researcher
Main activities and responsibilities	Conducting experiments and literature review on self organization of polymers
Name and address of employer	Koç University, Rumelifeneri Yolu 34450 Sarıyer İstanbul
Type of business or sector	University

Dates	June 2008- July 2008
Occupation or position held	Intern
Main activities and responsibilities	Conducting experiments and literature review on Synthesis and characterization of layered double hydroxides
Name and address of employer	Hacettepe University, Hacettepe Üniversitesi Beytepe / ANKARA
Type of business or sector	University
Dates	July 2007- Aug. 2007
Occupation or position held	Intern
Main activities and responsibilities	Determining efficiency of production processes
Name and address of employer	Levent Chemistry Industry A.Ş
Type of business or sector	Industrial Cleaning Supplies

Education and training

Dates	Oct 2009- February 2012
Title of qualification awarded	MSc
Principal subjects/occupational skills covered	Materials Science and Engineering
Name and type of organisation providing education and training	Sabanci University
Dates	Oct 2004- June 2009
Title of qualification awarded	BSc
Principal subjects/occupational skills covered	Chemistry
Name and type of organisation providing education and training	Hacettepe University

Annexes

M. Baysal, Y. YÜRÜM, Biogasification of Soma Lignite by Microorganisms, 6th Chemical Engineering Conference for Collaborative Research in Eastern Mediterranean Countries, EMCC-6, March 7-12, 2010, Antalya, Turkey, Book of Abstracts, ISBN: 978-125-036-6, Istanbul, 2010, p. 286

S. İnan, A. Dikbaş, S. Ergintav, F. Duygun, M. N. Yalçın, K. Tırpan, K. Yasar, E. Okandan, Y. YÜRÜM., M. Baysal, R. Saatçılar, M. Yılmaz, A. R. Toygar, A. Kösebalaban, S. Anaç, H. Duran, M. Onbası, M. Ersoy, M. Atayar, İ. Ergüder, Coalbed Gas Potential In the Miocene Soma Basin (Western Turkey), Twenty Seventh International, Pittsburgh Coal Conference Coal Energy, Environment and Sustainable Development October 11-14, 2010, Istanbul Hilton Session 22, Coal Science: CBM/Carbon Dioxide, Oral Presentation 22-3, Abstract Booklet, p.21.

M. Baysal, Y. YÜRÜM, S. İnan, Biogasification of Soma Lignite (A Preliminary Study), Twenty Seventh International, Pittsburgh Coal Conference Coal Energy, Environment and Sustainable Development October 11-14, 2010, Istanbul Hilton Poster Session 5, Coal Science: CBM/Carbon Dioxide, Poster Presentation P5-17, Abstract Booklet, p.59